DISS. ETH NO. 28829

FUNCTIONAL ROLE OF T REGULATORY CELLS IN PERIPHERAL IMMUNE TOLERANCE IN MULTIPLE SCLEROSIS

A thesis submitted to attain the degree of DOCTOR OF SCIENCES
(Dr. sc. ETH Zurich)

presented by

TIZIANA LORENZINI

Dr. med., University of Brescia

born on 03.03.1987

accepted on the recommendation of

Prof. Dr. Federica Sallusto (doctoral thesis supervisor)

Prof. Dr. Roland Martin (co-examiner)

Prof. Dr. Manfred Kopf (co-examiner)

2022

TABLE OF CONTENTS

LIST OF FIGURES

LIST OF TABLES

1.0 ABSTRACT (English)

Multiple sclerosis (MS) is considered a prototypic autoimmune disease of the central nervous system. It is the leading cause of chronic neurological disability in young adults, and not only T and B cells, but also regulatory T cells (Tregs) have been suggested to play important roles in its pathogenesis. Several studies have shown Treg dysfunction in patients with MS, but underlying mechanisms remain poorly understood. By combining immunophenotyping, functional assays, high-throughput T cell receptor (TCR) Vβ-chain-, and RNA sequencing we examined the Treg compartments in 41 patients with relapsing-remitting MS (RRMS) and 17 healthy donors (HDs). Patients with MS showed a reduced frequency of CD3+CD4+ cells and Foxp3+ Tregs and an increased frequency of CD39+ Tregs. The expression of CD127 was augmented, whereas the expression of CD49d was decreased in Tregs derived from patients. By using a novel staining strategy based on CD45RA and GPA33, we observed low t-Tregs in younger patients. When we determined Treg function, we found that this was reduced only in natalizumab-treated patients. Accordingly, only in this group we detected an altered gene expression in t-Tregs, but not in p-Tregs. Here we provide insights into the possible mechanisms underlying the functional Treg impairment in some patients with MS, such as an impaired proliferation and homeostasis of t-Tregs, leading to their depletion, and an increased Teff autoproliferation. In addition, we detected potential compensatory mechanisms, that might be beneficial or detrimental, such as CD39, CD127 and CD45RA upregulation. Our findings prompted us to investigate strategies to reestablish immune tolerance by adoptive transfer of Tregs. We provide the first description of suppressive, Foxp3 positive T cell clones specific for myelin basic protein (MBP) that could be used as source of TCRs for adoptive Treg therapy in selected patients.

1.1 ABSTRACT (Italian)

La sclerosi multipla (MS) è considerata un modello di malattia autoimmune del sistema nervoso centrale. Costituisce la principale causa di disabilità neurologica cronica in giovani adulti e non solo linfociti T e B, ma anche linfociti T regolatori (Treg) giocano un ruolo importante nella sua patogenesi. Diversi studi hanno evidenziato un difetto funzionale dei Treg nei pazienti con MS, tuttavia i meccanismi sottostanti rimangono scarsamente compresi. Attraverso l'utilizzo combinato di immunofenotipo, saggi funzionali e sequenziamento di TCRβ e RNA ad alte prestazioni abbiamo esaminato i Treg in 41 pazienti con sclerosi multipla recidivante remittente e 17 donatori sani. I pazienti presentavano una ridotta frequenza di cellule CD3+CD4+ e Treg Foxp3+, oltre ad un'aumentata percentuale di Treg CD39+. L'espressione di CD127 era incrementata, mentre l'espressione di CD49d era diminuita nei Treg dei pazienti. Utilizzando una nuova strategia di staining, basata su CD45RA e GPA33, abbiamo osservato una ridotti t-Treg nei pazienti più giovani. Analizzando la capacità inibitoria dei Treg, ne abbiamo riscontrato una diminuzione solo nei pazienti trattati con natalizumab. Consistentemente, solo questo gruppo presentava un'alterata espressione genica a livello dei t-Treg. In definitiva, i nostri risultati suggeriscono possibili meccanismi patogenici alla base del difetto funzionale dei Treg riscontrato in alcuni pazienti: una ridotta proliferazione e omeostasi dei t-Treg, causa di deplezione a livello periferico, e una maggiore autoproliferazione dei linfociti T. In aggiunta, abbiamo identificato possibili meccanismi compensatori, come un'aumentata espressione di CD39, CD127 e CD45RA. I nostri dati ci hanno indotto a studiare strategie per ristabilire la tolleranza immunologica mediante trasferimento adottivo di Treg. In questo studio descriviamo per la prima volta cloni cellulari T funzionali, positivi per l'espressione di Foxp3 e specifici per la proteina basica della mielina che potrebbero essere utilizzati come fonte di recettori T per la terapia cellulare a base di Treg in pazienti selezionati.

2.0 INTRODUCTION

2.1 Multiple sclerosis

Multiple sclerosis (MS) is a chronic inflammatory disease of the central nervous system (CNS), characterised by demyelination and neurodegeneration *(1)*. It affects 2.8 million people worldwide with a rising prevalence over the last years *(2)*. It is the most common cause of chronic neurological disability in young adults, with females being two to three times as likely to acquire MS as males, and with a mean age at diagnosis of 32 years *(2)*. It was described in 1868 by Jean-Martin Charcot as 'la sclerose en plaques' based on the histological characteristics of the demyelinating lesions *(3)*. Currently, the diagnosis of MS is based on McDonald criteria that have been revised in 2017 *(4)*. The following criteria support the diagnosis: clinical signs and symptoms that are typical for MS can derive from all areas of the CNS, which have been affected and occurred in temporal and spatial separation, i.e. dissemination in time and space, that is at least two different areas of the CNS should have been affected and at two different time points *(4)*. The most common symptoms at onset include lack of strength in one or more limbs, optic neuritis, paresthesias and dysesthesias, vision problems, dizziness, fatigue, and sexual, bowel and bladder dysfunction *(5)*. Furthermore, lesions detected using magnetic resonance imaging (MRI) that are typical for MS (juxtacortical, callosal, periventricular, and infratentorial, spinal cord) markers of inflammation in the cerebrospinal fluid (CSF), such as oligoclonal bands *(4)*, and abnormal visual evoked potentials are used for diagnosing MS. The majority of patients show a relapsing-remitting form of the disease (RRMS), characterised by phases of neurological symptoms alternating with recovery phases *(6)*. Differential diagnosis include acute disseminated encephalomyelitis, neuromyelitis optica, CNS vasculitis, systemic lupus erythematosus, Sjögren syndrome, sarcoidosis, infectious diseases, metabolic disorders, and malignancies *(5)*. Usually, within 15-25 years, RRMS can evolve into secondary progressive MS (SPMS) with progressive neurological disability, although today's use of highly effective treatments has protracted this time and less and less patients enter the SPMS stage. The minority of patients have a disease onset characterised by a progressive course from onset (primary progressive MS, PPMS) *(6)*. The expanded disability status scale (EDSS) is routinely adopted during clinical examination to measure the disability status of patients. It

ranges from 0 to 10, with 0 corresponding to normal neurological exam, 6 to loss of autonomy and 10 to death due to MS *(5)*.

A complex genetic etiology underlies MS, and more than 200 risk alleles have been identified *(7)*. The HLA (human leukocyte antigens)-DRB1*15:01 locus is the main genetic risk factor, and accounts for up to 60% of the genetic risk in MS patients *(8)*. Additional genes within the HLA complex have been identified as conferring risk or protection for MS *(8)*. Further susceptibility genes, which are involved in innate and adaptive immune pathways, in the peripheral immune system and brain resident microglia, have been discovered *(7)*. An excerpt of susceptibility genes, identified by the International Multiple Sclerosis Genetics Consortium and selected for their involvement in immune pathways, is shown in Table 1. Besides the complex genetic trait, several environmental factors contribute to the etiology of MS. These include viruses and infectious agents, smoking, diet, gut microbiota, stress, sex hormones, and vitamin D deficiency *(9)*. The strongest environmental risk factor for MS is considered to be Epstein-Barr virus (EBV) *(9)*. Important to note, the main genetic risk factor, the HLA-DR15 haplotype appears to act in concert with environmental risk factors such as smoking and EBV *(10)*.

Table 1. MS risk alleles involved in innate and adaptive immune pathways.

Gene	Locus	Function
NCAPH2	Chr. 22	T cell development
NCF4	Chr. 22	NADPH oxidase complex
CSF2RB	Chr. 22	Crosstalk between DC and NK
GRAP2	Chr. 22	TCR signaling
IFNGR2	Chr. 21	Th differentiation
TMEM50B	Chr. 21	IFN-γ signaling
CD40	Chr. 20	Th differentiation
CD37	Chr. 20	Humoral and cellular immune response
IFI30	Chr. 19	Antigen processing
TYK2	Chr. 19	Th1 and Th2 activation pathway
C3	Chr. 19	PI3K Signaling in B Lymphocytes
CD226	Chr. 18	Crosstalk between DC and NK
MALT1	Chr. 18	TCR signaling
HEATR6	Chr. 17	DC differentiation
STAT3	Chr. 17	Th differentiation
GRB2	Chr. 17	Th1 and Th2 activation pathway
IKZF3	Chr. 17	Lymphoid differentiation/T regulatory cell function
MAP3K14	Chr. 17	PKCθ signaling in T Lymphocytes

Gene	Locus	Function
IRF8	Chr. 16	DC maturation
NLRC5	Chr. 16	TLR and IL-1 receptor pathway
SEPT1	Chr. 16	Interaction with Foxp3
IQGAP1	Chr. 15	Rac and IL-8 signaling pathway
TRAF3	Chr. 14	CD40 signaling pathway
BATF	Chr. 14	Lineage-specific T cell differentiation
ZFP36L1	Chr. 14	B cell development
TRAFD1	Chr. 12	Control of innate immune response
SH2B3	Chr. 12	Cytokine signaling pathway
PTPN11	Chr. 12	Cytokine signaling pathway
LTBR	Chr. 12	Crosstalk between DC and NK
TNFRSF1A	Chr. 12	Th differentiation
ETS1	Chr. 12	BCR signaling
CXCR5	Chr. 12	Th differentiation and migration
CLECL1	Chr. 12	Costimulatory molecule
PLCB3	Chr. 11	Chemokine signaling pathway
CD6	Chr. 11	T cell differentiation
FKBP2	Chr. 11	Calcineurin inhibitor-binding protein in T cells
CD5	Chr. 11	Proliferation and T cell differentiation
SPI1	Chr. 11	Th1 and Th2 activation pathway
NR1H3	Chr. 11	Macrophage function
MADD	Chr. 11	TNFR1 signaling pathway
IFITM3	Chr. 11	Interferon signaling pathway
CAMK2G	Chr. 10	PKCθ signaling in T Lymphocytes
IL2RA	Chr. 10	Th differentiation
IL15RA	Chr. 10	IL-15 signaling pathway
GATA3	Chr. 10	Th differentiation, regulator of Foxp3
IRF5	Chr. 6	Virus- and interferon- signaling pathway
IKZF1	Chr. 6	Th1 and Th2 activation pathway
HOXA1	Chr. 6	ROS production in macrophages
CARD11	Chr. 6	TCR signaling
TAGAP	Chr. 6	T cell activation
IL22RA2	Chr. 6	IL-22 signaling pathway
AHI1	Chr. 6	Interaction with Foxp3
BACH2	Chr. 6	B- and T-lymphocyte differentiation
TNFAIP3	Chr. 5	CD40 signaling pathway
ETV7	Chr. 6	T cell development
JARID2	Chr. 6	Th17 cell function and T regulatory cell homeostasis
CD83	Chr. 6	Cytokine signaling pathway
IL12B	Chr. 5	Th differentiation
TCF7	Chr. 5	T cell differentiation
IL6ST	Chr. 5	Th differentiation
IL7R	Chr. 4	γc cytokine signaling pathway
MARCHF1	Chr. 4	MHC class II downregulation

Gene	Locus	Function
TNIP3	Chr. 4	TLR, IL-1 and TNF signaling pathway
LEF1	Chr. 4	Thymic T cell development
TET2	Chr. 4	DNA methylation in Tregs
NFKB1	Chr. 4	Th1 and Th2 activation pathway
TXK	Chr. 4	TCR signaling
TEC	Chr. 4	TCR signaling
BCL6	Chr. 4	Th differentiation
IL12A	Chr. 3	Cytokine that acts on T and NK cells
CD80	Chr. 3	Th differentiation
FOXP1	Chr. 3	Repressor of monocytes and macrophages
CCR4	Chr. 3	Th1 and Th2 activation pathway
EOMES	Chr. 3	Th1 differentiation
STAB1	Chr. 3	Defense against bacteria
CD28	Chr. 2	Th1 and Th2 activation pathway
STAT4	Chr. 2	Th differentiation
RND3	Chr. 2	ROS production in macrophages
REL	Chr. 2	IL-12 signaling pathway
ADCY3	Chr. 2	IL-1 signaling pathway
BATF3	Chr. 1	T cell development
CD58	Chr. 1	Cytokine signaling pathway
TGFBR3	Chr. 1	Th1 and Th2 activation pathway
BCL10	Chr. 1	TCR signaling
SLAMF7	Chr. 1	T and B cell signaling
JAK1	Chr. 1	Th1 and Th2 activation pathway
LCK	Chr. 1	TCR signaling
RUNX3	Chr. 1	Th1 and Th2 activation pathway- Treg function
TNFRSF14	Chr. 1	T cell activation
TNFRSF25	Chr. 1	Lymphocyte homeostasis

Abbreviations: NADPH= nicotinamide adenine dinucleotide phosphate; DC= dendritic cell; NK= natural killler; TCR= T cell receptor; Th= T helper; PI3K= phosphoinositide 3-kinase; PKCθ= protein kinase C-theta; TLR= Toll like receptor; BCR= B cell receptor; TNFR1= tumor necrosis factor receptor 1; ROS= reactive oxygen species; TNF= tumor necrosis factor; MHC= major histocompatibility complex.

2.2 Immune response in multiple sclerosis

The experimental autoimmune encephalomyelitis (EAE) is the animal model of MS and was developed to understand the pathogenesis of encephalomyelitis after rabies vaccination. In

contrast to rabies, post-vaccinial encephalomyelitis was characterised by lymphoid infiltrated and demyelination in the CNS, suggesting an autoimmune etiology *(11)*. The EAE model is induced by either active immunisation with myelin-derived proteins or peptides in adjuvant or by passive transfer of activated myelin-specific CD4+ T lymphocytes *(12)*. Data obtained from this model suggested that autoreactive CD4+ T cells play a crucial role in the pathogenesis of MS. In this model the immunisation induces these cells in the lymph nodes and spleen. The origin of these autoreactive T cells in MS is not clear, but they probably develop in the thymus by recognition of HLA-DR self peptides (SP) presented by thymic epithelial cells, dendritic cells and thymic B cells *(13)*. DR15 molecules might contribute to the positive selection of SP-reactive T cells with low avidity, whereas those with high avidity are probably negatively selected *(13)* (Figure 1). Autoreactive T cells are then released into the periphery where they are probably activated by high-avidity cross-recognition of peptides derived from foreign antigens, such as EBV and *Akkermansia (1, 13)* (Figure 1). It has been assumed that HLA-DR-SPs are also involved in homeostatic maintenance and proliferation (a process called autoproliferation) of memory CD4+ T cells. Furthermore, memory B cells present "pathogenic" CNS self-peptides that are recognised with high avidity and sustain the proliferation and brain homing of autoreactive T cells *(14)* (Figure 1). The specificity of autoreactive T cells has been mapped to immunodominat peptides of myelin proteins, such as myelin basic protein (MBP), proteolipid protein (PLP), and myelin oligodendrocyte glycoprotein (MOG) *(15)*. In addition, novel autoantigens, such as RAS Guanyl Releasing Protein 2 (RASGRP2) and guanosine diphosphate (GDP)-l-fucose synthase, have recently been discovered *(14, 16)*. The peripheral activation of autoreactive T cells by these peptides explains their specificity for antigens that are not expressed in the thymus.

Brain inflammation in MS is supposed to start with the disruption of blood-brain barrier caused by lymphocytes migrating into the CNS *(17)*. They recognise "pathogenic" CNS self-peptides presented by antigen presenting cells (APCs), such as macrophages, microglia and perhaps astrocytes, in the context of HLA class II molecules *(5)*. The secretion of proinflammatory cytokines, such as IFN-γ, TNF-α, IL-17 and GM-CSF, and chemokines leads to an increased permeability of the blood brain barrier due to the expression of adhesion molecules by endothelial cells *(5)*. In mice, T cell response is directed towards an immunodominant peptide during the early stages of the disease. Subsequently, the tissue damage releases new molecules and the immune response spreads from dominant to

subdominant epitopes and to different antigens (epitope spreading) *(5)*. T helper type 1 (Th1) cells, secreting IFN-γ and expressing the transcription factor T-bet and the chemokine receptor CXCR3, have been considered for a long time the main responsible for CNS inflammation *(18)*. Later, it has been shown that Th17 cells, producing IL-17 and expressing the transcription factor RORC and the chemokine receptor CCR6, as well as Th1/Th17 cells, also play a role in the development of EAE *(18)*. The relative role of Th1 and Th17 cells in MS is still not clear *(18)*. Both IFN-γ and IL-17 are present in MS brain lesions and, together with Th1/Th17 cells, have been associated with disease activity *(18)*. It has been shown that Th17 cells transmigrate more efficiently across the blood brain barrier than Th1 cells, highly express granzyme B, and kill neurons *(19)*. In the animal model, it has been shown that Th17 cells that migrate to the CNS originate in the intestine, thus linking diet and gut microbiota to MS *(20)*. In humans, a correlation between microbiota alterations, intestinal Th17 cell expansion and MS activity has been confirmed *(20)*. However, the relative contribution of Th1 and Th17 cells during different disease phases is not fully understood *(18)*. Moreover, a Th2 phenotype, characterised by IL-4 secretion and the expression of the transcription factor GATA3, has been identified in brain infiltrating lymphocytes of a patient with MS *(21)*. Not only autoreactive CD4+ T cells participate in the pathogenesis of MS, but also regulatory T cells (Tregs) have been suggested to play important roles in protecting against MS *(22)*. This role will be discussed in details below. CD8+ have been found to be more frequent than CD4+ T cells in brain lesions. They may recognise antigen in the context of HLA class I molecules expressed by neurons and oligodendrocytes and cause tissue damage *(15)*. However, in EAE model it has been shown that CD8+ T cell depletion or deficiency is associated with an increased disease severity, thus suggesting a protective or regulatory role *(18)*. Similarly, γδ cells have been found to be expanded in MS brain lesions and in the cerebrospinal fluid and to produce IL-17, but they may have protective functions during disease resolution *(18)*. As daclizumab therapy, used to treat MS, leads to the expansion of natural killer (NK) cells, their role has become of interest. It has been shown that NK cells have strong antibody-dependent cytotoxic effects and they might damage the myelin sheath *(23, 24)*. However, certain subsets, such as CD56 bright NK cells, show immunoregulatory properties and kill activated T cells *(23, 24)*.

The role of B cells in the pathogenesis of MS is still unclear. The beneficial effect of B-cell depleting therapies supports their detrimental role that can be related to their antigen

presenting function, sustaining autoreactive T cell activation and proliferation, as mentioned above *(14)*. Furthermore they produce proinflammatory cytokines and they are organised in tertiary lymphoid-like structures in the CNS which are the likely source of autoantibodies *(25)*. Indeed, autoantibodies directed against myelin and IgG oligoclonal bands, are sometimes detectable in serum and/or CSF fluid from MS patients *(15)* although their contribution to the pathogenesis is currently less clear and controversially discussed. It has been hypothesised that EBV is involved in B cell overactivation that leads to CNS inflammation *(25)*. By contrast, it has been shown that B cells protect mice from chronic EAE through the production of IL-10 and thus exert a regulatory function *(26)*. Microglia has a distinct origin from monocyte-derived macrophages and plays a role in active CNS inflammation by myelin phagocytosis, antigen presentation and proinflammatory cytokines secretion *(27)*. However, it has also anti-inflammatory functions by clearing myelin debris and promoting remyelination *(27)*. Neutrophils share some proinflammatory functions with microglia and in addition they can release neutrophil extracellular traps and produce reactive oxygen species *(28)*.

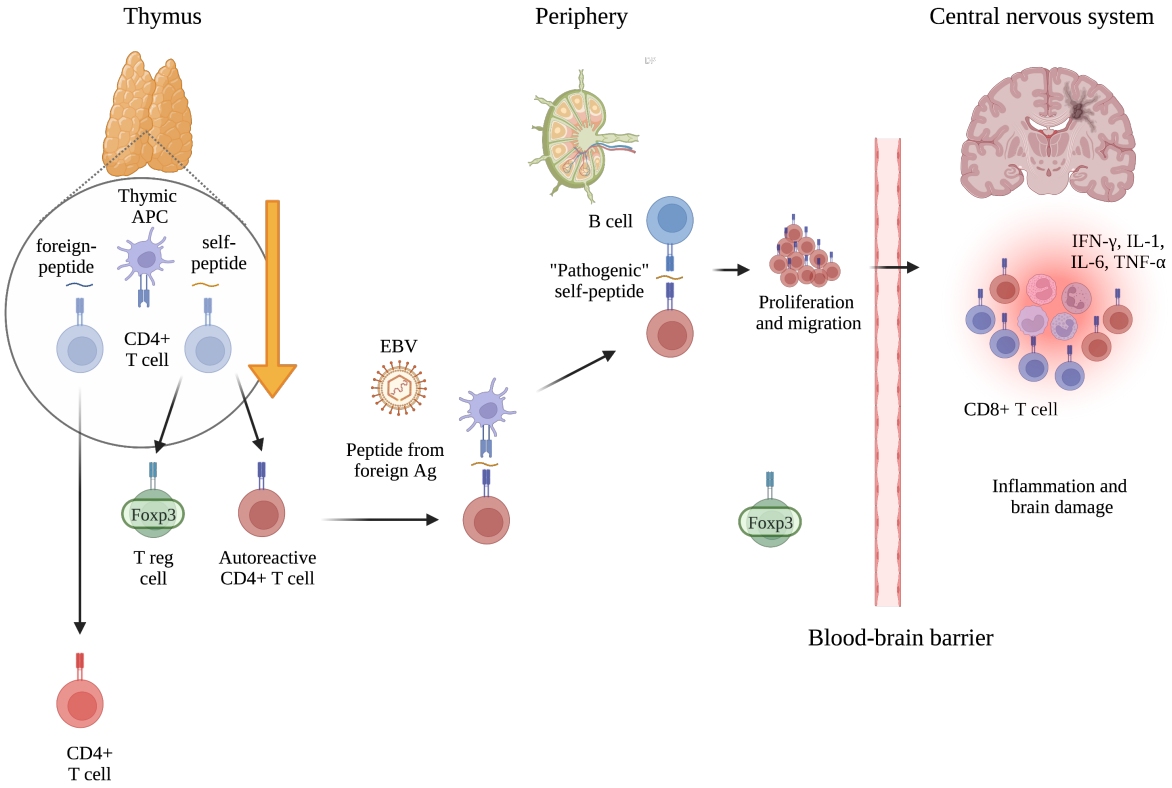

Figure 1. Autoreactive T cell development, activation, proliferation and migration into the CNS. Adapted from Wang J *(13)*. Created with Biorender.com.

2.3 Neuropathology of MS

Typically, MS lesions are characterised by demyelination, multifocal inflammation, oligodendrocyte loss, reactive gliosis and axonal degeneration *(6)*. An inflammatory perivascular infiltrate, with T and B cells, is observed in early active lesions which are more frequently observed in patients with RRMS *(6)*. Later, myelin phagocytosis is mediated by perivascular macrophages which are the most frequent cells in brain lesions. Initially oligodendrocytes can proliferate leading to a partial remyelination. However, subsequently there is a loss of oligodendrocytes and myelin and hypertrophic astrocytes eventually form a central glial scar, surrounded by a hypercellular rim of astrocytes, macrophages and lymphocytes *(5)*. Hence, a microglia and/or macrophage reaction is usually observed in inactive or chronic active MS lesions in patients with progressive MS *(6)*. Chronic inactive lesions contain a hypocellular, gliotic core and do not show active inflammation *(6)*. Axonal loss is a feature of either active and chronic MS lesions, but the latter are characterised by axonal swelling *(6)*.

In conclusion, the interplay between innate and adaptive immunity determines the histopathology of MS brain lesions during different disease phases. The shift from a predominant adaptive immune response to an innate immune response might influence the disease progression from an acute to a chronic form.

2.4 Regulatory T cell discovery

In 1970 Gershon and Kondo discovered a population of thymus-derived lymphocytes that were able to induce tolerance *(29)*. However, the “suppressor T cell hypothesis” collapsed in the mid 1980s, when the existence of the molecule I-J, which was supposed to mediate T cell suppressive function *(30)*, had been disproved. Mostly because of the lack of identifying markers, the nature of suppressive cells remained undefined until 1995, when Sakaguchi et al. described regulatory T cells (Tregs), as a subset of CD4+ T cells highly expressing the IL-2 receptor α-chain (CD25) *(31)*. IL-2 and CD25-deficient mice have a reduced number of CD25+CD4+ T cells and spontaneously develop severe autoimmunity and inflammation, suggesting that CD25 is not only a Treg marker, but is also implicated in their function and homeostasis *(30)*. In 1997 T regulatory cells 1 (Tr1), producing high levels of IL-10 and with

the ability to suppress antigen-specific immune responses have been defined *(32)*. In 1998 an in vitro functional assay to evaluate Treg suppressive function has been established *(30)*. In 2001 Scurfy mice were shown to carry mutations of *Foxp3* gene on X chromosome. They spontaneously develop lymphoproliferation and multiorgan infiltration leading to death 16-26 days after birth *(33)*. In 2003 Foxp3 has been discovered as the main transcription factor for Tregs *(30)*. Foxp3 is a member of the forkhead family of transcriptional regulators, it represses *NFAT* (nuclear factor of activated T cells) and *NFKB* and inhibits the expression of genes involved in cytokine secretion and T effector cell function *(34)*. When Foxp3 was retrovirally transduced into CD25-CD4+ cells they were converted into phenotypically and functionally Treg-like cells *(30)*. The stability of Foxp3 depends on epigenetic modifications in the *Foxp3* locus that is in the Treg-specific demethylated region (TSDR) *(35)*. Next, mutations of the human ortholog of murine *Foxp3* have been discovered as genetic cause of Immune dysregulation, Polyendocrinopathy, Enteropathy, X-linked (IPEX) syndrome which is characterized by multiple autoimmune manifestations involving the endocrine glands, skin and intestine *(36)*. In 2006 expression of CD127 was found to be inversely correlated with Foxp3 expression and low expression of CD127 was identified as an additional Treg marker *(37)*. Recently, Treg heterogeneity has been studied in detail and, in addition to the physiological state, also in several diseases ranging from tumors to autoimmune diseases. The understanding of Treg heterogeneity with respect to phenotypic markers and functions has important implications for therapies that aim at exploiting Tregs for example by adoptively transferring Tregs in autoimmune diseases.

2.5 Human Treg markers

The lack of unique and specific Treg identifying markers complicates Treg characterisation. Expression of the transcription factor Foxp3 is considered the gold standard marker of Tregs *(38)*. However, Foxp3 is not exclusively expressed by Tregs, but can also be expressed by T effector cells (Teffs) following activation *(38)*. Furthermore, as Foxp3 is localized in the nucleus, assessment of its expression requires intracellular staining with fixation and permeabilisation of the cells, which compromises their viability and renders detection more complicated *(38)*. High expression of CD25 and lack of CD127 are the most used identifying surface markers. Thus, Tregs are identified as CD3+ CD4+ CD25hi CD127lo cells.

CD4+CD25+ cells can constitute up of 30% of total peripheral blood mononuclear cells (PBMCs), but only the cells that highly express CD25 are Tregs *(39)*. Like Foxp3, CD25 and the lack of CD127 are not specific for Tregs, as they can also be expressed by Teffs after activation *(39)*.

Table 2. Human Treg markers.

Essential	Origin	Activation	Suppression	Migration	Stability
CD3	CD45RA (thymic)	CD137	CTLA4	CCR4	Helios
CD4	CD45RO (peripheral)	OX40	CD39	CCR6	TIGIT
CD25	CD31 (thymic)	CD121a/b	CD73	CCR9	
CD127lo	TNFR2 (peripheral)	LAP	HLA-DR	CD49d-	
Foxp3	GITR (peripheral)	GARP	LAG-3	CD103	
		CD69	ICOS		
		CD103	PD-1		
		CCR4			
		CD154-			

Besides the above molecules, some markers are helpful to identify Treg origin, and in particular to distinguish thymus- and peripherally-derived Tregs (the nature of these subsets will be discussed in detail below). CD45RA is expressed by thymus-derived Tregs (t-Tregs, alternatively named naïve/resting/fraction I), and its expression is low in peripherally-derived Tregs (p-Tregs, alternatively named effector/activated/fraction II). A third subset of CD45RA- cells, characterised by intermediate levels of Foxp3 and CD25 expression and named fraction III, has been defined as a mixture of Treg and non-Treg cells *(40)*. In addition, t-Tregs express CD31 (Platelet Endothelial Cell Adhesion Molecule-1, PECAM-1), an adhesion molecule that is highly expressed on recent thymic emigrants T cells *(41)*. Helios, an Ikaros transcription factor family member, has first been described as specific for t-Tregs in mice *(42)*. However, in humans, Helios positive and negative t-Tregs coexist, and the lack of Helios expression is associated with a more unstable phenotype *(43)*. The expression of Helios is correlated with

TIGIT (immunoreceptor with Ig and ITIM domains) *(44)*. Moreover, p-Tregs express higher levels of effector molecules, such as CTLA-4 (cytotoxic T lymphocyte antigen 4, CD152), and molecules involved in T cell activation, migration, and suppression, as shown in Table 2.

Some Treg-specific activation markers have been identified, including CD137 (4-1BB), CD121a/b, LAP (latent-associated peptide), GARP (glycoprotein A repetitions predominant), CD103 (integrin subunit alpha E, ITGAE), and OX40 *(39)*. The expression of low levels of CD49d, that is the α-chain of the integrin VLA-4, characterises Tregs. As integrins are involved in leukocyte adhesion, their expression is increased in activated Tregs. The expression of CD137, combined with the lack of CD154 expression, has been described as Treg activation signature *(45)*. We used two TNF receptor super family (TNFRSF) members-CD137 and OX40 (CD134, or TNFRSF4) - to recognise activated Tregs. Additional Treg markers have been associated with increased suppressive Treg function. For instance, TIM-3, HLA-DR, LAG-3, CD39, and ICOS (inducible costimulator) positive Treg are more suppressive than their negative counterpart *(46, 47)*. A list of Treg markers is shown in Table 2. Lastly, the assessment of *Foxp3* methylation status, that is a stable genetic modification, helps to distinguish between Tregs and activated Teffs transiently expressing Foxp3 *(35)*. Whereas Tregs show *Foxp3* demethylation and tend to remain demethylated even after in vitro expansion, activated Teffs display no *Foxp3* demethylation *(35)*.

2.6 Treg subsets

Based on their origin, Tregs can be classified as thymus-derived or peripherally-derived (Table 3). Both subsets are equally important to protect against autoimmunity. Thymus-derived Tregs (t-Tregs) develop in the thymus, probably by diversion of self-reactive thymocytes *(48)*. These cells escape the negative selection, which self-reactive double positive thymocytes usually undergo. The mechanisms that determine positive or negative selection are unclear, but the affinity and specificity of the interaction between self-peptide-TCR might support Treg precursor differentiation into mature Foxp3+ cells *(48)*. Since full Foxp3 expression requires Treg activation, t-Tregs have a reduced Foxp3 expression in comparison to p-Tregs. However, their Foxp3 expression is considered stable, due to the low TSDR methylation *(49)*. Foxp3 inhibits the transcription factor STAT4 (signal transducer and activator of transcription 4), which stimulates IFN-γ production *(40, 49)*. The frequency of t-

Tregs decline with age reflecting reduced thymic output due to thymic involution. Although sometimes defined as naïve, they are not antigen unexperienced, as they have already recognised a self-antigen in the thymus in an antigen-specific manner *(49)*. After t-Tregs have been released from the thymus they migrate to secondary lymphoid organs, using CCR7 and CXCR5, where they can be reactivated *(49)*. At this stage, they express activation markers, such as LAP and CD103, and it is difficult to distinguish them from peripherally-derived Tregs (p-Tregs) *(49)*. GPA33 has recently been discovered as marker of stable thymus-derived Tregs *(50)*. It has been identified in naïve Tregs just before exit from the thymus, but its expression remained detectable after Treg activation, thus identifying Tregs with a low propensity of conversion into T effector cells *(50)*.

In contrast to t-Tregs, p-Tregs are probably generated via the conversion of peripheral T effector cells under the influence of locally produced cytokines (i.e. TGF-β, IL-2, and IL-33) *(51)*. Thus, they are supposed to maintain tolerance to harmless foreign antigens, derived from food or commensal microbes and presented in mucosal tissues *(51)*. Their main regulatory mechanism is the secretion of immunosuppressive cytokines. Although they express higher levels of Foxp3 in comparison to t-Tregs, they are considered to be less stable and can convert into Teffs under inflammatory conditions. A reduced Helios expression and a lower TSDR demethylation could account for this instability *(49)*. Furthermore, recently generated p-Tregs might show an incomplete lineage commitment, which might require repeated antigen stimulation to become complete *(49)*. Such cells that are not fully committed can be found in the above mentioned fraction III subset, which is characterized by intermediate expression of Foxp3 and CD25. This subset expresses many of the markers found in p-Tregs, has an unclear inhibitory capacity and is unstable, as it can produce inflammatory cytokines and shows incomplete TSDR demethylation *(49)*. The frequency of p-Tregs increases with age.

Type 1 regulatory cells (Tr1) can be considered a subset of peripheral regulatory cells that do not constitutively express Foxp3, but can up-regulate it under activation. They are identified by co-expression of LAG-3 and CD49b *(32, 52)*. Even if they lack Foxp3 expression, they are fully suppressive not only via IL-10 secretion, but also through mechanisms adopted by Foxp3+ cells, such as the anti-inflammatory adenosine, cytotoxic molecules, and co-inhibitory molecules *(52)*. Th3 cells are another subset of cells with suppressive function, but lacking Foxp3 expression, and mainly characterised by TGF-β secretion *(38)*. Although

described in mice, CD8+ Tregs remain to be defined in humans *(53)*. Recently, they have been shown to suppress pathogenic CD4+ T cells in infections and autoimmune diseases *(54)*. In addition to T cells, natural killer T cells (NKT) have regulatory functions, and regulatory B cells and plasma cells have also been described *(55)*.

Based on the expression of distinct chemokine receptors, Tregs have been classified as Th17-like (CCR6+CXCR3-CCR4+), Th1-like (CCR4+CCR6-CXCR3+), and Th2-like (CCR4+CCR6-CXCR3-). These subsets display the master transcription factors RORγt, T-bet, and GATA3, respectively *(56)*. Even if Th17-like and Th1-like Tregs can produce little amounts of IL-17 and IFN-γ, respectively, they mainly produce IL-10, express Foxp3, and are phenotypically and functionally stable *(56)*. Interestingly, there is a developmental link between Th17 cells and Treg cells, as they both require TGF-β for initial differentiation *(57)*. By next generation RNA sequencing, we found that p-Tregs express genes associated with Th17-lineage commitment, such as *RORC*, *RORA*, *BATF*, and *IL17RB* (see below). Tissue-resident Tregs represent a heterogenous subset with a unique phenotype, and tissue-related functions *(49, 58)*. Lastly, it is important to specify if Tregs that have been generated *in vitro*, for example through TGF-β stimulation. In this case, the term "*in vitro*-induced Treg cells" should be adopted *(59)*.

Table 3.

Treg cell subsets
Thymus-derived Tregs (t-Tregs)
Periperally-derived Tregs (p-Tregs)
Type I regulatory cells (Tr1)
Th3 cells
CD8+ Tregs
Natural killer T cells (NKT)
Th17-like Tregs
Th1-like Tregs
Th2-like Tregs
Tissue-resident Tregs
In vitro-induced Tregs

2.7 Treg cell frequency, function and plasticity

The quantification of Treg frequency in peripheral blood is difficult due to the lack of unique and specific Treg-identifying markers, as discussed above.

As Tregs can be defined as CD25hiCD127loFoxp3+, the staining and gating strategies might differ, hampering the comparison between studies. Buckner suggested that, based on the expression of high levels of CD25, approximately 4% of CD4+ T cells in human blood can be defined as regulatory *(38)*. In our cohort of 16 HDs, Tregs, defined as CD25+CD127lo, represented 2.82% of CD4+ cells (range 1.06-4.58%, see below). IPEX elucidates the importance of Tregs in preventing autoimmunity *(36)*. In this disease, Foxp3-expressing cells are usually low or absent, but they can also be present, although unstable and impaired *(60)*. This example underscores the importance of Treg function over Treg cell number. Accordingly, patients with autoimmune diseases in most instances show only a modest reduction in Treg cell number *(38)*. Furthermore, the number of Tregs is quantified in peripheral blood, but may not reflect Treg number in peripheral tissues which is more relevant for Treg function *(38)*.

Beyond IPEX, an impaired Treg function is observed in several primary immunodeficiencies *(61)*. Mutations in the α-chain of the IL-2 receptor (*IL-2Rα*, *CD25*) lead to an IPEX-like syndrome associated with opportunistic infections related to T cell deficiency *(61)*. Mutations in *STAT5b* compromise the transcription of genes downstream of IL-2Rα and decrease Foxp3 expression *(61)*. STAT5b deficiency is characterised by dwarfism, infections, diarrhea, eczema and lymphocytic interstitial pneumonitis, suggesting immune dysregulation *(61)*. Autoimmune Polyendocrinopathy, Candidiasis and Ectodermal Dystrophy (APECED) syndrome is caused by autosomal recessive mutations in *AIRE* (autoimmune regulator) which plays a role in the generation of functional Tregs *(61)*. It is characterised by reduced Treg frequency, Foxp3 expression and functionality *(61)*. In Wiskott-Aldrich syndrome, caused by mutations in *WAS* (WASP Actin Nucleation Promoting Factor), Treg function is consistently impaired and patients develop thrombocytopenia, eczema, infection snd malignancies *(61)*.

Several mechanisms of suppression have been described, and their relative contribution to Treg function is unclear. Since Tregs express high levels of CD25, they can compete with effector T cells for IL-2, deplete it, and induce IL-2 deprivation-mediated apoptosis of effector T cells *(62)*. CD39 and CD73 are endonucleases that hydrolyse ATP, reducing its availability

for T cell proliferation. The consequent generation of adenosine inhibits Teffs binding to the adenosine A2A receptor *(63)*. Moreover, Tregs can induce cytolysis by the same mechanisms adopted by cytotoxic T cells and NK cells, such as granzyme A and perforin *(63)*. In addition, Tregs can suppress CD8+ T cells, but not CD4+ T cells, by Fas-mediated apoptosis *(64)*. Furthermore, Tregs can inhibit APCs by TIGIT-CD155 interaction, or by CTLA-4-CD80/ CD86 interaction *(49, 63)*. CTLA-4 additionally increases the expression of IDO by dendritic cells, thus lowering the concentration of tryptophan for T effector cell proliferation *(64)*. CTLA-4 (cytotoxic T-lymphocyte-associated protein 4) insufficiency due to heterozygous germline mutations leads to a complex immune dysregulation syndrome with multiple autoimmune manifestations *(65)*. This syndrome is characterised by an increased frequency of Tregs, albeit dysfunctional *(65)*. LAG-3 (lymphocyte-activation gene 3) can also block dendritic cell maturation and their immunostimulatory capacity *(63)*. In a mouse model, it has been shown that Tregs can acquire CD80 and CD86 from dendritic cells via trogocytosis. In particular, the acquisition of CD86 enhanced Treg activation and suppressive function *(66)*. Another mechanism mediating Treg function is the production of inhibitory cytokines, such as IL-10, TGF-β, and IL-35. As discussed above, these cytokines are crucial for Tr1 and Th3 cell function, but their role for t-Tregs function is still debated *(63)*. Thus, Tregs exert a broad immunosuppressive effect beyond the antigens they specifically recognize *(67)*. A summary of Treg suppressive mechanisms is provided in Table 4.

Tregs show some degree of plasticity, for example they can suppress using the same transcriptional program of their target Teffs *(68)*. During type-I immune responses, IFNγ is released by Teffs and induces *TBET* expression, leading to the polarisation of Th1-suppressive Tregs *(68)*. However, IFNγ induces *IL2RB2* expression, that makes Tregs susceptible to the effects of IL-12. IL-12 drives Treg polarisation into Th1-like Tregs with an impaired proliferative capacity *(68)*. Thus, the balance between IFNγ and IL12 in the microenvironment is responsible for Treg differentiation either into Th1-suppressive Tregs, or into Th1-like non-suppressive Tregs. It has been suggested that in pathological conditions, such as in multiple sclerosis, this balance is shifted towards an increased frequency of Th1-like defective Tregs *(68)*. Accordingly, Th17-like Tregs have been shown to contribute to pathological conditions, such as colon cancer, inflammatory bowel disease, psoriasis and arthritis, and Th2-like Tregs have been observed in patients with food allergies *(68)*. As discussed above Th1-, Th17-, and Th2-like cells are functionally and phenotypically stable

(56), but might become pathogenic in diseases characterised by type 1, -17, or -2 polarisation, respectively.

Table 4.

Treg suppressive mechanisms
IL-2 depletion and IL-2 deprivation-mediated apoptosis
CD39 and CD73-mediated adenosine production
Granzyme A and perforin-mediated cytolysis
Fas-mediated apoptosis
APCs inhibition through CTLA-4
APCs inhibition through TIGIT
LAG-3-mediated block of dendritic cell maturation
Trogocytosis of CD80 and CD86 from dendritic cells
Inhibitory cytokines, i.e. IL-10, TGF-β, and IL-35
Differentiation in Th1-suppressive Tregs

2.8 Treg cell antigen specificity and repertoire

As Tregs have an antigen-specific T cell receptor (TCR), one important question that has arisen concerns the specificity of their TCR. In particular, whether Tregs recognise self- or non self-antigens has been a matter of debate. According to the first hypothesis, medullary epithelial thymic cells (mTEC) present endogenous antigens under the control of AIRE and FEZF2 (FEZ family zinc finger 2), and positively select a t-Treg repertoire based on high affinity interactions *(69)*. In addition, in mice, the Treg TCR repertoire was found to be enriched for TCR complementarity determining regions 3 (CDR), which contained strongly interacting amino acids in comparison to the Teff TCR repertoire *(70)*. These TCRs might recognise self-antigens with high avidity, in contrast to Teffs. Therefore, t-Tregs specific for self-antigens have been found *(67)*. MOG, one of the major auto-antigens of autoreactive Teffs in multiple sclerosis, has been discovered as self-antigen for t-Tregs *(68)*. MOG-specific Treg TCRs had a higher functional avidity for MOG peptides in comparison to the T effector counterpart and Tregs, in contrast to Teffs, could not develop in the absence of MOG *(48)*. This might suggest that self-peptides are the unique and best agonists for Tregs, while autoreactive Teffs are more degenerate *(68)*. In contrast to this model, Pacholczyk et al.

suggested that non self-antigens are the cognate specificities of Tregs *(71)*. Supporting this hypothesis is the discovery of Tregs specific for bacteria, fungi, parasites, allergens and alloantigens *(67)*. In addition, it has been reported that thymic Treg differentiation does not require the recognition of a self-agonist. However, CD4+CD25+ thymocytes are less sensitive to agonist-induced deletion than their CD+CD25- counterpart, thus they are apparently enriched *(72)*. It could be argued that if Tregs are specific for self-antigens their TCR repertoire should be mostly distinct, with a limited overlap with Teff TCR repertoire. By contrast, a high overlap would suggest that Tregs recognise similar non self-antigens, like Teffs. However, the reports on this subject are often contradictory. Fazilleau et al. reported a 24% of overlap between the two repertoires, and suggested that Tregs have a repertoire size and diversity similar to those of Teffs *(73)*. As the current knowledge about this topic is limited, we tried to compare the diversity between Treg and Teff repertoire and to measure their overlap, by performing high-throughput TCR sequencing in patients with RRMS and HDs (see below).

It is probably clear from the above summary that many aspects that are involved in thymic Treg development and their antigen-specificity are complex and remain incompletely understood. Whether Tregs suppress in an antigen-specific fashion is another open question. To exploit their suppressive function, Tregs require activation by an antigen-specific TCR-MHC II interaction *(48)*. Once Tregs are activated in an antigen-specific manner, they can suppress Teffs with different antigen specificities. However, it has been suggested that the suppression is more effective when Tregs and Teffs have the same antigen specificity *(70)*. In conclusion, it is still unclear if Tregs are specific for self- or non self- antigens, but they require to be activated by their cognate antigen to become suppressive. Once they are activated, they can use specific and non-specific mechanisms to suppress Teffs. It might be possible that, whereas specific mechanisms require cell-cell interaction, non-specific mechanisms are mediated by cytokines that create a tolerogenic environment. Hence, the interaction of a Treg and a Teff sharing the same antigen-specificity might underlie an effective suppression.

2.9 Tregs in MS

Data obtained from the EAE model suggested that Tregs may also have protective roles in MS. When a disease-inducing trigger was applied, the adoptive transfer of CD4+CD25+ T cells prevented EAE or reduced its severity *(31)*, while targeted deletion of Treg resulted in increased susceptibility to the disease and prevented secondary EAE remission *(74)*. Protective Treg-mediated mechanisms include the inhibition of the capacity of dendritic cells to prime naïve autoreactive T cells *(49, 63)*, the suppression of proliferation and migration of autoreactive T cells *(63)*, and remyelination in the CNS. The latter is obtained not only by anti-inflammatory mechanisms, but also by induction of oligodendrocyte differentiation *(75* (Figure 2).

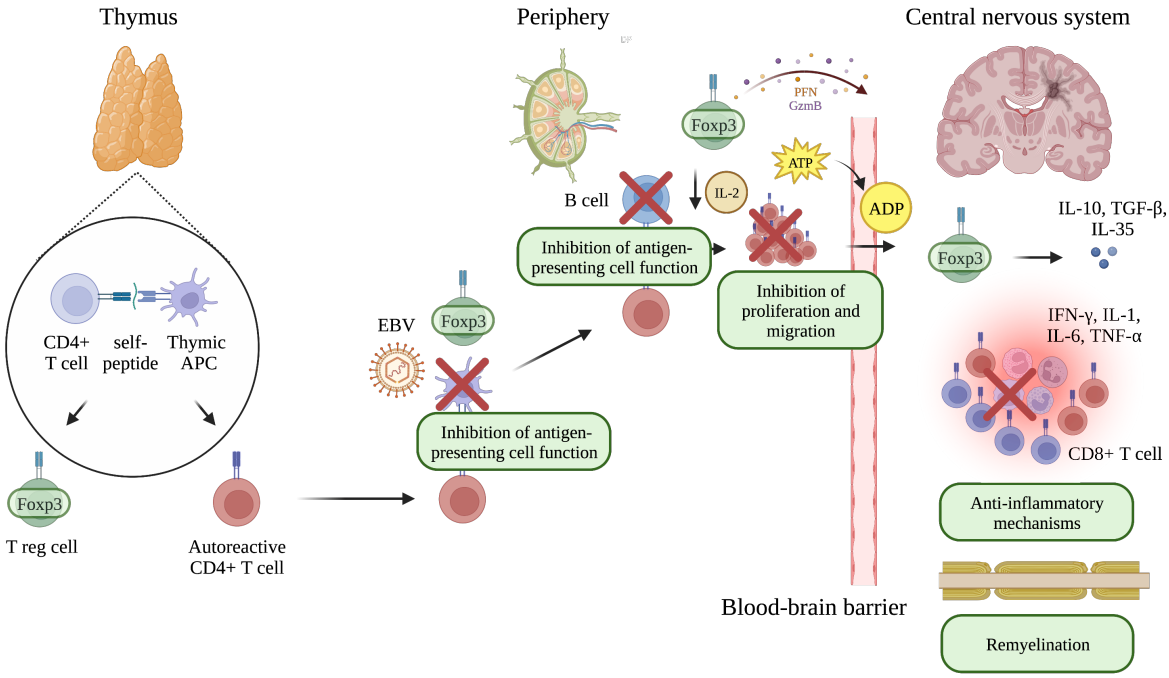

Figure 2. Mechanisms of Treg-mediated suppression of autoreactive T cells in MS. Adapted from Wang J *(13)*. Created with Biorender.com.

A failure of Treg-dependent immune tolerance has been supposed to contribute to several autoimmune diseases and in particular to MS. Numerous studies have assessed various Treg-related aspects in patients with MS *(22, 76-78)*, however, with sometimes controversial results, which is due to the lack of unique identifying markers for Tregs, the heterogeneity of cohorts and discrepancies in laboratory methods. For instance, a meta-analysis of 16 studies

found no evidence for reduced numbers of Tregs defined as CD4+CD25+ cells in peripheral blood of patients with MS *(79)*. However, when Tregs were defined as CD4+CD25+Foxp3+ cells, they were lower in patients with MS as compared to HDs *(79)*. Moreover, an accumulation of Tregs in the CSF, together with an increased expression of CD103 and CD49d, adhesion molecules involved in T cell homing, has been observed in RRMS patients *(77, 78)*. However, accumulating Tregs in the CSF might be more susceptible to apoptosis, resulting in a low frequency of Tregs in MS brain lesions *(80)*. In addition, Tregs derived from patients with MS show a functional impairment, when tested for their suppressive capacity against autologous lymphocytes stimulated polyclonally or antigen-specifically *(78, 81)*. In these experiments, the compromised Treg suppressive capacity was not related to an increased resistance of Teffs. In contrast, secondary progressive MS patients display a normal Treg function, and no correlation between Treg function and disease activity has been found *(82)*. Nevertheless, the mechanisms underlying the functional defect are still unknown. Overall, existing data hints at an impaired thymic function and a proinflammatory environment (Figure 3). Genetic susceptibility and environmental factors might influence both pathogenic mechanisms *(7, 9)*. The hypothesis of a reduced thymic output is supported by the reduced frequency of CD31+ recent thymic emigrant (RTE) Tregs and reduced TCR repertoire diversity based on a lower CDR3 (complementarity-determining region 3) complexity score of patients with MS *(83)*. A positive correlation between RTE-Tregs prevalence and Treg-mediated suppression has been found *(83)*. The frequency of RTE-Tregs physiologically declines with age, but a premature reduction has been observed in pediatric patients with MS *(84)*. The hypothesis of a proinflammatory environment that may reduce Treg stability and downregulate Foxp3 is supported by the higher frequency of Th1-like Tregs secreting interferon-γ (IFN-γ) and with reduced suppressive function in untreated patients with RRMS *(68, 85)*. This phenotype could be induced *in vitro* by IL-12, suggesting that proinflammatory cytokines can influence Treg plasticity. Similarly, IL-6 can induce a Th17-like non-suppressive phenotype *(86)*. Proinflammatory signals, as the ones found during a relapse in patients with MS, can increase CD39 and CD45RA expression in Tregs *(87, 88)*. Activated Tregs up-regulate could be mobilised to the CNS to exploit their anti-inflammatory effect *(87)*. However, an increased activation could lead to exhaustion, and finally reduce the concentration of CD39+ Tregs, as reported in some MS patients *(89)*. Lastly, inflammation drives post-translational modifications in Foxp3 causing its degradation *(87)*. A compromised

Tr1 function might additionally contribute to MS pathogenesis. Defects in the induction of Tr1 cells with CD46 co-stimulation have been observed in MS patients as reduced IL-10 secretion *(90)*.

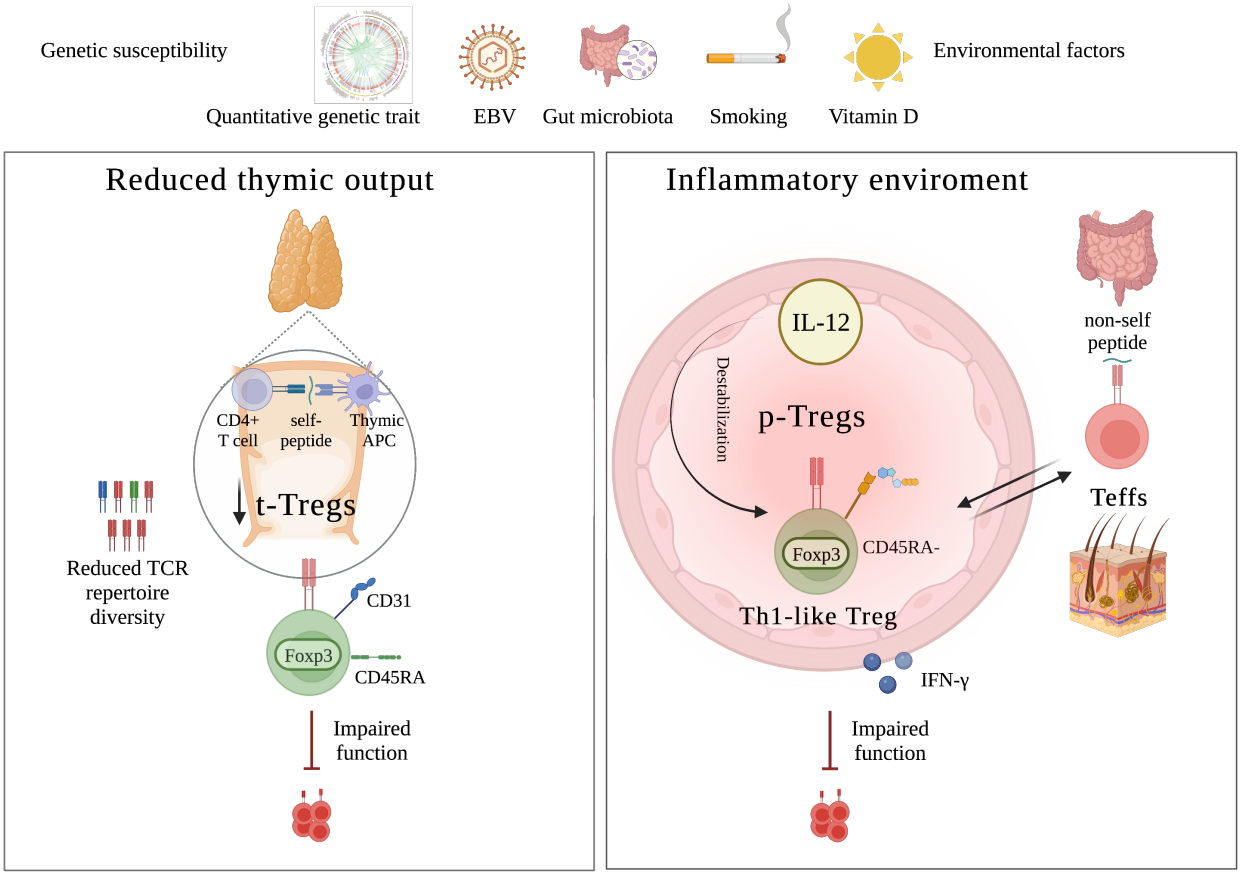

Figure 3. Possible pathogenic mechanisms underlying functional Treg defect in some patients with MS. Created with Biorender.com.

2.10 Current and future treatments for MS

Although there is no cure for MS yet, treatments include steroids during acute exacerbations and disease-modifying drugs to modify the course of the disease through immunomodulation or suppression *(15)*. Interferon-β (IFN-β) has a low/moderate efficacy in reducing relapse rates, is well tolerated, and has numerous immunomodulatory effects, including stabilisation of the brain-blood barrier, down-regulation of MHC class II molecules on APCs, and inhibition of proinflammatory cytokines *(15)*. Glatiramer acetate (GA) has a similar efficacy and tolerability profile, inhibits antigen presentation and proinflammatory cytokines, and induces the production of neurotrophic factors *(15)*. Natalizumab is a humanized monoclonal

IgG4κ antibody against α4-integrin, an adhesion molecule expressed by lymphocytes and monocytes that mediates their adhesion to the endothelium and extravasation across the blood-brain barrier into the CNS. It was designed following the observation of the importance of VCAM-1 in EAE model. The reduced CD49d expression on circulating lymphocytes is mediated by internalisation and degradation of CD49d *(91)*. Furthermore, the interaction between α4 integrins and VCAM-1 (vascular cell adhesion molecule 1) is important for lymphocyte activation and proliferation *(92)*, and natalizumab exerts a costimulatory effect via integrin α4 *(91)*. It has a high efficacy and good tolerability, except for one adverse effect: i.e. progressive multifocal leukoencephalopathy (PML), associated to JC polyoma virus infection (PML) *(15)*. This effect might be related to the low lymphocyte counts in the CSF and to the release of B cells from the bone marrow and the spleen, where JC virus is latent *(93, 94)*. Furthermore, drug cessation sometimes induces rebound disease activity, an effect that has been related to the accumulation of autoreactive lymphocytes T cells in the periphery that may enter the CNS *(91)*. It has been shown that natalizumab supports a proinflammatory gene expression profile and the retention of inflammatory activated lymphocytes is associated with increased IL-2, IFN-γ and IL-17 in some patients with MS *(14, 91)*. Fingolimod (FTY720) is an inhibitor of the sphingosin-1 phosphate receptor (S1PR) that is necessary for egress of CCR7 positive lymphocytes from the lymph nodes *(15)*. Thus, it prevents their migration to the CNS, without affecting CCR7 negative memory lymphocytes *(15)*. It is less effective than Natalizumab in reducing relapse rates, and it is associated with the risk of reactivation of latent infections, particularly of HSV-1 and VZV infection *(15)*. Dimethyl fumarate has an efficacy comparable to fingolimod and has immunomodulatory effects, such as dendritic cells and proinflammatory cytokines inhibition, and neurotrophic factors, and regulatory B cell induction *(15)*. Alemtuzumab is a monoclonal antibody against CD52, that is expressed by B and T cells. It blocks the inflammation by lymphocyte depletion, and, in some patients, is associated with secondary autoimmune diseases *(15)*. Anti-CD20 antibodies (rituximab, ocrelizumab, ofatumumab) efficiently reduce the inflammatory activity in MS by B cell depletion *(15)*. Their main mechanism is binding to CD20, expressed on the surface of all B cells, except early pro-B cells, plasma blasts and plasma cells, and inducing lysis by antibody-dependent complement- or cell-mediated cytotoxicity *(95)*. Whereas a small fraction of CD20-expressing T cells is depleted *(96)*, T cells are mostly diminished because in absence of B cells, they are not supported by antigen presentation, and are thus deprived of a stimulus

necessary for their activation and proliferation *(96)*. Daclizumab is a humanised monoclonal antibody against CD25 and its anti-inflammatory activity is mediated by the expansion of CD56 bright NK cells *(15, 23)*. Autologous hematopoietic stem cell transplantation (aHSCT) is a highly effective treatment of MS and can entirely suppress MS disease activity for long periods of time with 70–80% of patients remaining disease-free *(97)*. Autologous CD34+ stem cells are collected prior to the high-dose chemotherapy and are subsequently infused to the patient to reconstitute a functional immune system *(24, 97)*. Thus, the main mechanisms of action are eliminating autoreactive T cells, and establishing a new T cell repertoire *(24, 97)*.

The induction of specific tolerance against target antigens represents a strategy to re-establish immune tolerance in MS patients. One approach, which our group pursues, uses an infusion of autologous red blood cells chemically coupled with myelin peptides. The phase Ib study confirmed the tolerability and safety of the treatment and provided mechanistic indication of antigen-specific tolerization, such as a decrease of antigen-specific T cell response *(98)*. In table 5, the effects of MS treatments on Tregs are reported.

Table 5. Effects of MS treatments on Tregs

Treatment	Effect on Tregs
IFN-β	Increased frequency of t-Tregs and improved suppressive capacity *(99)*, higher number of Tregs and Tr1 cells *(100)*
Glatiramer acetate	Increased frequency of t-Tregs and improved suppressive capacity *(101)*, increased IL-10 production *(102)*
Natalizumab	Reduction of CD49d expression on Tregs, block of Treg transmigration, Treg frequency and suppressive capacity unchanged after treatment *(103)*
Fingolimod	Reduced Treg frequency, but increased Foxp3 and CD39 expression in the remaining CD4+ T cells *(104)*
Dimethyl fumarate	Increased responsiveness of Teffs for immunoregulation by Tregs *(105)*
Alemtuzumab	Tregs are not spared from depletion, expansion of CD45RA- Tregs after treatment due to homeostatic proliferation or T effector cell conversion, enhanced Treg inhibitory effect related to altered Teffs *(106)*
Anti-CD20 therapy	Slightly decreased CD4+ Treg frequency, increased frequency of CD8+ Treg *(95)*
Daclizumab	Reduced Treg frequency, impaired proliferation and suppressive capacity *(107)*, expansion of CD56+ NK cells *(108)*

Treatment	Effect on Tregs
aHSCT	Unknown
Antigen-specific toleration therapy	Unknown

2.11 Adoptive transfer of Tregs as treatment for MS

As discussed above, during the last 30 years, several disease-modifying drugs with immunomodulatory effects have been approved for MS. These treatments reduce relapse rates and slow the progression of RRMS *(15)*. However, they are ineffective in halting or reversing the disease that is dependent from neurodegenerative processes, especially in progressive forms of MS, and have side effects related to immunosuppression *(109)*. As already mentioned, Tregs have neuroregenerative properties that would help to treat patients with later-stage progressive disease *(75, 109)*. Thus, the reconstitution of regulatory T cell function, by means of adoptive cellular therapy (ACT), has been proposed as promising treatment for MS *(110)*. Successfully used to treat certain types of cancer, this therapy has already been applied to other diseases, such as graft-versus-host-disease, type I diabetes, systemic lupus erythematosus, and amyotrophic lateral sclerosis *(49)*. Currently, autologous polyclonal CD4+CD25+CD127lo Tregs are the most commonly used source for ACT *(49)*. By this therapy, Tregs are isolated, expanded *in vitro* and infused back to the patient *(111)*. They have been shown to be effective in reducing insulin resistance in paediatric patients with type I diabetes, but the results were less impressive in adults *(49)*. Furthermore, a phase Ia/II clinical trial has demonstrated the safety and tolerability of autologous polyclonal Tregs, either administered intravenously or intrathecally, in patients with MS *(112)*. However, clinical benefits have not been established yet *(49)*. As Tregs rely on antigen-specific recognition through TCR to be activated, the efficacy of polyclonal Tregs might be limited by the low number of antigen-specific cells, the short term lifespan, and the hurdles in reaching their target tissues *(49)*. Moreover, polyclonal Tregs might cause broad immunosuppression, for instance suppressing immunity against infections and tumors, and off-targets effects *(48)*. An highly specific TCR-antigen-MHC II interaction is necessary to activate Tregs *(69)*. Upon this activation, Tregs can suppress T effector cells (Teffs) with different antigen specificities,

but the suppression might be more efficient when Tregs and Teffs share the same antigen specificity *(67)*. This might be related to the multiple suppressive mechanisms adopted by Tregs, some requiring a direct cell-cell interaction, such as granzyme A and perforin-mediated cytolysis, and Fas-mediated apoptosis, some mediated by IL-2 depletion, anti-inflammatory cytokines, or inhibition of APCs *(63)*. These factors strongly support the use of antigen-specific Tregs, which are more potent, should carry a lower risk of general immunosuppression and target specific tissues *(49)*.

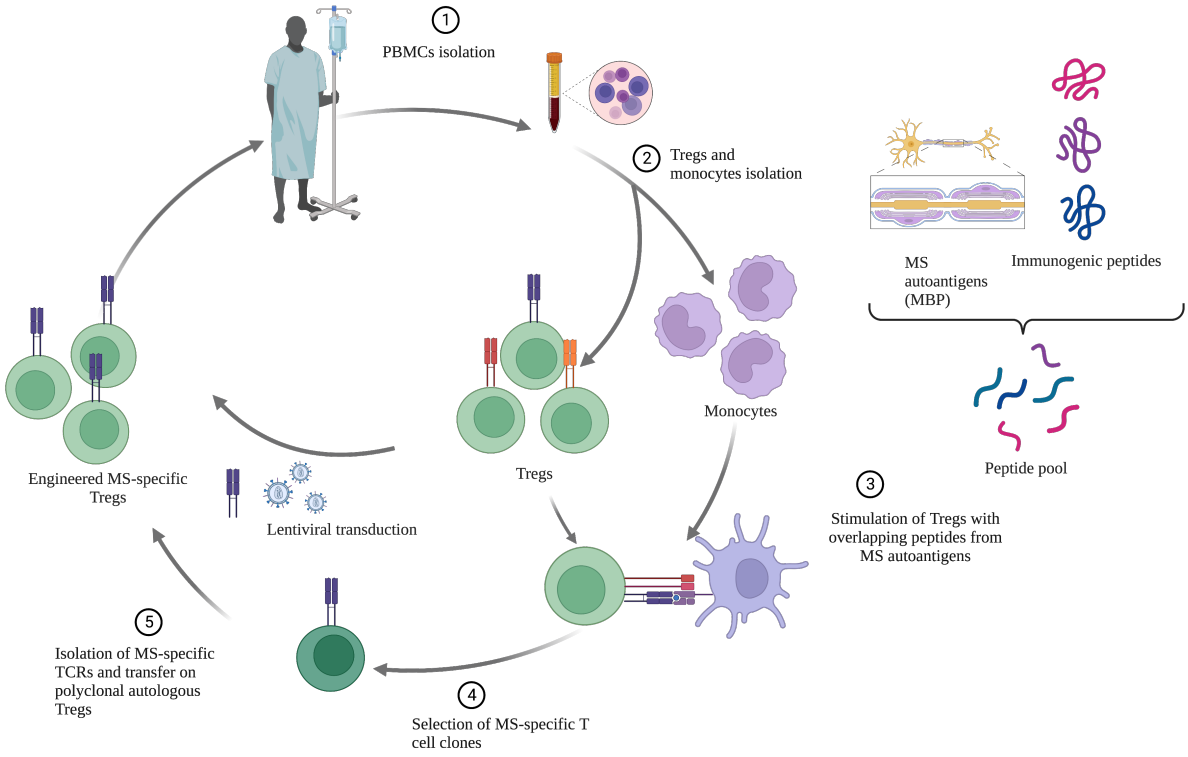

Figure 4. Overview of adoptive T cell therapy. Polyclonal T cells are isolated from patients and edited to express TCRs specific for MS autoantigens. Engineered MS-specific Tregs are then expanded and re infused. Created with Biorender.com.

Nevertheless, purification and expansion of self-antigen-specific Treg cells is hindered by the low precursor frequency *(111)*. An alternative approach is to edit polyclonal Tregs to express antigen-specific TCRs *(111)*. By this approach T cells are isolated from patients and stimulated with autologous monocytes pulsed with pools of overlapping peptides derived from MS autoantigens (Figure 4). Autoreactive Teffs which recognize MBP and MOG can

been found in peripheral blood of MS patients as well as in healthy individuals *(113)*. These cells can be selected and used as source of TCRs that are expressed into autologous Tregs by retroviral or lentiviral transduction. In this way, engineered autoantigen-specific Tregs are obtained and can be expanded to be infused back to the patient *(110)*. In this context, antigen recognition is HLA-restricted. Indeed, a TCR derived from an MBP-specific clone of a patient with MS has been isolated and expressed in human Tregs *(114)*. These Tregs could be activated in response to stimulation with MBP, and suppress MBP-stimulated Teffs *(114)*. In addition, they ameliorated EAE in MOG-immunized DR15 transgenic mice *(114)*. Fransson et al. modified Treg cells with a lentivirus vector system to express a chimeric antigen receptor (CAR) targeting MOG in trans with the Foxp3 gene *(115)*. These cells were able to migrate to the CNS and to reduce the severity of EAE in the chronic phase *(115)*. In another study from Malviya et al., transgenic T cells expressing a TCR specific for MOG (35-55) were equally efficient in EAE induced by MOG (35-55), and induced by an unrelated antigen, PLP (178-191) *(116)*.

However, it has been shown that engineered Tregs are less effective in preventing EAE when they express an autoreactive Teff-derived TCR in comparison to a self-reactive Treg-derived TCR *(48)*. Namely, the suppressive capacity is influenced by the avidity and Tregs have a higher functional avidity for self-peptides, which are their unique and best agonists, in comparison to Teffs, which are more degenerate *(48, 69)*.

Therefore, Treg-derived TCRs might be the best choice for ACT *(49)*. However, to our knowledge, self-antigen-specific Tregs have never been isolated from patients with MS. With our study, we aimed to isolate and characterize myelin-specific Tregs from patients with MS, and to investigate their potential use for ACT. Moreover, it is not clear which Treg cell subsets are more suited to engineer for Treg therapy *(111)*. One concern is the eventual presence of Teffs in the product infused, due to a contamination or due to a Treg conversion into Teff *(49)*. As t-Tregs are supposed to be more stably committed to Treg lineage, they might be the safest source for ACT *(49)*. Additional Treg properties, such as the expression of migratory or suppressive molecules, might influence Treg selection. Another issue is that any defect in Treg cells derived from MS patients should be corrected before autologous transfer of these cells *(49)*. However, Treg suppressive capacity should be studied not only at bulk level, but also at clonal level, as functional Treg clones might be present in MS patients. New

technologies, such as chimeric antigen receptors and genome editing, are currently under development to increase Treg specificity and functionality *(85)*. Furthermore, Tr1 cells have been generated from Teffs by lentiviral vector-mediated IL-10 gene transfer and expanded for clinical application. Clinical trials have shown the safety and feasibility of this approach *(117)*.

2.12 TCR repertoire in MS

The adaptive immune system can recognize almost any antigen through a repertoire of theoretically billions of TCRs *(118)*. A diverse TCR repertoire is crucial to ensure an adequate immune response to foreign antigens and it is influenced by genetic and environmental factors, such as thymic selection, age, HLA haplotype, and infections *(119)*. Such diversity is mostly contained in the hypervariable CDR3 region of the TCR. The CDR3 stems from rearrangements of V, D, and J gene segments (Vβ chain) and V, J segments (Vα chain), with random insertions and deletions, that contribute to the large diversity of the TCR repertoire *(118)*. Following antigen stimulation, specific TCCs are selectively expanded and the repertoire becomes less diverse. Molecular methods such as Sanger sequencing and CDR3 spectratyping have been used to characterise the immune repertoire in past *(120)*. However, the limited resolution and the low throughput have given rise to conflicting results. High-throughput sequencing technologies are currently used to assess the TCR repertoire and enable to capture the full immune repertoire including individual clones *(118)*. Up to 10% of T cells may express two functional α chains, whereas less then 1% express two functional β chains *(120)*. Thus, sequencing of TCR β genes is usually preferred to estimate the number of single clones in the total repertoire. Despite previous data suggested a reduced TCR repertoire diversity in patients with MS in comparison to HDs, recent evidences support a higher diversity in patients *(120, 121, 122)*. Furthermore TCR repertoire has been analysed both in CSF and blood. Highly diverse repertoire and increased clonal expansion have been found in both compartments *(120, 121)*. Whereas Lossius et al. detected a significant overlap indicating that most CSF cells have entered from blood *(120)*, de Paula Alves Sousa et al. found only few shared clones between the compartments *(121)*. In addition, it has been shown that CD8+, more than CD4+ clonotypes, are shared between peripheral blood and brain lesions in patients with MS *(21)*. Planas et al. suggested that clonally expanded CD8+

clonotypes in brain lesions most likely derive from TCCs that are clonally expanded outside the CNS *(21)*. By contrast, the most frequent CD4+ clonotypes identified within the CSF and the brain were infrequent in blood, indicating a local expansion that was stable for at least one year or specific recruitment of CD4+ clonotypes into the brain *(21, 120)*. The observation of identical TCR sequences encoded by different nucleotide combinations has been interpreted in support of an antigen-driven T cell response *(120)*. Some studied have investigated the specificity of the TCR repertoire against microbial antigens. Public EBV-reactive CD8+ T cells shared across individuals were found to be enriched in the CSF of patients with MS, but not of HDs *(120)*. CMV-specific TCRs have been recognised in patients with MS and positively correlated with HLA-DRB1*04:05 haplotype and mild disability *(121)*. The studies cited above refer to T cell TCR repertoire without distinction between Teffs and Tregs. Evidences available on Treg TCR repertoire suggest that it displays a high level of diversity, similar to that of Teffs, shows a preference for high-affinity self-antigens, and is mostly, but not totally distinct, in comparison to Teff repertoire *(123)*. In addition, it has been shown that the thymic and peripheral Treg TCR repertoires are similar, but not identical, suggesting a peripheral reshaping of TCR diversity based on the availability of local antigens *(123)*. Föhse et al. demonstrated that high TCR repertoire diversity is crucial for Treg expansion, peripheral reshaping of Treg TCR repertoire and *in vivo* suppressive capacity *(124)*. As Tregs are more suppressive when they share the same antigen-specificity of Teffs, a high TCR diversity would positively influence Treg inhibitory capacity by increasing the frequency of antigen-specific Tregs *(123)*. Thus, a limited TCR diversity may be a risk factor in autoimmune disease *(123)*.

The hypothesis of public TRCs shared across patients supported the use of databases of CDR3 sequences *(120, 125)*. A TCR is defined as public on the basis of identical amino acid sequences shared across multiple individuals *(126)*. In response to a dominant antigen, selective pressure might drive convergent recombination towards the generation of the same public amino acid CDR3 *(126)*. Thus, the identification of a public TCR repertoire in individuals exposed to the same antigen might lead to the detection of antigen-specific TCRs. Whereas McPAS-TCR database is a catalogue of TCRs that have been found in T cells associated with various pathological conditions in humans and in mice *(127),* VDJdb database lists TCR sequences with known antigen specificities *(128)*.

The detection of antigen-specific TCRs is of interest for adoptive Treg therapy that, as mentioned above, is based on editing polyclonal Tregs to express autoantigen-specific TCRs. MHC tetramers have been developed to identify T cells specific for known antigens *(129)*. Originally designed as class I MHC tetramers for CD8+ T cells, they have been adapted as class II MHC tetramers for CD4+ T cells. However, broad application of this technology has encountered several limitations, including the low frequency of CD4+ T cells of interest, that require expansion or enrichment, the low TCR-MHC avidity, and the HLA class II restriction *(129)*. Due to the low frequency of autoantigen-specific T cells, tetramer staining has still not be used in the context of adoptive Treg therapy.

3.0 MATERIALS AND METHODS

3.1 Patient samples

EDTA-anticoagulated blood samples were collected from 19 untreated, 12 natalizumab-treated, 10 anti-CD20-treated patients with RRMS, and 17 healthy controls. MS was diagnosed according to the revised McDonald criteria *(121)*. Patients and controls were recruited from the NIMS-Neuroimmunology and MS Research Section, Department of Neurology, University Hospital Zurich. Samples were collected in the context of previous research projects which had been approved by the Cantonal Ethical Committee of Zurich, Switzerland (EC-No. 2013-0001 and EC-No. ERC 2014-0699). All study participants had given their written informed consent to use their samples for research. PBMCs were isolated from blood samples using Ficoll-Paque™ density gradient-centrifugation. They were cryopreserved in 90% heat-inactivated fetal calf serum (Eurobio, Courtaboeuf, France) and 10% Dimethyl sulfoxide (Sigma-Aldrich) for 24-48 hours at -80°C prior to long-term storage in liquid nitrogen. 36 individuals were typed for HLA class I and II molecules at Histogenetics LLC, NY, USA. DNA was isolated from whole blood using a standard DNA isolation protocol using a Triton-X100 (Sigma Aldrich, St Louis, MO, USA) lysis buffer and Proteinase K (Roche) treatment. Samples containing a final DNA concentration of 15 ng/ml were typed for HLA-class I (A* and B*) and HLA-class II (DRB1*, DRB3*, DRB4*, DRB5*, DQA1* and DQB1*) using high-resolution HLA sequence-based typing (SBT).

3.2 Treg isolation and culture

Tregs were purified from previously frozen PBMCs by using EasySep™ Human CD4+CD127loCD25+ Regulatory T cell Isolation kit (STEMCELL™ Technologies). First, CD25+ cells were positively selected and CD4+ cells were enriched. Then, CD127hi cells were targeted for depletion. EasySep™ Human CD4+ Isolation kit (STEMCELL™ Technologies) was used in parallel to isolate CD4+CD25- Teffs. After isolation, Tregs were immediately analysed or kept in T cell medium. T cell medium had the following composition: Iscove's modified Dulbecco's medium (Gibco™), 5% human serum (Blood Bank Basel, Switzerland), 2 mM L-glutamine (Gibco™), 100 U/ml penicillin (Corning), 100 µg/ml streptomycin (Corning), and 50 µg/mL gentamicin (Sigma-Aldrich). Except when used to perform functional assays, Tregs were kept in short-term culture with high concentrations of IL-2 (500 U/mL). hIL-2 containing supernatant were produced by T6 cell line that was kindly provided by F. Sallusto, IRB, Bellinzona- ETH, Zurich, Switzerland. To expand Tregs, we used 1 µg/mL phytohemagglutinin (PHA, Sigma-Aldrich), IL-2 (500 U/mL), and irradiated allogenic feeders (45 Gy). To prevent Foxp3 downregulation due to Teff expansion, we tested rapamycin and IL-7. However, the results obtained and shown below induced us to avoid long-term Treg culture. To generate TCCs, we used SH800S Cell Sorter (Sony) to sort and plate one single Treg/well in T cell medium. Then, we added 1 µg/mL PHA (Sigma-Aldrich), allogenic irradiated feeders (45 Gy) and IL-2 (500 U/mL). At day 10 after cloning, growing wells were identified by eye and transferred to a new plate with fresh medium with IL-2. Clones were splitted when necessary, and eventually restimulated after 14 days. To confirm their monoclonality, we performed a staining for the expression of Vβ-chain of TCR. Table 6 shows the fluorophore-conjugated anti-human antibodies used for staining.

Table 6. Fluorophore-conjugated anti-human antibodies used for staining of TCR Vβ-chain.

Antibody	Fluorochrome	Company
anti-human TCR Vb 1	PE	Beckman Coulter
anti-human TCR Vb 2	PE	Beckman Coulter
anti-human TCR Vb3	FITC	Beckman Coulter
anti-human TCR Vb4	PE	Beckman Coulter
anti-human TCR Vb5.1	FITC	Beckman Coulter
anti-human TCR Vb5.2	FITC	Beckman Coulter
anti-human TCR Vb5.3	PE	Beckman Coulter

anti-human TCR Vb6.7	FITC	Endogen, Pierce
anti-human TCR Vb7	PE	Beckman Coulter
anti-human TCR Vb8	FITC	Beckman Coulter
anti-human TCR Vb9	PE	Beckman Coulter
anti-human TCR Vb11	FITC	Beckman Coulter
anti-human TCR Vb12	PE	Beckman Coulter
anti-human TCR Vb13.1	PE	Beckman Coulter
anti-human TCR Vb13.6	FITC	Beckman Coulter
anti-human TCR Vb14	PE	Beckman Coulter
anti-human TCR Vb16	FITC	Beckman Coulter
anti-human TCR Vb17	FITC	Beckman Coulter
anti-human TCR Vb18	PE	Beckman Coulter
anti-human TCR Vb20	PE	Beckman Coulter
anti-human TCR Vb21.3	FITC	Beckman Coulter
anti-human TCR Vb22	FITC	Beckman Coulter
anti-human TCR Vb23	PE	Beckman Coulter
anti-human TCR Vb12	FITC	Beckman Coulter

3.3 Immunophenotyping

We used three flow cytometry panels to stain previously frozen PBMCs derived from 41 patients with RRMS and 16 HDs. In addition to the fundamental Treg markers (CD3, CD4, CD25, CD127, Foxp3), we analysed origin and memory markers (GPA33 and CD45RA), functional markers (CD39), and migratory markers (CD103 and CD49d). PBMCs were thawed, washed, stained with the LIVE/DEAD fixable dye Aqua (Invitrogen™) and the unspecific antibody binding to Fc-receptors was blocked with purified human IgG (Sigma-Aldrich). Surface staining was performed using the following fluorophore-conjugated anti-human antibodies: anti-CD3 BV786, anti-CD25 BV421, anti-CD127 APC/Cyanine7, anti-CD39 PE, anti-CD45RA BV711, anti-CD103 BV605, anti-CD49d PerCP/Cyanine5.5 (BioLegend), anti-CD4 PE-Texas Red (Invitrogen™), anti-GPA33 PE (R&D Systems®). Then, cells were fixed and permeabilised with Foxp3 Transcription Factor Fixation/ Permeabilization buffers (eBioscience™). Intracellular staining was performed using Alexa Fluor 647 anti-FOXP3 antibody (BioLegend). Samples were acquired using the flow cytometer BD LSR Fortessa and analysed using the software FlowJo (FlowJo LLC). Table 7 shows the fluorophore-conjugated anti-human antibodies used for staining.

Table 7. Fluorophore-conjugated anti-human antibodies for Treg immunophenotyping.

Marker	Fluorophore	Clone	Isotype	Catalog Nr.	Lot.
CD3	BV785	37895	Mouse IgG2a, κ	317330	B239283

CD4	PE-Texas Red	S3.5	Mouse / IgG2a	MHCD0417	
CD25	BV421	BC96	Mouse IgG1, κ	302630	B228942
CD127	APC-E780	eBioRDR5	Mouse / IgG1, kappa	47-1278-42	4309179
GPA33a	PE	402104	Monoclonal Rat IgG2a	FAB3080P	
FOXP3	Alexa Fluor-647	206D	Mouse IgG1, κ	320114	B241845
CD45RA	BV711	HI100	Mouse IgG2b, κ	304138	B235784
CD39	PE	A1	Mouse IgG1, κ	328208	B199643
CD103	BV605	Ber-ACT8	Mouse IgG1, κ	350218	B215929
CD49d	PerCp-Cy5.5	9F10	Mouse IgG1, κ	304306	

3.4 Antigen-specific activation, expansion and cloning of Teffs and Tregs

Following CD45RA+ naïve T cell depletion by using CD45RA MicroBeads human (Miltenyi Biotec), CD45RA− PBMCs were seeded at 2 ×10^5 cells/well in 200 µl X-VIVO 15™ medium (Lonza) in 96-well U-bottom plates (Greiner Bio-One). Cells were either untreated or *ex vivo* stimulated with pools of overlapping peptides derived from foreign or self antigens at a final concentration of 10 µM. The following autoantigens have been used: MBP, MOG, RASGRP2, TSTA3 (GDP-l-fucose synthase), HLA and PLP. In addition, we investigated the response to EBNA 1 (EBV nuclear antigen 1), BLLF1 (EBV major glycoprotein), and CEF II (from Cytomegalovirus, EBV and Influenza virus). Peptides were provided by Peptides & Elephants, Hennigsdorf, Germany. As positive control, CD45RA- PBMCs were stimulated with anti-biotin MACSiBead particles loaded with biotinylated antibodies against human CD2, CD3, and CD28 at a bead-to-cell ratio of 1:2 (Miltenyi Biotec). To evaluate antigen-specific T cell response, proliferation as compared to unstimulated condition and positive control, was used as readout. To quantify T cell proliferation, wells were pulsed with 1 µCi/ well [3H] thymidine for 7 days. After 16 hours, cells were harvested on a membrane (Filtermat A, GF/C, Perkin-Elmer) using a harvester machine (Tomtec) and [3H] thymidine uptake was detected using Wallac 1450 Microbeta TriLux scintillation counter (Perkin Elmer). Cell proliferation was measured as counts per minute (cpm) or stimulatory index (SI). The SI indicates the ratio of cpm in the presence of the peptide versus cpm in the unstimulated control. Only if T cells showed a stimulatory index above 2, i.e. two times above background, they were considered antigen-specific.

This method is sensitive but doesn't allow further analysis of the proliferative compartment. An alternative method was labelling CD45RA- PBMCs at a final concentration of 0.5 μM carboxyfluorescein diacetate N-succinimidyl ester (CFSE, Sigma-Aldrich) before stimulation. After 7 days cells were collected, stained for Live/Dead® Aqua (Invitrogen) and surface markers, analysed by flow cytometry and responding T cells were identified as CFSE diluting cells. Alternatively, after staining responding T cells can be recognised by flow cytometry by expression of activation markers around 5-7 days after stimulation. Antigen-responding T cells have been isolated as bulk population or single clones, as described above. As the fraction of CFSElo T cells might contain bystander cells, expanded TCCs were co-cultured with APCs and stimulated a second time to confirm their reactivity by [3H] thymidine proliferation assay. Antigen specificity is defined by a stimulatory index above 2, i.e. two times above background.

In order to isolate antigen-responding Tregs, CD14+ and CD4+CD25+ T cells were isolated, by using EasySep™ Human CD14 Positive Selection Kit II, and EasySep™ Human CD4+CD127loCD25+ Regulatory T Cell Isolation Kit, respectively. Tregs were *ex vivo* stimulated using autologous irradiated (45 Gy) CD14+ cells that were either untreated or pulsed with specific peptides. As Tregs have been shown to be hyporesponsive and hypoproliferative *in vitro (130)*, it might be challenging to evaluate their response to antigens, thus we selected activation markers as readout. After 5 days, cells were collected and stained for Live/Dead® Aqua (Invitrogen) and surface markers. The following antibodies were used for staining: anti-CD4 APC/Cyanine7, anti-CD3 PerCP/Cyanine5.5, anti-CD137 BV421 and anti-OX40 APC (Biolegend) (Table 8). We sorted and cloned CD137+OX40+ cells after stimulation with autoantigens. Cloning methods are described above. Expanded TCCs were co-culterd with irradiated monocytes as APCs and restimulated with autoantigens. The next day following secondary stimulation, cells from clones were incubated with human IgG (Sigma-Aldrich), labeled with Live/Dead® Aqua (Invitrogen), and stained using the following fluorophore-conjugated anti-human antibodies: anti-CD3 BV786, anti-CD137 BV421, anti-CD69 APC/Cyanine7 (BioLegend), and anti-CD4 PE-Texas Red (Invitrogen™) (Table 8). The antigen specificity was confirmed by upregulation of the activation markers CD69 and CD137 and downregulation of CD3. The stimulatory index is defined as the ratio between mean fluorescence intensity (MFI) of activation markers observed in stimulated and unstimulated conditions, respectively. Antigen specificity is defined by a stimulatory index

above 2, i.e. two times above background. Supernatants were harvested at day 1 after stimulation. Cytokines in the supernatants were measured with a bead-based immunoassay using the Human T Helper Cytokine Panel (13-plex) kit (LEGENDplex, BioLegend) according to the manufacturer's instructions. The following cytokines were measured: IL-5, IL-13, IL-2, IL-6, IL-9, IL-10, IFN-γ, TNF-α (tumor necrosis factor–α), IL-17A, IL-17F, IL-4, and IL-22. IL-17F and IL-4 had low concentrations and therefore are not shown. Myelin-specific TCCs were obtained from a HLA-DR15+ patient. In the resting phase, cells from clones were fixed and permeabilised with Foxp3 Transcription Factor Fixation/ Permeabilization buffers (eBioeBioscience™). Intracellular staining was performed using Alexa Fluor 647 anti-FOXP3 antibody (BioLegend). The suppressive capacity was tested as ability to inhibit the proliferation of polyclonal stimulated CD25-CD4+ cells from the same donor as discussed below.

To understand if generated clones recognised their antigen in the context of one of the HLA-DR15 haplotype expressing HLA class II alleles, we used B cell lines isolated from a bare lymphocyte syndrome (BLS) patient as APCs. These cells were transfected to stably express DR2a (DRB5*01:01) or DR2b (DRB1*15:01) *(14)* and were kindly provided by B. Kwok (Benaroya Research Institute, Seattle). When a clone responded to the stimulation with BLS cells it was confirmed to be restricted for the respective HLA class II allele.

Table 8. Fluorophore-conjugated anti-human antibodies for Treg sorting and screening of TCC activation.

Marker	Fluorophore	Clone	Isotype	Catalog Nr.	Lot
CD3	BV785	37895	Mouse IgG2a, κ	317330	B239283
CD3	PerCP/ Cyanine5.5	SK7	Mouse IgG1, κ	344807	
CD4	PE-Texas Red	S3.5	Mouse / IgG2a	MHCD0417	
CD4	APC/Cyanine7	SK3	Mouse IgG1, κ	344615	
CD137	BV421	4B4-1	Mouse IgG1, κ	309819	B325666
CD134 (OX40)	APC	Ber-ACT35	Mouse IgG1, κ	350007	B326766
CD69	APC/Cyanine7	FN50	Mouse IgG1, κ	310913	

3.5 Suppression assay

The protocol for Treg suppressive activity characterisation was adapted from Gregori *et al. (130)*. Tregs and Teffs were purified from previously frozen PBMCs by using EasySep™ Human CD4+CD127loCD25+ Regulatory T cell Isolation kit (STEMCELL™ Technologies) and EasySep™ Human CD4+ Isolation kit (STEMCELL™ Technologies), respectively. CD4+CD25- Teffs were stimulated with anti-biotin MACSiBead particles loaded with biotinylated antibodies against human CD2, CD3, and CD28 at a bead-to-cell ratio of 1:2 (Miltenyi Biotec). Then, 5 x 10^4 Teffs/well were plated alone or in presence of Tregs at different ratios in T cell medium in a 96-well U-bottom plate (Greiner Bio-One). The ratio Treg:Teff ranged from 1:8 to 2:1. In addition, Tregs were cultured alone to monitor an intrinsic proliferative capacity. In parallel, Teff cells were plated in presence of the respective ratio of CD4+CD25-. This control condition ensured that the suppression was not due to the increasing number of cells/well with higher ratios Treg:Teff, with subsequent IL-2 consumption in the medium. At day 5, wells were pulsed with 1 µCi/well [3H] thymidine. In parallel, supernatants were harvested and stored at -20°C for subsequent cytokine analysis. After 16 hours, cells were harvested and [3H] thymidine uptake was detected. Cell proliferation was measured as counts per minute (cpm). Percent suppression was calculated using the following formula: [1-(cpm Teffs co-cultured with Tregs/cpm Teffs co-cultured with CD4+CD25- cells)] x 100. The mean suppressive capacity was calculated as the mean of five percent suppression values calculated at different Treg:Teff ratios.

As the suppression calculated at the ratio Treg:Teff 1:1 was the closest to the mean suppressive capacity, we used the supernatants harvested from that condition to quantify cytokines. Cytokine concentration were quantified using the Human T Helper Cytokine Panel (13-plex) kit (LEGENDplex, BioLegend) according to the manufacturer's instructions. The following cytokines were measured: IL-5, IL-13, IL-2, IL-6, IL-9, IL-10, IFN-γ, TNF-α (tumor necrosis factor–α), IL-17A, IL-17F, IL-4, and IL-22. IL-17F and IL-4 had low concentrations and therefore are not shown.

3.6 Next generation TCR Vβ-chain sequencing

Tregs (CD4+CD25+CD127lo) and Teffs (CD4+CD25-) were isolated from 9 patients with RRMS and 3 HDs as described above and cryopreserved. We extracted DNA from 50,000 to 100,000 cells with QIAamp® DNA Mini kit (QIAGEN) according to the manufacturer's

instructions. NanoDrop ND-1000 spectrophotometer was used to measure DNA quantity and purity. TCR Vβ library preparation and sequencing were performed at Adaptive Biotechnologies (Seattle, WA, USA) using the immunoSEQ platform. This assay employs a bias-controlled multiplex PCR to amplify genomic DNA extracted from immune cells and generate sequences of TCR genes *(118)*. We used TCRB assay at survey level. Diversity metrics and number of overlapping nucleotide sequences were estimated using immunoSEQ™ ANALYZER 3.0. The following applications were used:

- rearrangement details and top rearrangements: give information for each rearrangement present in a sample and identifies the most abundant clones;
- track rearrangements, combined rearrangements, pair-wise scatter plot, sample overlap, and Venn diagram: display the frequency of selected rearrangements across multiple samples, allows to find individual clones shared between samples or exclusive to one sample;
- gene usage: shows the V or J usage among the rearrangements present in a sample, can be compared between two samples;
- CDR3 length: it is Gaussian-like in a polyclonal sample. If a clone is expanded the corresponding CDR3 sequence shows a higher frequency;
- differential abundance: identifies rearrangements significantly increased or decreased in frequency between two samples;
- diversity metrics: diversity is considered as number of unique receptors (richness) and their relative abundance (evenness). Whereas a monoclonal sample has a very skewed distribution of frequencies, with more variation in abundance, a polyclonal sample is more even, as every rearrangement is present nearly at the same frequency. Several metrics are available, such as Pielou evenness, Simpson clonality, and clone distribution slope.

The diversity of Treg TCRs overlapping with Teffs as compared to the non-overlapping ones was calculated using the Simpson function in the vegan package in R (R Core Team, 2022). RNA was purified from T cells clones (TCCs) using QIAzol Lysis Reagent (QIAGEN) and isolated using the PicoPure RNA Isolation Kit (Life Technologies) according to the manufacturer's instructions. TCR Vαβ library preparation, sequencing and data analysis were performed at CD Genomics (Shirley, NY, USA). The 5' Rapid Amplification of cDNA Ends (5' RACE) approach was used for library construction. MiXCR software was employed to

obtained quantitated clonotypes from raw sequences. TCRs defined on the basis of amino acid sequences were searched in the publicly available databases mentioned above.

3.7 RNA extraction, sequencing and analysis

Whereas the genome is static, the transcriptome, which is the set of all RNA molecules transcribed in a cell population, is dynamic, can be influenced by experimental conditions, and is quantitative *(131)*. RNA sequencing (RNA-seq) is a revolutionary tool for transcriptomics, as it allows to generate millions of sequences in short time at low costs. In particular, third-generation technologies do not require amplification, and allow sequencing on single molecules, with long reads and low number of reads *(131)*. The basic work-flow of RNA-seq includes the following steps: RNA extraction, mRNA enrichment, conversion of mRNA to cDNA, preparation of a library with adapters, library denaturation, generation of reads, and analysis *(131)*. Purified Tregs (CD4+CD25+CD127lo) were separated by fluorescence-activated cell sorting (FACS) into t-Tregs (CD45RA+GPA33+) and p-Tregs (CD45RA-GPA33-) using SH800S Cell Sorter (Sony). RNA was purified using QIAzol Lysis Reagent (QIAGEN) and isolated using the PicoPure RNA Isolation Kit (Life Technologies) according to the manufacturer's instructions. It is known that the sorting process induces cellular stress and reduces T cell viability, leading to RNA degradation *(132)*. Despite immediate cell lysis and protein denaturation, final RNA concentrations were found to be less than expected. Thus, the libraries were prepared with the kit SMARTer Stranded Total RNA-Seq Kit v2 (Takara). RNA sequencing (RNAseq) was performed using Illumina’s NovaSeq 6000 at the Functional Genomics Center Zurich. The raw reads were first cleaned by removing adapter sequences, trimming low quality ends, and filtering reads with low quality (phred quality <20) using Fastp. Sequence pseudo alignment of the resulting high-quality reads to the human reference genome (build GRCh38.p13) and quantification of gene level expression were carried out using Kallisto *(133)*. The differential expression analysis was performed using DESeq2 *(134)*. By differential expression analysis, the difference in read counts between experimental conditions was assessed. Log2 ratio indicates the fold-change in gene expression. Differentially expressed genes (DEGs) between two samples were represented as comparison of average expression, Volcano-plot, or Heatmap of top DEGs. Whereas the first two combine threshold of p-values and fold-change to define set of DEGs,

the third one is a rank-based method *(131)*. Genes were considered differentially expressed when the false discovery rate (FDR) was <0.05. The FDR was calculated adjusting the p-value for multiple hypothesis testing. Gene Ontology (GO) functional database was consulted to explore DEGs. There were three GO domains: molecular function (MF), biological process (BP), and cellular component (CC). Genes can have multiple annotations. If more DEGs than expected belong to the same pathway, probably that pathway plays a role in the tested condition. The overrepresentation analysis identified these pathways. Gene set enrichment analysis (GSEA) determined whether a set of genes was randomly distributed or was overrepresented at the extremes, in a list of genes ranked according to their differential expression *(131)*. In contrast to bulk RNA-seq, which cannot capture the differences at the cellular level, single-cell RNA-seq reveals the molecular identity of each cell, resolves heterogeneous cell populations, and allows trajectory analysis and spatial transcriptomics *(131)*. The basic work-flow of RNA-seq includes the following steps: cell isolation from tissues with microfluidics or nanodroplets systems, barcoding of individual cells and transcripts with unique cell and molecule identifiers, cell lysis for RNA extraction, generation and amplification of cDNA, sequencing and data analysis *(131)*. Clustering are obtained by grouping cells with similar gene expression profiles. Using trajectory analysis it is possible to order the cells along a developmental path. However, sc-RNA-seq is still ten times more expensive than bulk RNA-seq, and allows to analyse a limited number of cells (around 10,000). Thus, we preferred bulk RNA-seq to analyze t-Tregs and p-Tregs in MS patients as compared to healthy controls (see below).

3.8 Tetramer constructs and assembly

Tetramer constructs were provided by from F. Momburg, DKFZ. Monomeric MHC-II molecules (HLA-DRB1*15:01 tethered with MBP 83-99) were coupled to streptavidin Alexa-647 (SA-647) in 100 µl of phosphate-buffered saline (PBS). Coupling was performed by stepwise incubation of monomers with 0.2 ug/µl SA-647 in PBS five times x 10 minutes, protected from light. The final solution was applied on T cells. Around 3-5 x 10^4 cells/well were incubated in a 96 well flat-bottom plate with Dasatinib (50nM) for 30min prior to and during labelling with tetramers. After 30 minutes, an aliquot of assembled tetramers, typically 0.3-0.6 µg were added to cells and incubated for 30 minutes at 37°C. Then, 0.5 µl magnetic

beads/well were added and incubated for 30 more minutes. After that the plate was transferred on ice for 30 minutes prior to staining and FACS analysis. As negative controls we used a tetramer composed of a HLA-DRB1*15:01 molecule tethered with the CLIP peptide and coupled to SA-647 and beads couples to anti-mouse IgG, respectively.

3.9 Statistics

Statistical analysis was performed by using GraphPad Prism 9.0 (GraphPad Software, La Jolla, CA). To test whether the data followed a Gaussian distribution we performed the D'Agostino-Pearson omnibus normality test. We employed unpaired t test to analyse two sets of data with a normal distribution and Mann-Whitney U test to analyse two sets of data with a non-normal distribution. We used one-way ANOVA test to compare more than two sets of data with a normal distribution and Kruskal-Wallis test to compare more than two sets of data with a non-normal distribution. Following the global test, we corrected for multiple comparisons using Tukey and Dunn's statistical hypothesis testing, respectively. To test whether two categorial variables were related we adopted the Chi-square test of independence. Correlations were assessed with Spearman correlation analysis. One-tailed P values were significant if the slope was significantly non-zero and, together with the goodness of fit (r^2), were used to define the correlation. Overall, p values were considered significant when equal or less than 0.05. Only statistically significant p values are reported.

3.10 Study approval

Samples were collected in the context of previous research projects which had been approved by the Cantonal Ethical Committee of Zurich, Switzerland (EC-No. 2013-0001 and EC-No. ERC 2014-0699). All study participants had given their written informed consent to use their samples for research prior to inclusion in the study. The study was conducted according to Declaration of Helsinki principles.

4.0 RESULTS

4.1 Treg isolation and culture

When Tregs are selected, the isolation method and the stringency of selection influence the purity of the population *(38)*. By using EasySep™ Human CD4+CD127loCD25+ Regulatory T cell Isolation kit, we obtained reproducible results and the purity of the final isolated fraction, calculated as Treg content (CD3+CD4+CD25+CD127loFOXP3+), was around 80% (Figure 5). The percentage of Tregs isolated from the initial number of PBMCs was around 0.5-1% (data not shown).

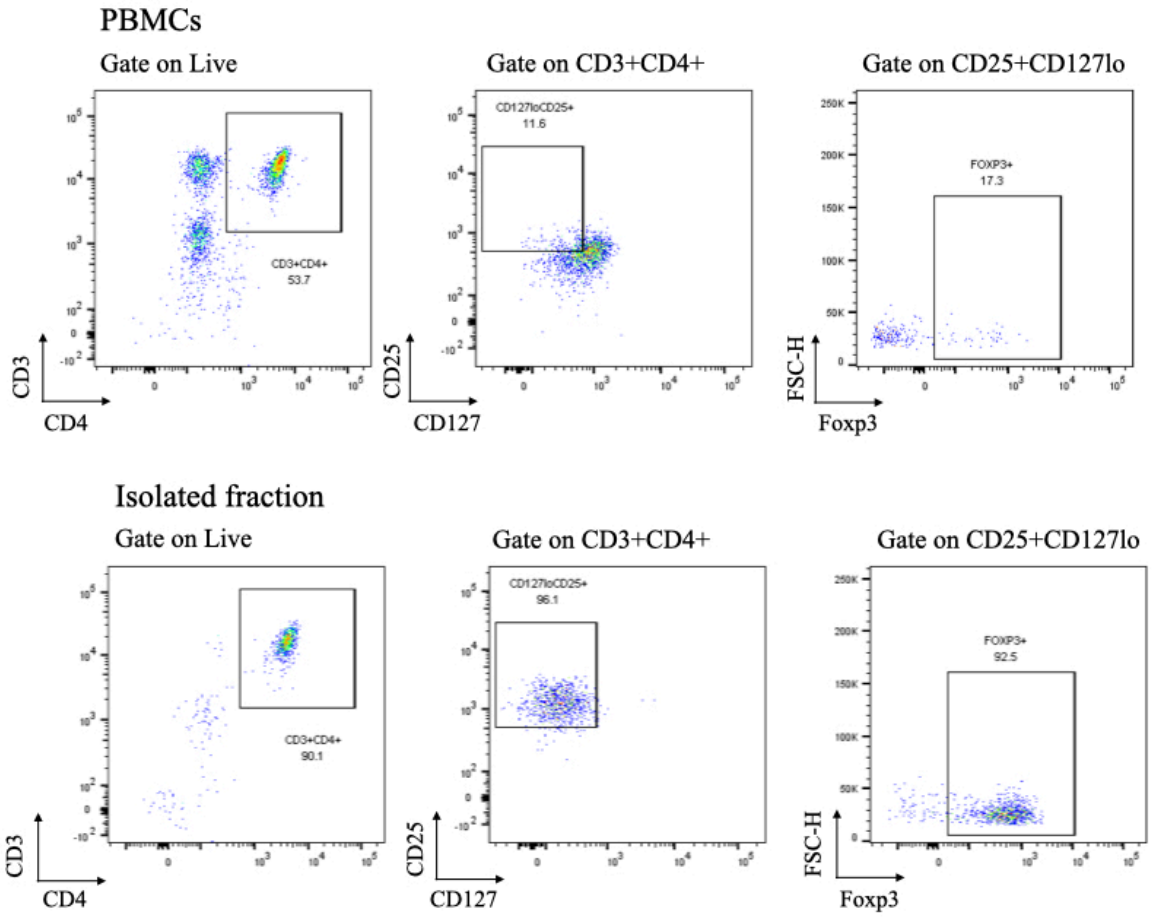

Figure 5. Representative experiment showing CD25+CD127loFoxp3+ enrichment after isolation using EasySep™ Human CD4+CD127loCD25+ Regulatory T cell Isolation kit.

As Tregs grow slowly and culture conditions favour the expansion of Teffs *(130)*, we found that the expression of Foxp3 in the isolated population tended to decrease in long-term cultures. When Tregs were expanded with PHA and IL-2, the frequency of Foxp3+ cells in CD25+CD127lo fraction was around 95% at day 7 and 10% at day 14 (Figure 6 and 7). For

this reason, it is preferable to keep Tregs in short-term culture, unless they are periodically enriched by sorting *(130)*. It has been shown that rapamycin inhibits the mammalian target of rapamycin (mTOR). Therefore, it blocks T cell cycle progression after activation, promotes TCR-induced T cell anergy even in the presence of costimulation, and allows induction of tolerance *(130, 135)*. This tolerance is induced by selective expansion of Tregs which suppress proliferation of Teffs *(135)*. For this reason, it is used to expand Tregs for ex vivo cellular therapy *(135)*. By adding rapamycin to T cell medium with IL-2 we observed an increased Foxp3 expression in expanded Tregs. At day 11 after stimulation, the frequency of Foxp3+ cells in CFSElo fraction was 34.6% without and 55.7% with rapamycin (Figure 6). However, we observed that rapamycin slightly decreased Treg viability, as shown by a reduced percentage of total and CFSElo lymphocytes, respectively (Figure 6).

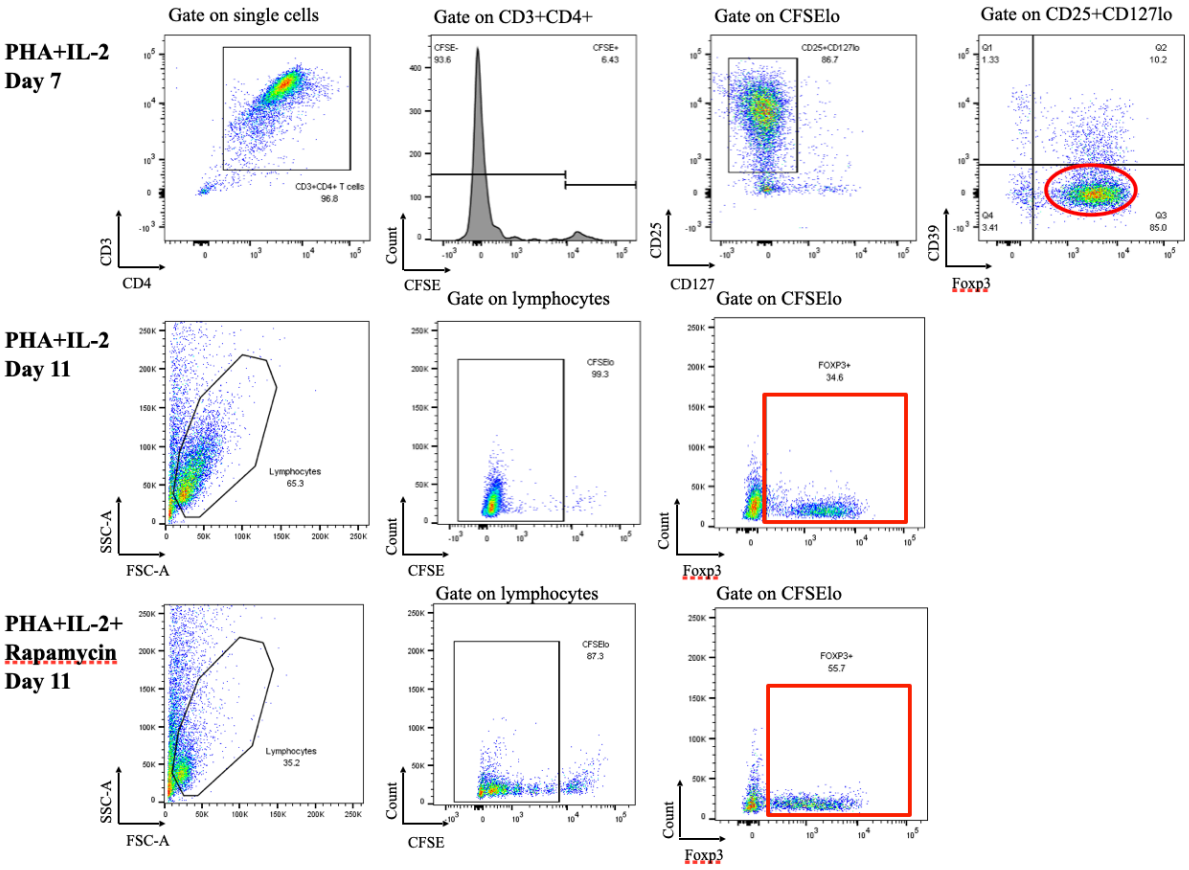

Figure 6. Generation of Treg cell lines. The loss of Foxp3 expression after 11 days of expansion is partially prevented by Rapamycin.

As an alternative approach, we added IL-7 to Treg culture. It has been shown that IL-7 enhances Treg survival, stabilises Treg molecular signature, increases surface expression of

CD25, and improves IL-2 binding of Tregs, thus reducing Teff proliferation *(136)*. However, we observed that, after 14 days of expansion, like rapamycin, it enhanced Foxp3 expression while diminishing Treg viability, as shown by reduced frequency of Tregs within CD3+CD4+ fraction (Figure 7). We found that at day 14 the percentage of Foxp3+ cells in Tregs was 10.1% with IL-2 and 70% with IL-7. Interestingly, with the combination of IL-2 and IL-7 the frequency of Foxp3+ cells in Tregs was 16% (Figure 7).

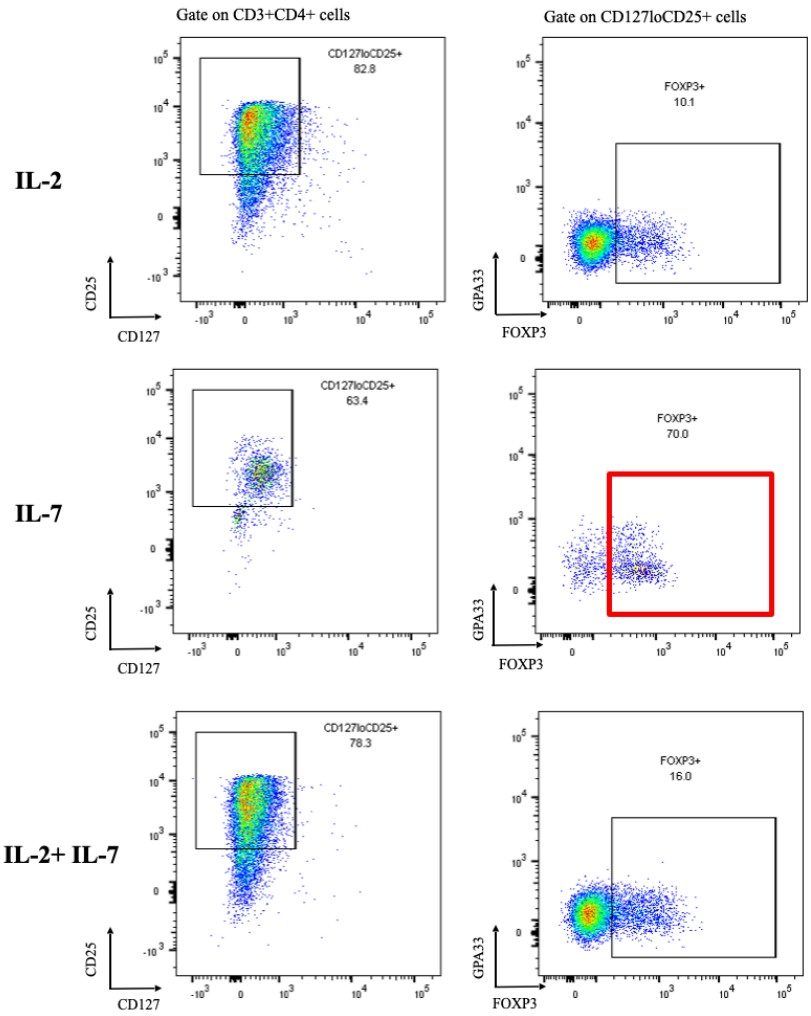

Figure 7. Generation of Treg cell lines. The loss of Foxp3 expression after 14 days of expansion is partially prevented by IL-7.

4.2 Tregs and Teffs differ for their activation profile under polyclonal or antigen-specific stimulation

CD45RA-depleted PBMCs include monocytes and memory T cells, but not naïve T cells and B cells. When an antigen is provided monocytes exploit their antigen presenting cell function.

In the memory repertoire, T cells specific for recall antigens are clonally expanded and frequent, while T cells specific for primary antigens are absent *(137)*. By contrast, in the naïve repertoire T cells specific for primary and recall antigens have been estimated to have a frequency ranging from 5 to 170 cells per 10^6 naïve T cells *(137)*. Thus, the depletion of CD45RA+ cells is supposed to enrich the population of potentially antigen specific T cells. Furthermore, in patients with MS, the depletion of B cells reduces T cell autoproliferation *(13)*. CD45RA-depleted PBMCs from three patients with MS were stimulated with MBP at a final concentration of 10 µM. At day 7 cells were analysed by flow cytometry. Whereas memory CD4+ T cells from patient 1 showed no reactivity to MBP, memory CD4+ T cells from patient 2 showed a proliferative response that appeared as CFSE dilution (Figure 8). As Tregs are hypoproliferative *in vitro (130)*, we used a readout alternative to proliferation to evaluate their response to autoantigens. Furthermore, under activation Teffs express Treg markers, such as CD25 and CD127lo, and are difficult to distinguish from Tregs (Figure 8).

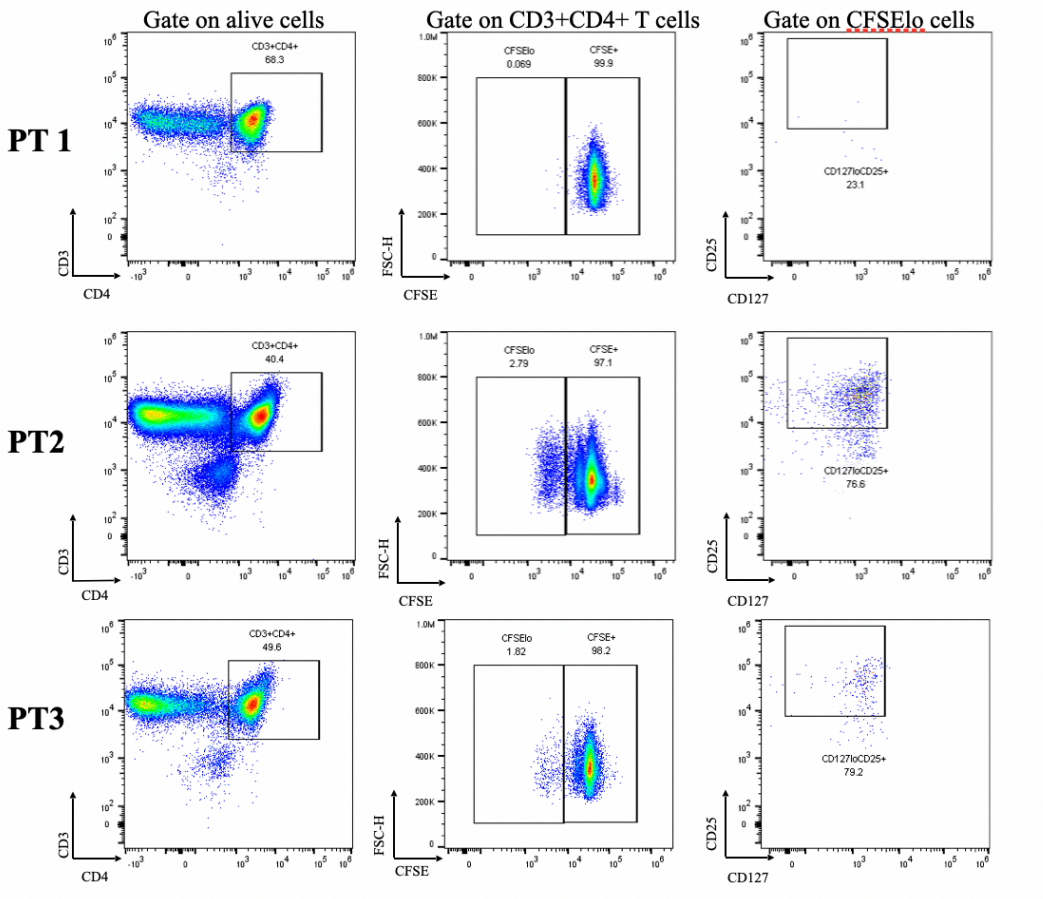

Figure 8. Teff proliferation and activation following stimulation with MBP in three patients with MS.

Thus, we evaluated Treg response based on upregulation of activation markers. The most commonly used activation markers for CD4+ T cells are ICOS, HLA-DR, CD25 (not shown), CD69, CCR4, CD80, and CD86 (Figure 9). Each marker has a different expression kinetics, for instance CD69 is considered an early activation marker, as its expression is maximal 12-24 hours after stimulation (Figure 9). In order to select activation markers specific for Tregs, we analysed the expression of several surface markers after polyclonal stimulation. We found that CD137 was specific for activated Tregs, as it was upregulated by Tregs, but weakly expressed by Teff, under stimulation (Figure 9).

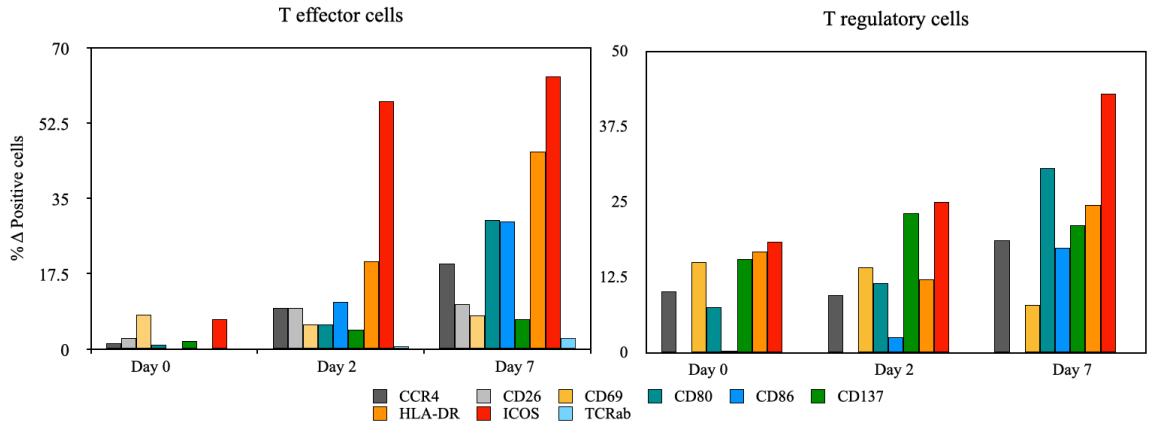

Figure 9. Following polyclonal stimulation (with anti-CD3 and anti-CD28 beads), Tregs and Teffs differ in their activation kinetics.

Isolated CD25+CD127lo T cells from three patients with MS were stimulated with autologous monocytes pulsed with MBP at a final concentration of 10 μM. At day 7 cells were analysed by flow cytometry. Whereas around 5% of Tregs from patient 2 reacted to MBP, as demonstrated by upregulation of CD137 and ICOS, in patient 1 and 3 Treg response to MBP was barely detectable (Figure 10). This finding demonstrates the high interindividual variability in both Treg and Teff in response to MBP. Despite not tested in this experiment, we then used the expression OX40, together with CD137, to identify activated Tregs (see below).

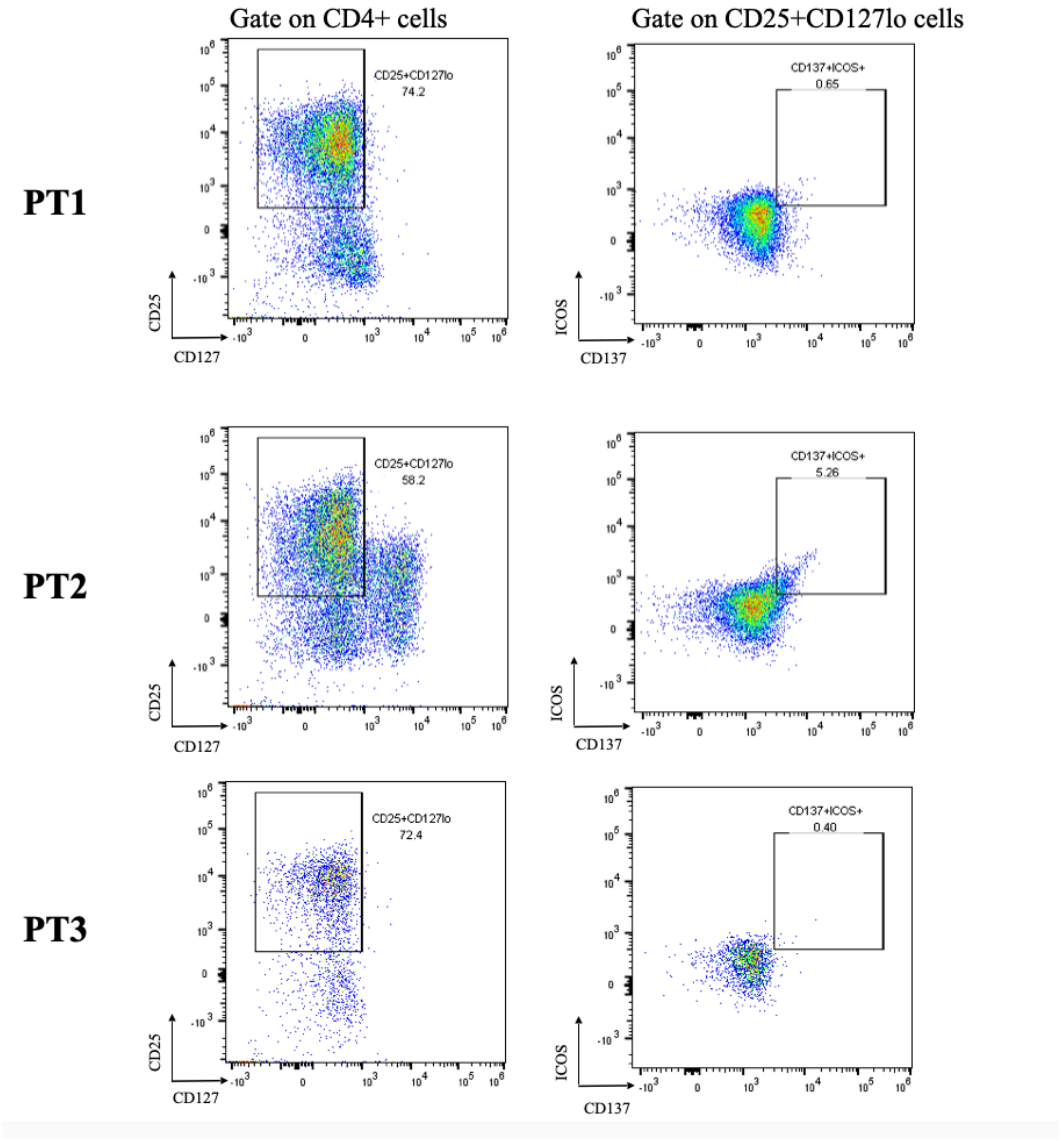

Figure 10. Treg activation following stimulation with MBP in three patients with MS.

Having obtained TCCs from CFSElo T effector cells after stimulation of CD45RA-PBMCs from patient 2 (Figure 8), we tested whether they reacted to MBP. TCC1 was confirmed to be specific for MBP, as demonstrated by [3H] thymidine incorporation assay (Figure 11). By contrast, TCC2 did not react to the stimulation with MBP and might have been obtained from bystander Teff activation (Figure 11).

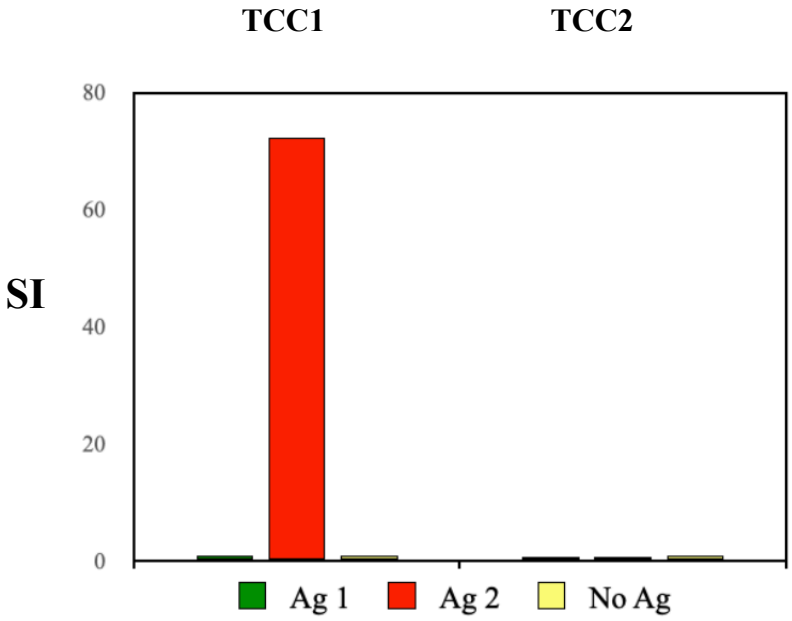

Figure 11. Thymidine incorporation assay following antigen-specific stimulation. In contrast to TCC2, TCC1 is specific for MBP (Ag 2), but not for MOG (Ag 1). SI indicates the ratio of cpm in the presence of the antigen versus cpm in the unstimulated control.

4.3 Evaluation of Treg suppressive capacity

Besides the classical *in vitro* suppression assay based on [3H] thymidine incorporation, an approach that is considered more precise is based on the labelling of Teffs with CFSE. CD4+CD25- Teffs isolated from a healthy donor were stimulated polyclonally in absence or presence of autologous Tregs at ratio 1:1. After 5 days cells were analysed by flow cytometry. Only one division cycle could be visualised when Teffs were stimulated in absence of Tregs (Figure 12). In Treg:Teff co-culture the frequency of dividing Teffs was lower and an increased proportion of cells was CFSEhi (Figure 12). However, we could not clearly distinguish between dividing Teffs and Tregs, both CFSElow (Figure 12). It has been described that Tregs derived from patients with MS have a reduced capacity to suppress Teffs stimulated with MOG *(81)*. However, due to the low frequency of circulating myelin-specific Teffs, it has been suggested that a high number of Teffs and Tregs would be needed to detect antigen specific responses in a co-culture approach *(138)*.

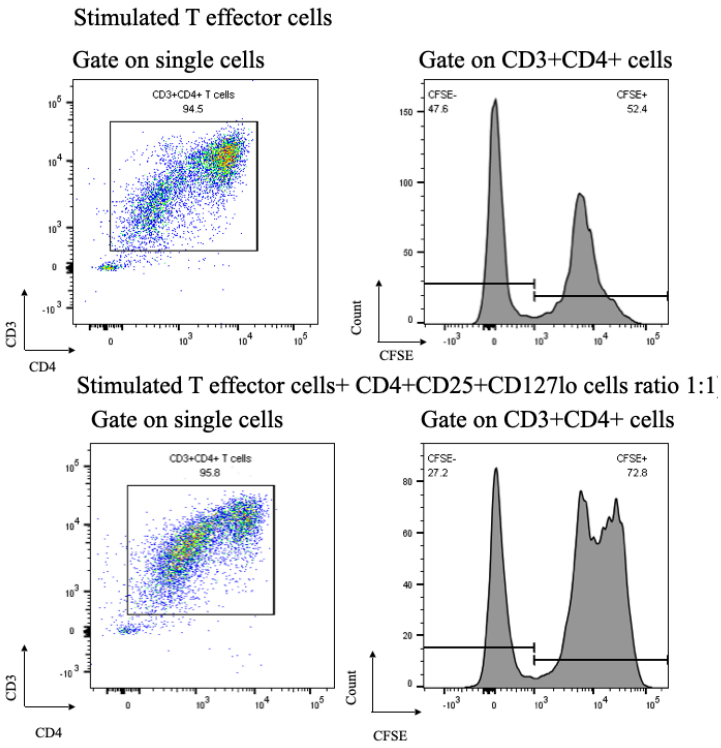

Figure 12. Teff proliferation after stimulation in absence or presence of Tregs (ratio 1:1) quantified by CFSE dilution in a healthy donor.

4.4 Phenotypic Treg alterations in patients with MS

We used flow cytometry to assess Treg frequency and phenotype in a cohort of 57 individuals. Patients with RRMS included untreated (UNT, n=19), natalizumab-treated (NAT, n=12), and anti-CD20-treated (a-CD20, n=10) patients. The control group was composed of 16 HDs. Untreated patients had either never been treated with immunomodulatory drugs, but were shortly after blood collection started on treatment, or were clinically stable after receiving the base therapy, but had not been treated in the last three months. Natalizumab-treated and a-CD20-treated patients had been on treatment since 18.6 and 14.4 months on average, respectively. The sex ratio was not significantly different between patients and HDs (chi-square test of independence). The mean age at the time of blood collection ranged from 35.3 in HDs to 40.7 years in a-CD20-treated patients and did not differ significantly among groups (one-way ANOVA). The percentage of HLA-DRB1*15:01 positive individuals was 9.1% among HDs, while it was 76% among patients, confirming the known positive association between MS and HLA-DRB1*15:01 (p=0.002, Chi-square t test of independence). Additional clinical and laboratory information is provided in Table 9 and 10. The gating strategy is

described in Figure 13A. Generally, the term Tregs was used to refer to CD25+CD127lo T cells.

We initially compared patients and HDs. Patients with MS displayed a reduced frequency of CD3+CD4+ cells (p=0.03. Figure 13B). The proportion of Tregs within this subset was comparable to the percentage observed in HDs, but the variation was greater in patients (Figure 13C). Nevertheless, the frequency of Foxp3+ cells in Tregs was significantly lower in patients (p=0.001. Figure 13D). We evaluated CD127 expression on Tregs gating on CD25+Foxp3+ T cells. Hence, we found an increased expression of CD127 in this fraction in patients (p=0.032. Figure 13E). Furthermore, the frequency of CD39+ cells in Tregs was increased in patients (p=0.038. Figure 13F). The expression of the adhesion molecules CD103 and CD49d was measured as MFI. Whereas the MFI of CD103 was not significantly different (Figure 13G), we detected a lower MFI of CD49d on Tregs in patients (p=0.045. Figure 13H).

Next, to understand whether patients displayed differences in Treg phenotype related to the treatment, we performed a multiple comparison between untreated, natalizumab-treated ad a-CD20-treated patients. Only parameters showing a significant difference between patients and HDs were considered. We found that a-CD20-treated patients had a decreased percentage of Foxp3+ Tregs (p=0.001. Figure 13I) and an increased expression of CD127 on CD25+Foxp3+ T cells (p=0.02. Figure 13L) as compared to untreated patients. It has been shown that natalizumab induces internalization and degradation of CD49d on circulating lymphocytes and does not bind in a competitive manner with the anti-CD49d antibody used for staining *(91)*. Accordingly, we observed a lower MFI of CD49d on Tregs in natalizumab-treated patients than in untreated and a-CD20-treated patients (p=0.011 and p=0.03, respectively. Figure 13H). We did not find any difference in frequency of CD3+CD4+ and CD39+ Tregs within groups of MS patients (Figure 14).

Thus, an altered Treg immunophenotype is observed in patients with MS.

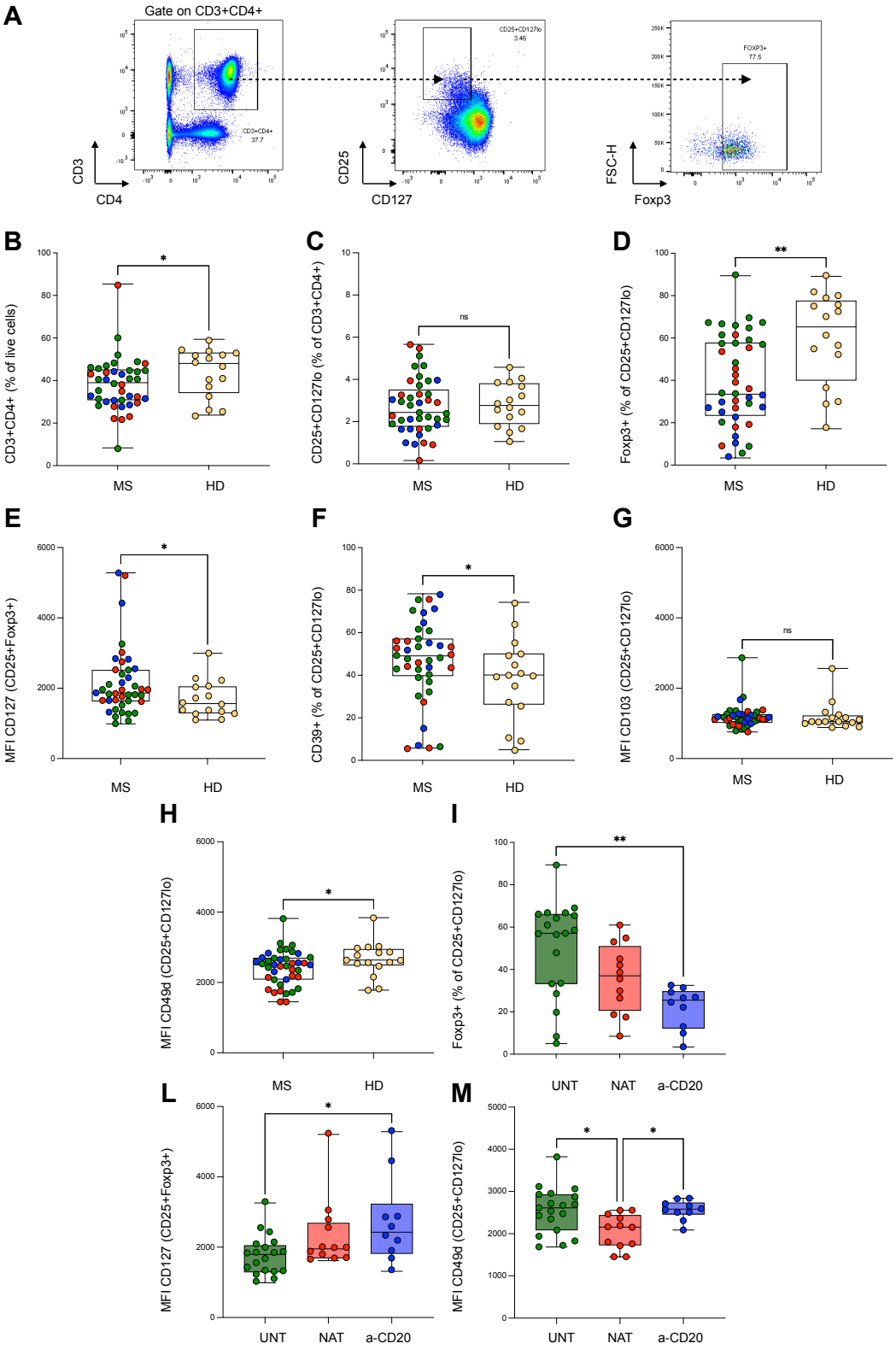

Figure 13. Treg phenotype in patients with RRMS and HDs. (A) Gating strategy for Treg immunophenotyping. Tregs were defined as CD25+CD127lo gated on CD3+CD4+ cells. The expression of Foxp3, CD39, CD49d, CD103 was evaluated on this subset as percentage of positive cells or MFI (only Foxp3 expression is shown). **(B-H)** Patients with MS (MS) were

compared to HDs (HD). Patients included untreated (green), natalizumab- (red), and a-CD20-treated (blue). **(B-C)** Frequency of CD3+CD4+ cells and Tregs. **(D)** Frequency of Foxp3+ cells in Tregs. **(E)** The expression of CD127 was analyzed on CD25+Foxp3+ cells and is reported as MFI. **(F)** Percentage of Tregs expressing CD39. **(G-H)** MFI of CD103 and CD49d on Tregs. **(I-M)** Multiple comparison between untreated (UNT), natalizumab-treated (NAT) and a-CD20-treated patients (a-CD20). Frequency of Foxp3+ cells in Tregs and MFI of CD127 and CD49d on Tregs are shown, respectively. **(B-M)** Dots represent frequency of each donor, boxes extend from the 25th to 75th percentiles, and whiskers from min to max. The line in the middle of the box is the median. Unpaired t test or Mann-Whitney test were used to compare two sets of data. One-way ANOVA or Kruskal-Wallis test followed by Tukey or Dunn's statistical hypothesis testing, respectively, were adopted to compare more than two sets of data. * $p<0.05$; ** $p<0.01$.

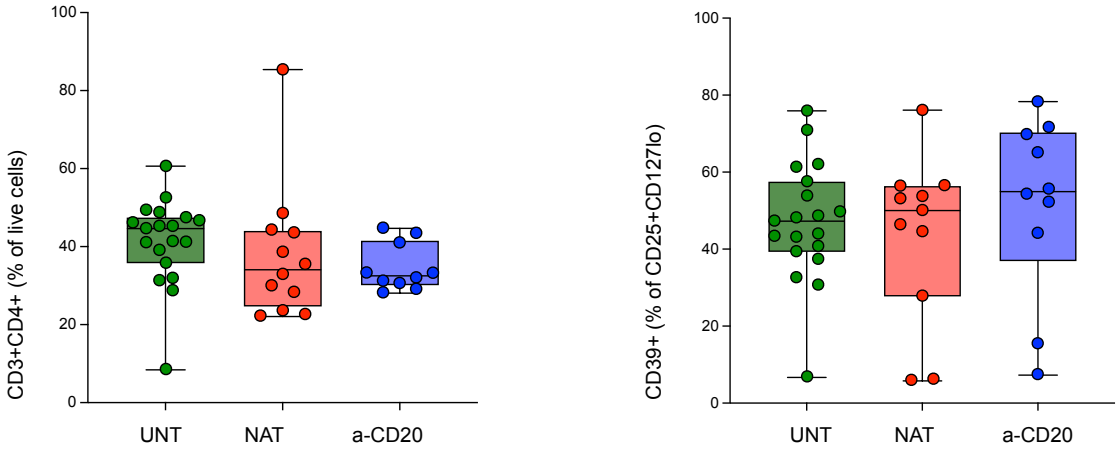

Figure 14. Multiple comparison between untreated (UNT), natalizumab-treated (NAT) and a-CD20-treated patients (a-CD20). Frequency of CD3+CD4+ cells and CD39+ Tregs are shown, respectively. Kruskal-Wallis test and one-way ANOVA were performed respectively and were not significant.

Table 9. Clinical and demographic characteristics of 41 patients with RRMS and 17 healthy donors.

Donor	Age (at blood collection)	Diagnose	Sex	Treatment duration (months)	HLA-typing	Immunophenotyping	Suppression assay	Multiplex cytokine profiling	High-throughput TCR Vβ-chain sequencing	Bulk RNA sequencing
UNT_01	40	RRMS	F	NA	DRB1*15:01 POS	✓	✓	✓	✗	✗
UNT_02	26	RRMS	F	NA	DRB1*15:01 POS	✓	✗	✗	✗	✗
UNT_03	21	RRMS	F	NA	NA	✓	✗	✗	✗	✗
UNT_04	27	RRMS	M	NA	DRB1*15:01 POS	✓	✓	✗	✓	✓
UNT_05	25	RRMS	F	NA	DRB1*15:01 POS	✓	✓	✗	✗	✗
UNT_06	50	RRMS	F	NA	DRB1*15:01 NEG	✓	✓	✗	✓	✓
UNT_07	32	RRMS	F	NA	NA	✓	✓	✓	✗	✗
UNT_08	28	RRMS	F	NA	NA	✓	✓	✓	✗	✗
UNT_09	35	RRMS	F	NA	NA	✓	✓	✓	✗	✗
UNT_10	48	RRMS	M	NA	DRB1*15:01 POS	✓	✓	✗	✓	✓
UNT_11	53	RRMS	F	NA	NA	✓	✗	✗	✗	✗
UNT_12	47	RRMS	M	NA	DRB1*15:01 POS	✓	✗	✗	✗	✗

UNT_13	48	RRMS	F	NA	NA	✓	✗	✗	✗	✗
UNT_14	40	RRMS	F	NA	DRB1 *15:01 POS	✓	✓	✓	✗	✗
UNT_15	26	RRMS	F	NA	DRB1 *15:01 NEG	✓	✓	✓	✗	✗
UNT_16	48	RRMS	M	NA	DRB1 *15:01 NEG	✓	✓	✗	✗	✗
UNT_17	37	RRMS	F	NA	DRB1 *15:01 NEG	✓	✗	✗	✗	✗
UNT_18	38	RRMS	F	NA	DRB1 *15:01 POS	✓	✗	✗	✗	✗
UNT_19	33	RRMS	M	NA	DRB1 *15:01 POS	✓	✓	✓	✗	✗
19	**37**	**RRMS**	**14 F/ 5 M**	**NA**	**9 DRB1 *15:01 POS/ 4 NEG**	**19**	**12**	**7**	**3**	**3**
NAT_01	30	RRMS	F	7	NA	✓	✗	✗	✗	✗
NAT_02	32	RRMS	F	12	DRB1 *15:01 POS	✓	✓	✓	✓	✓
NAT_03	46	RRMS	F	23	NA	✓	✓	✓	✗	✗
NAT_04	25	RRMS	M	10	DRB1 *15:01 POS	✓	✓	✓	✗	✗
NAT_05	33	RRMS	M	9	DRB1 *15:01 POS	✓	✓	✓	✓	✓
NAT_06	43	RRMS	M	31	DRB1 *15:01 POS	✓	✓	✓	✗	✗
NAT_07	38	RRMS	M	7	DRB1 *15:01 POS	✓	✓	✗	✗	✗

NAT_08	29	RRMS	M	19	DRB1 *15:01 POS	✓	✓	✗	✓	✓
NAT_9	36	RRMS	F	51	DRB1 *15:01 POS	✓	✓	✓	✗	✗
NAT_10	42	RRMS	F	10	NA	✓	✓	✓	✗	✗
NAT_11	47	RRMS	M	25	DRB1 *15:01 NEG	✓	✓	✓	✗	✗
NAT_12	40	RRMS	F	NA	DRB1 *15:01 POS	✓	✗	✗	✗	✗
12	**37**	**RRMS**	**6 F/ 6 M**	**12**	**8 DRB1 *15:01 POS/ 1 NEG**	**12**	**10**	**8**	**3**	**3**
aCD20_01	29	RRMS	M	4	NA	✓	✓	✓	✗	✗
aCD20_02	49	RRMS	F	1	DRB1 *15:01 POS	✓	✓	✓	✗	✗
aCD20_03	49	RRMS	M	NA	NA	✓	✓	✓	✗	✓
aCD20_04	46	RRMS	F	11	NA	✓	✓	✓	✓	✗
aCD20_05	35	RRMS	F	24	DRB1 *15:01 NEG	✓	✓	✓	✓	✓
aCD20_06	33	RRMS	M	6	NA	✓	✓	✓	✗	✗
aCD20_07	25	RRMS	M	3	NA	✓	✓	✓	✗	✗
aCD20_08	35	RRMS	F	52	NA	✓	✓	✓	✓	✓
aCD20_09	62	RRMS	M	NA	NA	✓	✗	✗	✗	✗

aCD20_10	44	RRMS	F	NA	DRB1 *15:01 POS	✓	✗	✗	✗	✗
10	**39.5**	**RRMS**	**5 F/ 5 M**	**6**	**2 DRB1 *15:01 POS/ 1 NEG**	**12**	**8**	**8**	**3**	**3**
HD_01	46	None	F	NA	NA	✓	✓	✓	✗	✗
HD_02	33	None	F	NA	NA	✓	✗	✗	✗	✗
HD_03	45	None	F	NA	NA	✓	✓	✓	✗	✗
HD_04	49	None	M	NA	DRB1 *15:01 NEG	✓	✗	✗	✗	✗
HD_05	28	None	F	NA	DRB1 *15:01 NEG	✓	✗	✗	✗	✗
HD_06	35	None	F	NA	DRB1 *15:01 NEG	✓	✗	✗	✗	✗
HD_07	25	None	M	NA	DRB1 *15:01 NEG	✓	✗	✗	✗	✗
HD_08	27	None	M	NA	DRB1 *15:01 NEG	✓	✓	✗	✗	✗
HD_09	25	None	F	NA	NA	✓	✓	✓	✗	✗
HD_10	47	None	F	NA	NA	✓	✓	✗	✗	✗
HD_11	37	None	M	NA	DRB1 *15:01 NEG	✓	✗	✗	✗	✗
HD_12	36	None	F	NA	DRB1 *15:01 NEG	✓	✓	✓	✗	✗
HD_13	53	None	M	NA	NA	✓	✓	✓	✗	✗
HD_14	26	None	F	NA	DRB1 *15:01 NEG	✓	✓	✗	✗	✗

HD_15	31	None	M	NA	DRB1*15:01 NEG	✓	✓	✓	✓	✓
HD_16	22	None	M	NA	DRB1*15:01 POS	✓	✓	✗	✓	✓
HD_17	35	None	M	NA	DRB1*15:01 NEG	✗	✓	✓	✓	✓
17	**35**	**None**	**9 F/ 8 M**	**NA**	**1 DRB1*15:01 POS/ 10 NEG**	**16**	**11**	**7**	**3**	**3**

Table 9: rows highlighted in bold show the summary of the characteristics of the respective group of patients or HDs.

Table 10. Immunophenotyping of 41 patients with RRMS and 16 healthy donors.

Donor	CD3+CD4+ (% of live cells)	CD25+CD127lo (% of CD3+CD4+)	Foxp3+ (% of CD25+CD127lo)	MFI CD127 (CD25+Foxp3+)	CD39+ (% of CD25+CD127lo)	MFI CD49d (CD25+CD127lo)	MFI CD103 (CD25+CD127lo)
UNT_01	46.1	3.13	66.9	1959	39.3	3120	1326
UNT_02	46.6	2.1	61	2106	57.5	3823	2870
UNT_03	41.1	1.9	66.2	2397	40.7	2879	1748
UNT_04	31.8	2.07	66.8	1286	75.9	2429	1050
UNT_05	45.2	2.23	56.9	1832	48.1	1827	790
UNT_06	49.3	2.78	58.6	987	47.3	2956	1366
UNT_07	31.2	3.72	47.9	1636	49.7	2932	1181
UNT_08	83.6	3.94	65.5	1794	37.3	1685	831
UNT_09	52.5	2.15	89.4	2056	43.1	1722	850
UNT_10	41.3	4.15	28.5	1066	32.5	2697	1220
UNT_11	48.7	2.39	33.2	1390	53.8	2717	1265
UNT_12	41	5.13	57.1	1300	30.6	2083	1092
UNT_13	45.2	3.31	83	2517	61.3	2535	935
UNT_14	35.7	4.64	19.7	1808	70.9	3065	1172
UNT_15	47.4	4.66	50	3258	43.9	2611	1360
UNT_16	44.6	1.68	69.1	1267	62	2349	1099
UNT_17	39	2.13	56.5	1515	48.6	2474	970
UNT_18	60.6	2.95	64.3	1185	43.3	2671	1084

UNT_19	28.6	2.4	33.5	1814	6.69	1939	941
NAT_01	22.5	0.16	8.5	5207	53.1	1453	757
NAT_02	44.2	1.66	17.4	2750	44.5	1801	970
NAT_03	48.5	3.3	38.6	1660	76.1	2556	1154
NAT_04	22.1	5.48	53.1	2525	5.76	2466	1219
NAT_05	32.8	3.95	61	1954	56.5	1757	924
NAT_06	43.5	5.66	54.9	1948	46.3	2150	1384
NAT_07	35.4	2.91	26.4	1842	53.7	2193	1092
NAT_08	23.5	0.91	45	1969	50	2164	1122
NAT_9	85.4	0.99	42	3017	6.1	2370	1128
NAT_10	28.2	3.02	18.6	1758	27.7	1714	1116
NAT_11	38.5	2.28	29.8	1648	56.4	2551	1154
NAT_12	29.9	3.27	35.5	1616	53.1	1453	757
aCD20_01	33.1	2.9	29.2	1865	52.2	2087	1229
aCD20_02	31.1	1	24.5	2839	71.7	2311	1194
aCD20_03	30.5	1.64	31.4	2158	69.8	2568	992
aCD20_04	33.2	3.05	3.4	5284	44.1	2505	1172
aCD20_05	31.9	1.65	32.5	1649	55.6	2841	1675
aCD20_06	40.9	0.93	26.8	2821	54.3	2710	1042
aCD20_07	28.1	2.12	22.1	2552	65.1	2508	1272
aCD20_08	44.7	1.37	12.9	4424	78.3	2828	1257

aCD20_09	43.4	1.84	9.8	1315	7.3	2594	1234
aCD20_10	29	3.97	26.5	2297	15.3	2657	1142
HD_01	50.9	1.49	17.2	2225	49.6	2546	928
HD_02	26.6	4.06	36.0	1376	4.98	1781	882
HD_03	47.1	1.06	29.4	1585	55.6	2981	1161
HD_04	25.8	2.57	51.7	1106	74.3	2867	1051
HD_05	40.9	2.67	75.2	1777	50.4	2578	1052
HD_06	52.2	3.23	56.1	1331	10.9	1823	1106
HD_07	49	4.58	89.1	1372	41.2	2640	1049
HD_08	37.6	3.68	72.1	1716	25.8	3029	2564
HD_09	52.5	3.88	81.4	2277	40.3	3845	1617
HD_10	53.4	2.86	78.5	1275	45.2	2774	1038
HD_11	54.3	3.03	69.7	1095	40	2569	996
HD_12	54.9	1.78	79.6	2058	35.3	2470	1319
HD_13	33	3.86	54.4	1269	64.3	3012	1164
HD_14	59.4	2.46	74.6	1541	39.6	2852	1246
HD_15	41.4	1.67	28.3	2995	27.6	2161	902
HD_16	23.8	2.23	60.8	2030	9.32	2636	1023

4.5 Distinct transcriptional profiles of thymus- versus peripherally-derived Tregs

Opstelten et al. previously discovered GPA33 as a cell surface marker predominantly expressed in CD4+CD25+CD45RA+ T cells as compared to their CD45RA- counterpart and CD4+CD25- T cells *(50)*. In an exemplary experiment, Tregs were isolated from a healthy donor and analysed by flow cytometry. We confirmed the previous observation, but we noted that histograms of GPA33 expression in CD45RA+ and CD45RA- Tregs partly overlapped (Figure 15A). Next, we designed a gating strategy to identify two Treg subsets. We distinguished t-Tregs, which expressed both CD45RA and GPA33 (CD45RA+GPA33+), and p-Tregs, which did not express CD45RA nor GPA33 (CD45RA-GPA33-) (Figure 15A). Aiming to apply this panel to compare the immunophenotype of patients with MS and healthy individuals, we selected 12 subjects of the cohort, including 9 patients with RRMS (3 untreated, 3 natalizumab-treated and 3 anti-CD20-treated) and 3 HDs. From these subjects we isolated t-Tregs and p-Tregs defined as above by fluorescence activated cell sorting. From these cell subsets we extracted RNA for bulk RNA sequencing. A total of 802 genes were differentially expressed between these t-Tregs and p-Tregs (False Discovery Rate<0.05). The 50 most differentially expressed genes are shown in Figure 15B. Differentially upregulated genes in t-Tregs were enriched for genes involved in transcription and translation, while in p-Tregs for genes playing a role in chemotaxis, chemokine- and cytokine-mediated signaling pathway, and immune response (Figure 15C). Whereas t-Tregs expressed higher levels of genes identifying naïve Tregs (TCF7, BACH2, LEF1, AFF3, SATB1) and implicated in recirculation through lymphoid tissues (CCR7 and CXCR5), p-Tregs upregulated migration and tissue homing genes (CCR3, CCR4, CCR6, CCR8, CCR10, ITGB1, and CXCR6). In addition, p-Tregs expressed higher levels of MHC class II genes (HLA-DRA, HLA-DPB1, HLA-DQB1), T cell activation genes (CD80 and TNFRSF9), and negative regulators of T cell response (CTLA-4, LGALS1, LGALS3, GZMA). By contrast, t-Tregs highly expressed AREG, encoding for amphiregulin, an autocrine growth factor essential for Treg function. Interestingly, p-Tregs up-regulated genes associated with Th17 lineage commitment (RORC, RORA, BATF, and IL17RB) (Figure 15D).

GPA33 is supposed to be stably expressed on t-Tregs, but was also expressed on a subset of cells among CD45RA- Treg cells (Figure 15A). It has been argued that the CD45RA-GPA33+ Treg subset might contain activated t-Tregs *(50)*. Thus, we speculated that they might be t-

Tregs that, after having migrated from the thymus to the secondary lymphoid organs, are reactivated by self-antigens. Due to the loss of cell viability after sorting, leading to RNA degradation *(132)*, we could not further investigate this hypothesis by transcriptome analysis. Collectively, these findings confirm that CD45RA and GPA33 can be used to identify two distinct subsets of Tregs, which differentially express genes related to their thymic or peripheral origin.

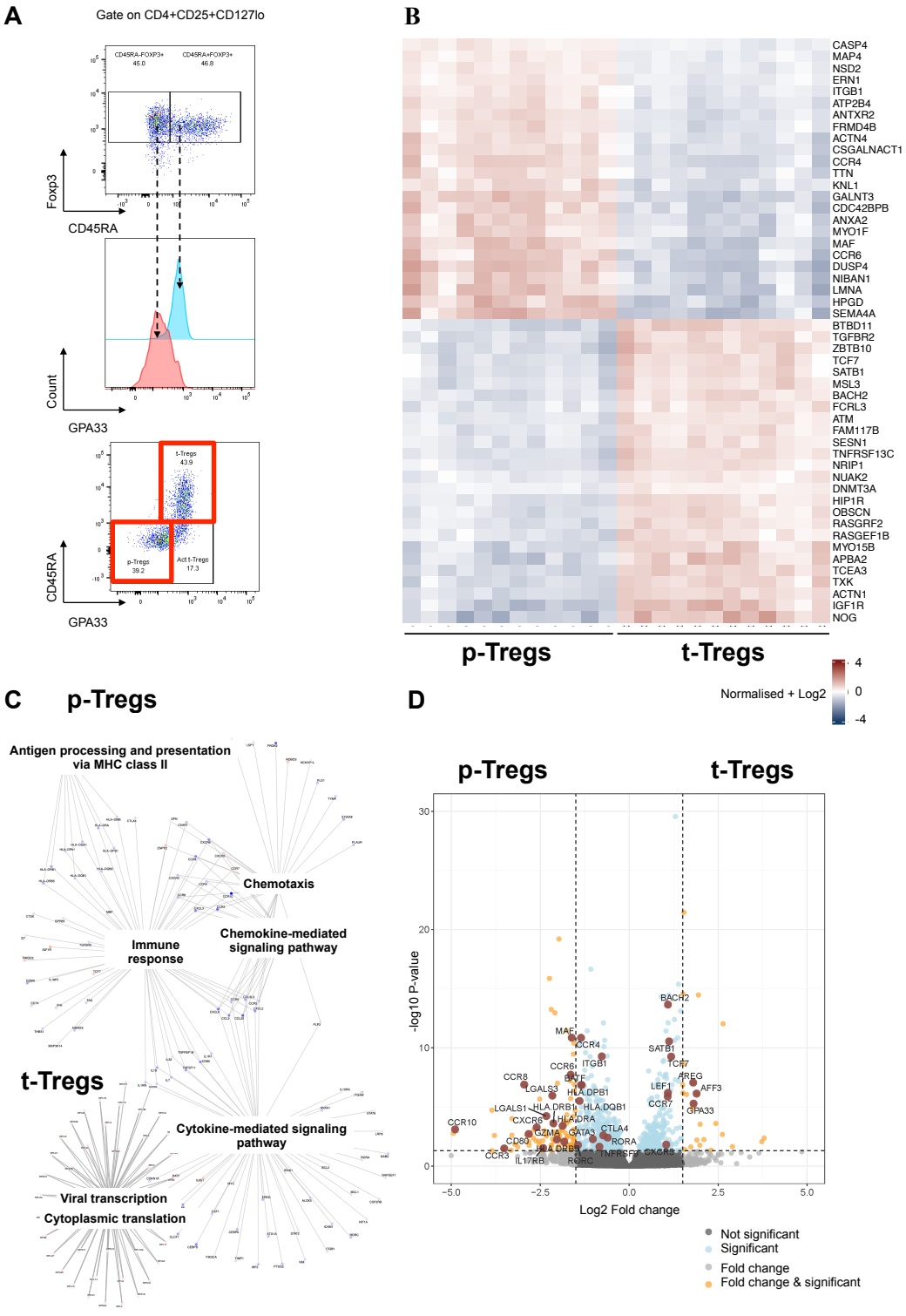

Figure 15. Transcriptome analysis of thymic- and peripherally-derived Tregs in 9 MS patients and 3 HDs. (A) Exemplary dot plots and histogram of Foxp3, CD45RA and GPA33 expression in Tregs isolated from a HD showing the gating strategy designed to define two subsets: p-Tregs (CD45RA-GPA33-) and t-Tregs (CD45RA+GPA33+). A minor cell subset was CD45RA-GPA33+. The first two subsets (red squares) were analysed by RNA sequencing. The third subset was speculated to contain activated (Act.) t-Tregs but was not further investigated by transcriptome analysis. (B) Heatmap showing the expression counts of the top 50 differentially expressed genes across t-Tregs and p-Tregs. Both positive and negative log fold changes are displayed. (C) Genes belonging to different Gene Ontology (GO) Biological Process (BP) terms were up-regulated in p-Tregs and t-Tregs, respectively. (D) Volcano plot showing genes involved in Treg homeostasis, homing, activation, and function differentially expressed between t-Tregs and p-Tregs (log2 fold change threshold > 1.5; false discovery rate <0.05).

4.6 Age-dependent altered distribution of t-Tregs in patients with MS

Previous studies have employed the expression of CD45RA, CD31 or Helios to discriminate between t-Tregs and p-Tregs *(83, 87, 50)*. To examine the relative proportion of t-Tregs and p-Tregs in patients with MS as compared to HDs, we used the gating strategy defined above (Figure 15A), based on the combination of CD45RA and GPA33. In addition, even though CD45RA-GPA33+ subset was not completely characterised, we were interested to analyse its frequency in patients and HDs.

In agreement with previous data *(83, 84)*, we found that the production of t-Tregs decreases during ageing in HDs, reflecting a progressive thymic involution (r^2=0.25, p=0.048. Figure 16A). Accordingly, p-Tregs increase (r^2=0.42, p=0.007), and CD45RA-GPA33+ t-Tregs decline with age (r^2=0.45, p=0.004. Figure 16A). In patients with MS, we observed the same trend for t-Tregs (r^2=0.1, p=0.037), and p-Tregs (r^2=0.18, p=0.005), despite the change was less evident in comparison to HDs (Figure 16A). Furthermore, we did not find a significant decline of CD45RA-GPA33+ t-Tregs with ageing in patients (Figure 16A).

Given the influence of age on Treg subset distribution, we used the median age of the cohort (37 years) as cut-off to define two age-groups. Next, we compared matched age groups of patients and HDs. We detected a decreased frequency of t-Tregs in younger (p=0.047), but not

in older patients with MS (Figures 16B and C). The percentage of p-Tregs was not significantly altered both in younger and older patients (Figures 16D and E). Moreover, in contrast to younger patients, older patients displayed an increased frequency of CD45RA-GPA33+ t-Tregs in comparison to HDs (p=0.008. Figures 16F and G). The frequency of t-Tregs in younger patients and of CD45RA-GPA33+ t-Tregs in older patients was compared between untreated, natalizumab-treated ad a-CD20-treated patients by multiple comparison analysis. However, no significant differences between treatment-groups were apparent (Figure 17). Further we wondered whether Foxp3 expression in patients with MS was equally or unevenly decreased in Treg subsets when compared to HDs. We observed that the reduction of Foxp3 expression equally affected t-Tregs, CD45RA-GPA33+ t-Tregs and p-Tregs (p=0.046, 0.011 and 0.010, respectively. Figure 16H). When we compared treatment-groups, we found that the expression of Foxp3 was especially reduced in CD45RA-GPA33+ t-Tregs and p-Tregs derived from a-CD20-treated as compared to untreated patients (p=0.007, respectively. Figure 16I).

Hence, whereas younger patients show a reduced frequency of t-Tregs, older patients display an increased frequency of CD45RA-GPA33+ t-Tregs and Foxp3 expression is consistently reduced in each subset.

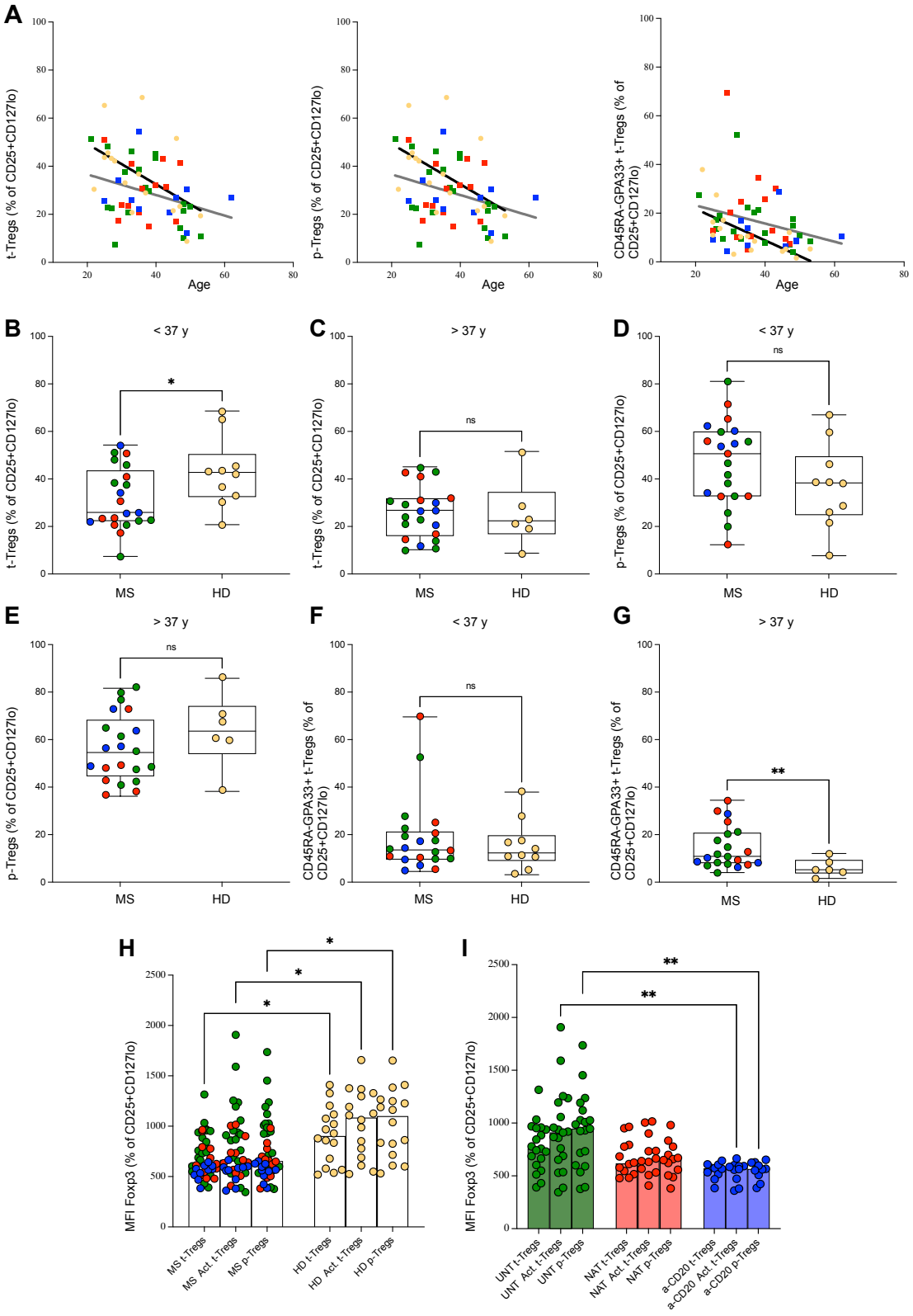

Figure 16. Balance between t-Tregs, p-Tregs, and CD45RA-GPA33+ t-Tregs in patients with RRMS. (A-H) Patients with MS (MS) were compared to HDs (HD). Patients included untreated (green), natalizumab- (red), and a-CD20-treated (blue). **(A)** Age-dependent course of t-Tregs, p-Tregs and CD45RA-GPA33+ Tregs in patients with MS (dark grey line) and

HDs (black line) (XY correlation). **(B-C)** Frequency of t-Tregs in younger and older patients, respectively. **(D-E)** Frequency of CD45RA-GPA33+ t-Tregs in younger and older patients, respectively. **(F-G)** Frequency of t-Tregs in younger and older patients, respectively. **(B-G)** Dots represent frequency of each donor, boxes extend from the 25th to 75th percentiles, and whiskers from min to max. The line in the middle of the box is the median. Unpaired t test or Mann-Whitney U test. * $p<0.05$; ** $p<0.01$. **(H)** Multiple comparison of the median MFI of Foxp3 in t-Tregs, p-Tregs, and CD45RA-GPA33+ t-Tregs between patients and HDs. **(I)** Multiple comparison of the median MFI of Foxp3 in t-Tregs, p-Tregs, and CD45RA-GPA33+ t-Tregs between treatment-groups. UNT: untreated. NAT: natalizumab-treated. a-CD20: anti-CD20-treated. **(H-I)** Scatter plot with bar graph. Kruskal-Wallis test. * $p<0.05$; ** $p<0.01$.

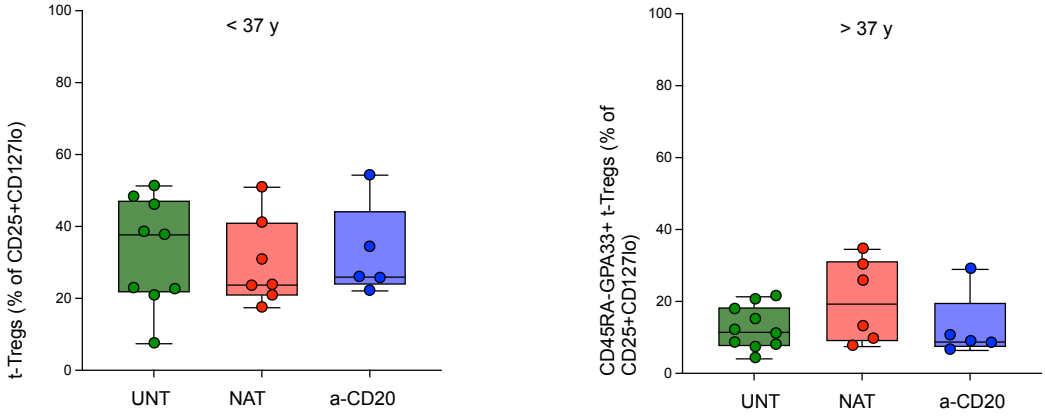

Figure 17. Multiple comparison between untreated (UNT), natalizumab-treated (NAT) and a-CD20-treated patients (a-CD20). Frequency of t-Tregs and of CD45RA-GPA33+ t-Tregs are shown, respectively. One-way ANOVA and Kruskal-Wallis test were performed respectively and were not significant.

4.7 Treg function is impaired in natalizumab-treated patients and correlates with a reduced frequency of t-Tregs

Towards the functional characterization of Tregs we performed suppression assays with Tregs (CD4+CD25+CD127lo) and T effector cells (Teffs, CD4+CD25-) isolated from 30 patients with RRMS and 11 HDs (Table 9). Suppression values were calculated at five Treg:Teff ratios (from 1:8 to 2:1) (Figure 18A). Additional details are provided in the Materials and Methods section. The mean Treg inhibitory capacity of natalizumab-treated patients was consistently

lower than in HDs and untreated and a-CD20-treated patients at several Treg:Teff ratios (Figure 18A). At ratio 1:2, the mean Treg suppressive capacity was 11.2% in natalizumab-treated patients and 34.2% in HDs. At ratio 2:1, the mean Treg suppressive capacity was 27.5% in natalizumab-treated patients and 48.1% in HDs (Figure 18A).

We further quantified cytokines in cell culture supernatants harvested from suppression assays in 24 patients with RRMS and 7 HDs (Table 9 and 11). Th1/Th2 cytokines were detected in the supernatants (Figure 18B). The mean concentration of IL-5 was 295.8 pg/mL in natalizumab-treated patients and 82.4 pg/mL in HDs. The mean concentration of IL-2 was 348.3 pg/mL in natalizumab-treated patients and 118.9 pg/mL in HDs. IFN-γ had a mean concentration of 634.8 pg/mL in natalizumab-treated patients and 281.4 pg/mL in HDs (Figure 18B).

To understand the main functional mechanisms of Tregs, we plotted the mean suppressive capacity, calculated at five Treg:Teff ratios, against the flow cytometry and cytokine secretion data using a correlation analysis (Table 12). We found a significant correlation between Treg inhibitory function and percentage of t-Tregs (r^2=0.11, p=0.038. Figure 18C). In addition, there was an inverse correlation between Treg suppressive capacity and IFN-γ concentration in supernatants (r^2=0.14, p=0.041. Figure 18D). By contrast, the correlation between Treg function and frequency of Foxp3+ cells within CD25+CD127lo fraction was not significant (Figure 18E). Moreover, the frequency of CD39+ cells within CD25+CD127lo subset was not positively correlated to Treg suppressive capacity (Table 12), but inversely correlated to the frequency of t-Tregs (r^2=0.22, p=0.003. Figure 18F).

Thus, the frequency of t-Tregs appears to be the main determinant of Treg function.

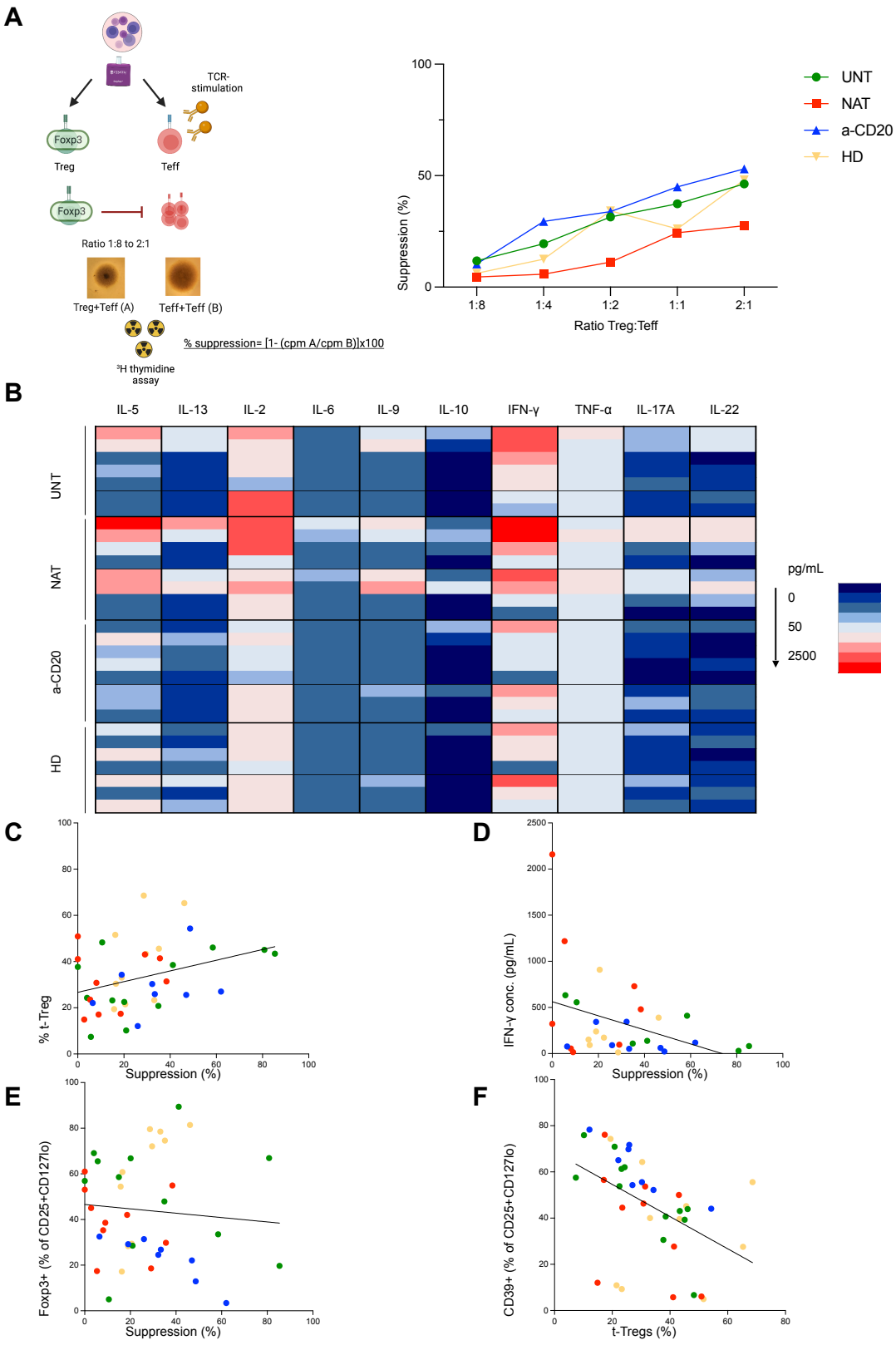

Figure 18. Determinants of Treg function in RRMS. (A) Schematic representation of suppression assay: polyclonally stimulated Teffs were co-cultured with different ratio of Tregs and the proliferation was measured at day 5. The mean Treg inhibitory capacity was calculated at five Treg:Teff ratios. UNT: untreated (green). NAT: natalizumab-treated (red). a-

CD20: anti-CD20-treated (blue). HD: healthy donor (yellow). **(B)** Concentrations of cytokines were detected in the supernatants harvested from the suppression assay at ratio Treg:Teff 1:1 by a bead-based immunoassay. Cytokine concentrations ranged from 0 (dark blue) to 2500 (dark red) pg/mL. **(C)** XY correlation between Treg suppressive capacity and frequency of t-Tregs within CD25+CD127lo subset. **(D)** XY correlation between Treg suppressive function and IFN-γ concentration in the supernatants. **(E)** XY correlation between Treg function and frequency of FOXP3+ cells within CD25+CD127lo fraction. **(F)** XY correlation between frequency of t-Tregs and CD39+ cells within CD25+CD127lo subset.

Table 11. Cytokine concentrations (pg/mL) in cell culture supernatants harvested from suppression assays.

Donor	IL-5	IL-13	IL-2	IL-6	IL-9	IL-10	IFN-γ	TNF-α	IL-17 A	IL-22
UNT_01	15.5	8.74	730.97	16.02	23.37	2.26	30.34	99.9	6.71	6.6
UNT_07	15.5	8.74	35.06	16.02	23.37	2.36	109.06	99.9	16.11	10.48
UNT_08	173.88	77.34	103.26	16.02	163.34	6.52	632.82	99.9	35.76	53.36
UNT_09	44.2	8.74	142.02	16.02	23.37	5.28	137.71	99.9	10.49	10.41
UNT_14	15.5	8.74	755.37	16.02	23.37	2.26	81.32	99.9	6.74	20.34
UNT_15	275.88	91.19	383.3	16.02	93.98	33.1	555.82	130.12	26.47	54.85
UNT_19	15.5	8.74	147.06	16.02	23.37	2.26	410.01	99.9	8.59	4.81
UNT_01	402.47	58.76	697.8	30.78	72.38	28.3	1218.63	170.14	106.8	171.47
NAT_02	15.5	8.74	132.79	16.02	23.37	2.26	16.49	99.9	2.8	3.06
NAT_03	1173.61	439.48	610.58	52.84	209.26	13.26	2159.47	99.9	178.8	111.42
NAT_04	54.83	8.74	559.15	16.02	23.37	14.08	322.36	99.9	21.23	48.12
NAT_05	360.48	105.34	379.32	18.59	275.22	76.2	480.43	160	94.52	212.23
NAT_06	15.5	8.74	98.92	16.02	23.37	2.26	55.49	99.9	7.76	4.26
NAT_09	15.5	10.66	133.48	16.02	23.37	2.26	96.41	99.9	19.69	36.51
NAT_10	328.32	50.66	174.77	27.8	127.25	17.4	729.31	127.33	53.36	45.18
NAT_11	15.5	8.88	79.82	16.02	23.37	28.43	343.8	99.9	15.18	14.92
aCD20_01	38.66	11.95	140.06	16.02	25.95	16.46	345.4	99.9	6.81	20.59
aCD20_02	24.94	8.74	223.2	16.02	23.37	3.53	91.59	99.9	12.1	9.02

aCD20_03	49.97	10.45	144.67	16.02	23.37	5.24	118.16	99.9	30.13	15.4
aCD20_04	129.21	48.67	173.6	16.02	23.37	6.59	77.39	99.9	7.41	4.71
aCD20_05	49.14	15.94	91.75	16.02	23.37	2.29	52.38	99.9	7.91	5.63
aCD20_06	54.28	12.83	50.87	16.02	23.37	4.79	61.83	99.9	5.24	12.04
aCD20_07	15.5	8.74	38.46	16.02	23.37	2.26	23.41	99.9	6.2	4.07
aCD20_08	110.97	43.69	154.2	16.02	23.37	2.26	91.95	99.9	15.86	8.09
HD_01	163.42	66.1	165.09	16.02	33.6	5.96	909.33	99.9	37.44	11.28
HD_03	50.65	13.53	104.81	16.02	23.37	16.02	390.18	99.9	39.05	8.1
HD_09	23.88	12.72	61.56	16.02	23.37	2.26	13.54	99.9	7.86	6.56
HD_12	15.5	8.74	114.98	16.02	23.37	3.53	152.28	99.9	6.68	14.33
HD_13	15.5	8.74	100.22	16.02	23.37	5.84	239.42	99.9	8.33	14.93
HD_15	197.07	29.53	131.74	16.02	23.37	2.8	172.79	99.9	12.23	5.6
HD_17	15.5	8.74	730.97	16.02	23.37	2.26	30.34	99.9	6.71	6.6
HD_01	15.5	8.74	35.06	16.02	23.37	2.36	109.06	99.9	16.11	10.48
HD_03	173.88	77.34	103.26	16.02	163.34	6.52	632.82	99.9	35.76	53.36

Table 12. Determinants of Treg function.

	Slope	r^2	P value	N of X values
Treatment duration	0.05208 ± 0.2068	0.004212	0.8046	17
Age	0.03718 ± 0.06861	0.007666	0.5911	40
CD3+CD4+ (% of live PBMCs)	0.05600 ± 0.1008	0.008053	0.5819	40
CD25+CD127lo (% of CD3+CD4+)	0.006588 ± 0.01015	0.01068	0.5202	40
Foxp3+ (% of CD25+CD127lo)	-0.09565 ± 0.1791	0.007451	0.5964	40
CD39+ (% of CD25+CD127lo)	0.1274 ± 0.1694	0.01467	0.4566	40
t-Treg (% of CD25+CD127lo)	**0.2316 ± 0.1076**	**0.1087**	**0.0378**	**40**
p-Treg (% of CD25+CD127lo)	-0.1758 ± 0.1370	0.04154	0.2072	40
Act. t-Treg (% of CD25+CD127lo)	-0.07719 ± 0.1053	0.01393	0.4682	40
MFI FOXP3 t-Treg	-0.3612 ± 1.900	0.0009503	0.8502	40
MFI FOXP3 p-Treg	0.5025 ± 2.496	0.001065	0.8415	40
MFI FOXP3 Act. t-Treg	-0.7429 ± 2.746	0.001922	0.7882	40
MFI CD127 (CD25+Foxp3+)	-0.09565 ± 0.1791	0.007451	0.5964	40
MFI CD103 (CD25+CD127lo)	-1.841 ± 2.571	0.01332	0.4783	40
MFI CD49d (CD25+CD127lo)	2.575 ± 3.571	0.01350	0.4753	40
t-Treg/p-Treg	0.008353 ± 0.01091	0.01520	0.4485	40
t-Treg/Act. t-Treg	0.03177 ± 0.02299	0.04786	0.1750	40
IL-5 conc. (pg/mL)	-4.203 ± 2.077	0.1275	0.0527	30
IL-13 conc. (pg/mL)	-0.8753 ± 0.4386	0.1245	0.0558	30
IL-2 conc. (pg/mL)	1.529 ± 1.652	0.02968	0.3626	30
IL-6 conc. (pg/mL)	-0.09708 ± 0.05781	0.09148	0.1043	30
IL-9 conc. (pg/mL)	0.6896 ± 0.5955	0.04570	0.2567	30
IL-10 conc. (pg/mL)	-0.08674 ± 0.1139	0.02028	0.4528	30
IFN-γ conc. (pg/mL)	**-10.65 ± 4.968**	**0.1410**	**0.0409**	**30**
TNF-α conc. (pg/mL)	-0.4253 ± 0.3151	0.06109	0.1879	30
IL-17A conc. (pg/mL)	-0.4255 ± 0.2430	0.09873	0.0908	30

IL-22 conc. (pg/mL)	-0.3136 ± 0.2382	0.05832	0.1986	30
Unique TCR Vβ clonotypes/Total	0.0002515 ± 0.002040	0.001517	0.9043	12
Clonal expansion	-0.0004915 ± 0.001760	0.007739	0.7857	12
Shannon clonality	-0.0001969 ± 0.0003166	0.03723	0.5480	12
Clone distribution slope	-0.001937 ± 0.005718	0.01135	0.7418	12
Shared TCRs/Total	-0.01214 ± 0.01689	0.04911	0.4888	12

4.8 No major alterations of Treg TCR repertoire are found in patients with MS

The TCR repertoire of effector T cells in patients with MS has been studied in considerable detail *(21, 120, 125)*, but much less is known about the TCR repertoire of Tregs. It has been shown that a highly diverse Treg repertoire increases the frequency of antigen-specific Tregs and probability of antigen-specific Treg-Teff interactions, thus enhancing Treg inhibitory capacity *(123, 124)*. By contrast, a limited TCR diversity may be a risk factor in autoimmune disease *(123)*. Therefore, we aimed to analyse the diversity of Treg TCR repertoire in patients with MS and to investigate how it correlates with Treg function. We initially compared the characteristics of Treg and Teff TCR repertoires in 9 patients with RRMS and 3 HDs by high-throughput TCR Vβ-chain sequencing (Table 9). We obtained a median of 27,860 productive TCR templates from all the samples (Table 12). Interestingly, Tregs show a reduced repertoire diversity in comparison to Teff based on a reduced percentage of unique/total TCR Vβ clonotypes (p=0.01. Figure 19A), and, conversely, an increased clonal expansion (p=0.03; Figure 19B). The clone distribution slope quantifies the diversity of the TCR repertoire based on the distribution of low frequency clones, and this diversity measure was also decreased in Tregs as compared to Teff (p=0.002. Figure 19C). Furthermore, Tregs and Teffs show a largely distinct repertoire, as the mean overlap between Tregs and Teffs was 7.2%, and Treg TCRs that overlapped with Teff were more diverse than the non-overlapping ones (Figure 19D).

When we compared patients with MS and HDs, we found that Treg TCR repertoire was reduced, but not significantly, in patients and Treg-Teff overlap based on nucleotide sequences was comparable (Figure 19E-G). We found no correlation between Treg suppressive capacity and Treg TCR diversity metrics (Table 14). However, there was a positive correlation between the frequency of thymus-derived Tregs and fraction of unique TCR Vβ unique clonotypes (r2=0.38, p=0.043. Figure 19H), and clone distribution slope (r2=0.45, p=0.023. Figure 19I).

Our findings indicate that Treg TCR repertoire diversity, being not significantly reduced, does not play a major role in determining Treg function in our cohort.

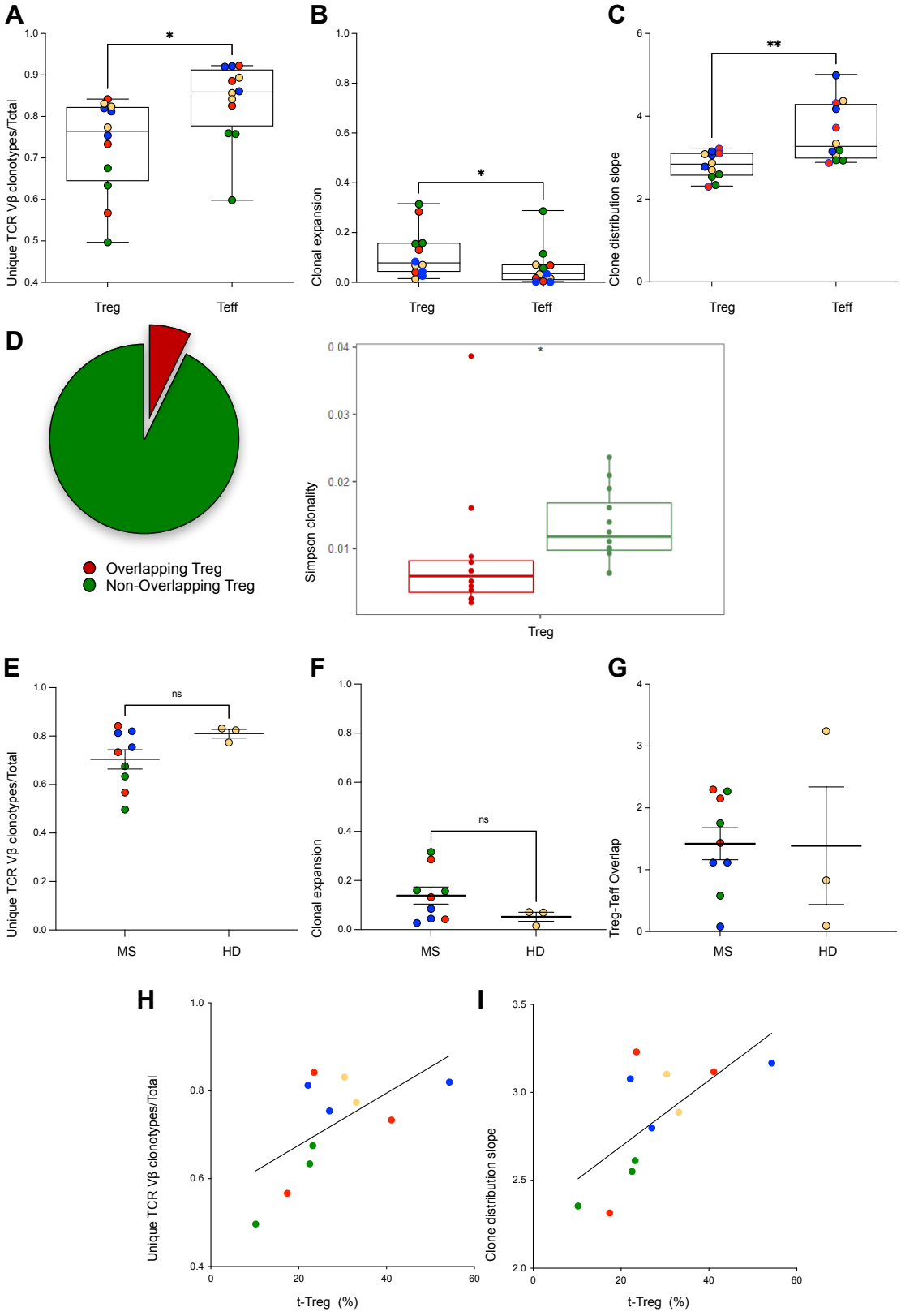

Figure 19. Treg TCR repertoire in patients with RRMS. (A) Comparison of the ratio unique TCR Vβ clonotypes/total TCR Vβ clonotypes between Tregs and Teffs. **(B-C)** Clonal expansion and clone distribution slope in Tregs in comparison to Teffs. **(A-C)** Box and

whiskers min to max; Mann-Whitney U test. * $p<0.05$; ** $p<0.01$. **(D)** Overlap between Tregs and Teffs. Diversity of Treg TCRs overlapping with Teffs as compared to the non-overlapping ones calculated as Simpson clonality. Box and whiskers min to max; Mann-Whitney U test. * $p<0.05$. **(E-G)** Patients with MS (MS) were compared to HDs (HD). Patients included untreated (green), natalizumab- (red), and a-CD20-treated (blue). **(E)** Ratio unique TCR Vβ clonotypes/total TCR Vβ clonotypes. **(F)** Clonal expansion. **(G)** Treg-Teff overlap based on nucleotide sequences. **(E-G)** Scatter plot graph. Mean with SEM. Unpaired t test or Mann-Whitney U test. **(H-I)** XY correlation between frequency of t-Tregs and ratio unique TCR Vβ clonotypes/total TCR Vβ clonotypes, and clone distribution slope.

Table 13. Immune repertoire analysis of T effector and T regulatory cell compartment in 12 patients with RRMS and 3 healthy donors.

Sample	Unique Rearrangements	Total Productive Templates	Unique TCR Vβ clonotypes/Total	Clonal expansion	Pielou Evenness	Shannon clonality	Simpson Clonality	Simpson's D
UNT_04_Teff	34237	57256	0.5979	0.2879	0.8125	0.1874	0.2092	0.0437
UNT_04_Tregs	5437	8580	0.6336	0.1600	0.9589	0.0410	0.0219	0.0004
UNT_06_Teff	28165	37178	0.7575	0.1168	0.9575	0.0424	0.02575	0.0006
UNT_06_Tregs	29599	43834	0.6752	0.1564	0.9636	0.0363	0.0111	0.0001
UNT_10_Teff	19305	25422	0.7593	0.0590	0.9789	0.0210	0.01102	0.0001
UNT_10_Tregs	15252	30706	0.4967	0.3162	0.9353	0.0646	0.0179	0.0003
NAT_02_Teff	11280	12229	0.9224	0.0057	0.9956	0.0044	0.0101	0.0001
NAT_02_Tregs	26357	31312	0.8418	0.0417	0.9855	0.0145	0.0093	0.0001
NAT_05_Teff	32914	37156	0.8858	0.0181	0.9919	0.0081	0.0067	0.0000
NAT_05_Tregs	11645	15879	0.7334	0.1321	0.9497	0.0503	0.0398	0.0016
NAT_08_Teff	13963	16906	0.8259	0.0699	0.9764	0.0236	0.0175	0.0003
NAT_08_Tregs	25474	44934	0.5669	0.2858	0.9422	0.0578	0.0142	0.0002
aCD20_04_Teff	42802	49719	0.8609	0.0356	0.9884	0.0116	0.0065	0.0000

aCD20_04_Tregs	9734	12907	0.7542	0.0849	0.9749	0.0251	0.0153	0.0002
aCD20_05_Teff	46938	50942	0.9214	0.0026	0.9969	0.0031	0.0049	0.0000
aCD20_05_Tregs	3939	4848	0.8125	0.0272	0.9851	0.0149	0.0191	0.0004
aCD20_08_Teff	28424	30902	0.9198	0.0028	0.9963	0.0037	0.0063	0.0000
aCD20_08_Tregs	15351	18724	0.8199	0.0448	0.9844	0.0156	0.0110	0.0001
HD_15_Teff	38211	44613	0.8565	0.0176	0.9912	0.0088	0.0061	0.0000
HD_15_Tregs	14615	18884	0.7739	0.0700	0.9792	0.0208	0.0117	0.0001
HD_16_Teff	26012	29103	0.8938	0.0338	0.9833	0.0167	0.0195	0.0004
HD_16_Tregs	2520	3058	0.8241	0.0150	0.9855	0.0145	0.0237	0.0006
HD_17_Teff	7695	9139	0.8420	0.0723	0.9732	0.0268	0.0240	0.0006
HD_17_Tregs	22120	26617	0.8310	0.0715	0.9740	0.0260	0.0173	0.0003

Sample	**Simpson's Evenness**	**iChao1**	**Efron Thisted Estimator**	**Clone Distribution Slope**	**Daley Smith Estimator**	**Maximal productive frequency**	**Overlap by nucleotide**
UNT_04_Teff	0.0007	186716	85069	2.95	63979	0.2087	0.0058
UNT_04_Tregs	0.3811	22988	25190	2.55	29333	0.0038	
UNT_06_Teff	0.0535	159469	86492	2.95	74395	0.0168	0.0175
UNT_06_Tregs	0.2699	133486	78447	2.61	64675	0.0026	

UNT_10_Teff	0.8687	102802	60219	4.33	71452	0.0016	0.0215
UNT_10_Tregs	0.4389	164760	89538	3.23	79564	0.0028	
NAT_02_Teff	0.6674	249422	108096	3.74	90613	0.0014	0.0230
NAT_02_Tregs	0.0543	58445	46681	3.12	49961	0.0309	
NAT_05_Teff	0.2337	91763	61185	2.89	63569	0.0097	0.0143
NAT_05_Tregs	0.1946	122238	68554	2.31	54818	0.0037	
NAT_08_Teff	0.5461	322139	121229	3.17	92825	0.0015	0.0112
NAT_08_Tregs	0.4381	55560	46252	2.80	51537	0.0057	
aCD20_04_Teff	0.9011	342637	128860	4.19	100174	0.0006	0.0008
aCD20_04_Tregs	0.6940	21697	22754	3.08	30616	0.0031	
aCD20_05_Teff	0.8897	227703	102376	5.01	91043	0.0008	0.0112
aCD20_05_Tregs	0.5337	90336	63207	3.17	64692	0.0033	
aCD20_08_Teff	0.8687	102802	60219	4.33	71452	0.0016	0.0215
aCD20_08_Tregs	0.4389	164760	89538	3.23	79564	0.0028	
HD_15_Teff	0.7140	236291	110076	3.35	88054	0.0011	0.0083
HD_15_Tregs	0.4962	84231	60721	2.89	61043	0.0033	

HD_16_Teff	0.1014	206913	93752	4.39	84715	0.0161	0.0009	
HD_16_Tregs	0.7068	14786	15351	2.71	24023	0.0062		
HD_17_Teff	0.2255	66144	44675	3.06	58776	0.0111	0.0324	
HD_17_Tregs	0.1514	165929	85050	3.10	79202	0.0086		

4.9 Thymus-derived Tregs from natalizumab-treated patients show profound gene expression alterations in comparison to HDs

Next we investigated factors, other than the frequency of t-Tregs, that could explain the fact that an impaired Treg function was observed exclusively in natalizumab-treated patients. Towards this end, we compared the gene expression profile between 9 patients (3 untreated, 3 natalizumab-treated and 3 a-CD20-treated) and 3 HDs. We isolated both t-Tregs and p-Tregs and we performed bulk RNA sequencing as previously discussed. A total of 512 genes were differentially expressed between t-Tregs derived from natalizumab-treated patients and HDs (false discovery rate <0.05. Figure 20A). Most of the differentially expressed genes (DEGs) were downregulated in t-Tregs derived from natalizumab-treated patients in comparison to HDs (Figure 20A and B). In stark contrast, no DEGs were observed between t-Tregs from untreated and a-CD20-treated patients respectively in comparison to HDs (Figure 21A and C). The DEGs between patients and HDs in p-Tregs were 0 in untreated, 6 in a-CD20-treated patients and 1 in natalizumab-treated, respectively (Figure 21B, D, and E). As many DEGs were found between t-Tregs from natalizumab-treated patients and HDs, we explored their function using biological process (BP) domain of the Gene Ontology (GO) functional database. We observed that 26 out of 512 DEGs showed a significant correlation with Treg function (Table 14). Genes implicated in RNA splicing and mRNA processing were up-regulated in natalizumab-treated patients-derived Tregs in comparison to HDs (Figure 20C). By contrast, genes involved in ion transmembrane transport, signaling pathway, positive regulation of cell proliferation, chemotaxis, and cell adhesion were downregulated in t-Tregs derived from natalizumab-treated patients as compared to HDs (Figure 20C). Among the genes that were negatively correlated to Treg suppressive capacity, and were over-expressed in natalizumab-treated patients, we found IL7R (CD127), genes playing a role in RNA processing, and TXNIP (Figure 20D). Interestingly, the latter represses glucose uptake and inhibits Thioredoxin-1 that promotes the synthesis of deoxyribonucleotides to allow rapid cell proliferation *(139)*. T cell activation results in rapid downregulation of TXNIP and induction of glycolysis to sustain T cell proliferation *(139)*. By contrast, the increased expression of TXNIP restrains lymphocyte proliferation *(140)*. Genes positively correlated to Treg response, and downregulated in natalizumab-treated patients were related to signal transduction, metabolic processes, and positive regulation of T cell activation and proliferation, that might

explain the functional Treg impairment observed in natalizumab-treated patients (Figure 20D).

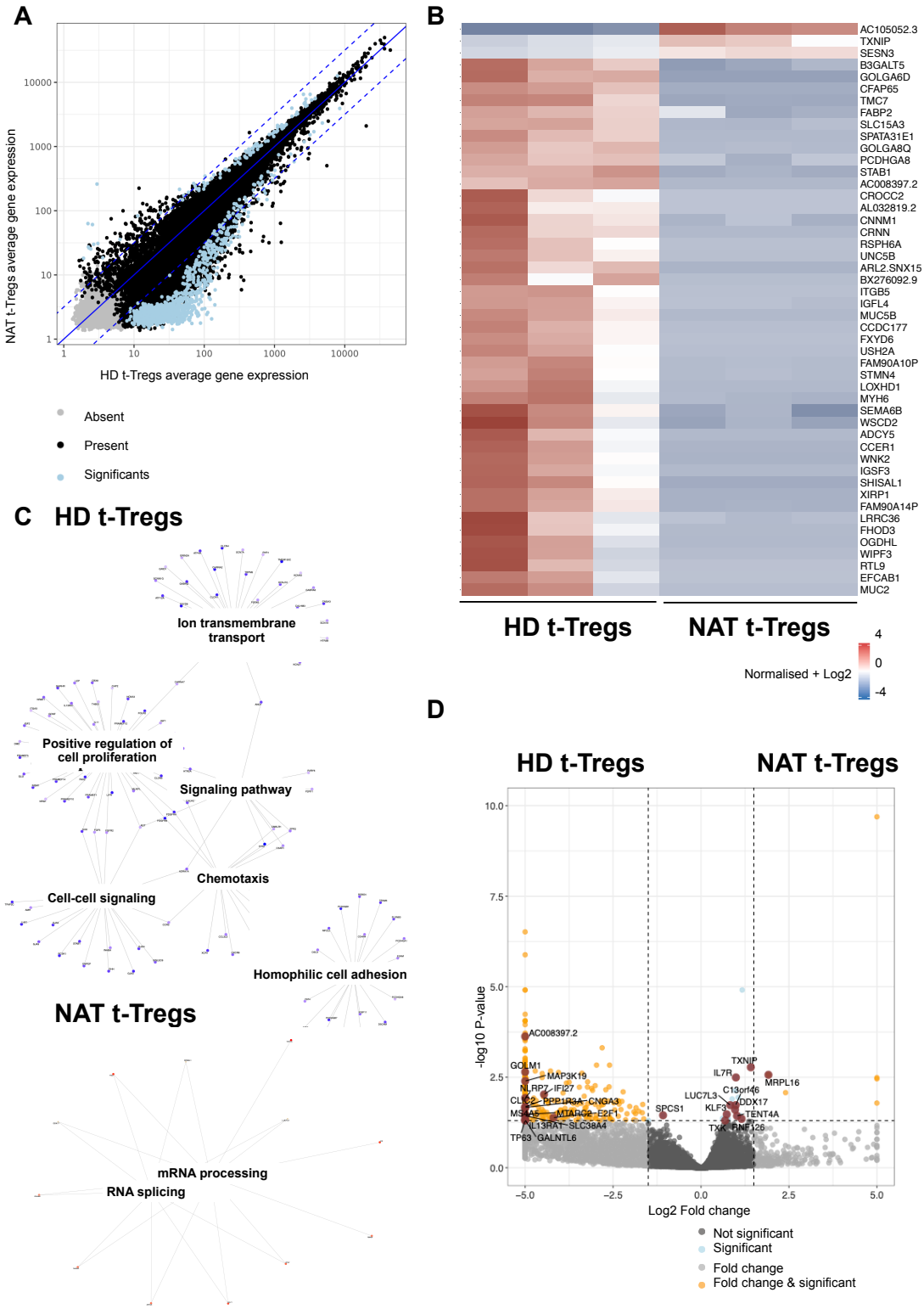

Figure 20. Transcriptomic analysis of t-Tregs derived from natalizumab-treated patients and HDs. (A) Comparison of average gene expression showing significantly differentially expressed genes between t-Tregs derived from natalizumab-treated patients and HDs. Present

(black) indicates genes with read counts > = 10 in more than one sample, absent (grey) indicates all genes that are not flagged as present, and significant (blue) indicates genes with log2 ratio > 0.5 and p value < 0.01. Log2 ratio indicates the fold-change in gene expression. **(B)** Heatmap showing the expression counts of the top 50 differentially expressed genes across t-Tregs derived from Natalizumab-treated patients and HDs. Both positive and negative log fold changes are displayed. **(C)** Genes belonging to different Gene Ontology (GO) Biological Process (BP) terms were up-regulated in t-Tregs derived from natalizumab-treated patients and HDs, respectively. **(D)** Volcano plot showing genes involved in T cell activation, proliferation, metabolism, and RNA processing differentially expressed between t-Tregs derived from natalizumab-treated patients and HDs (log2 fold change threshold > 1.5; False Discovery Rate <0.05).

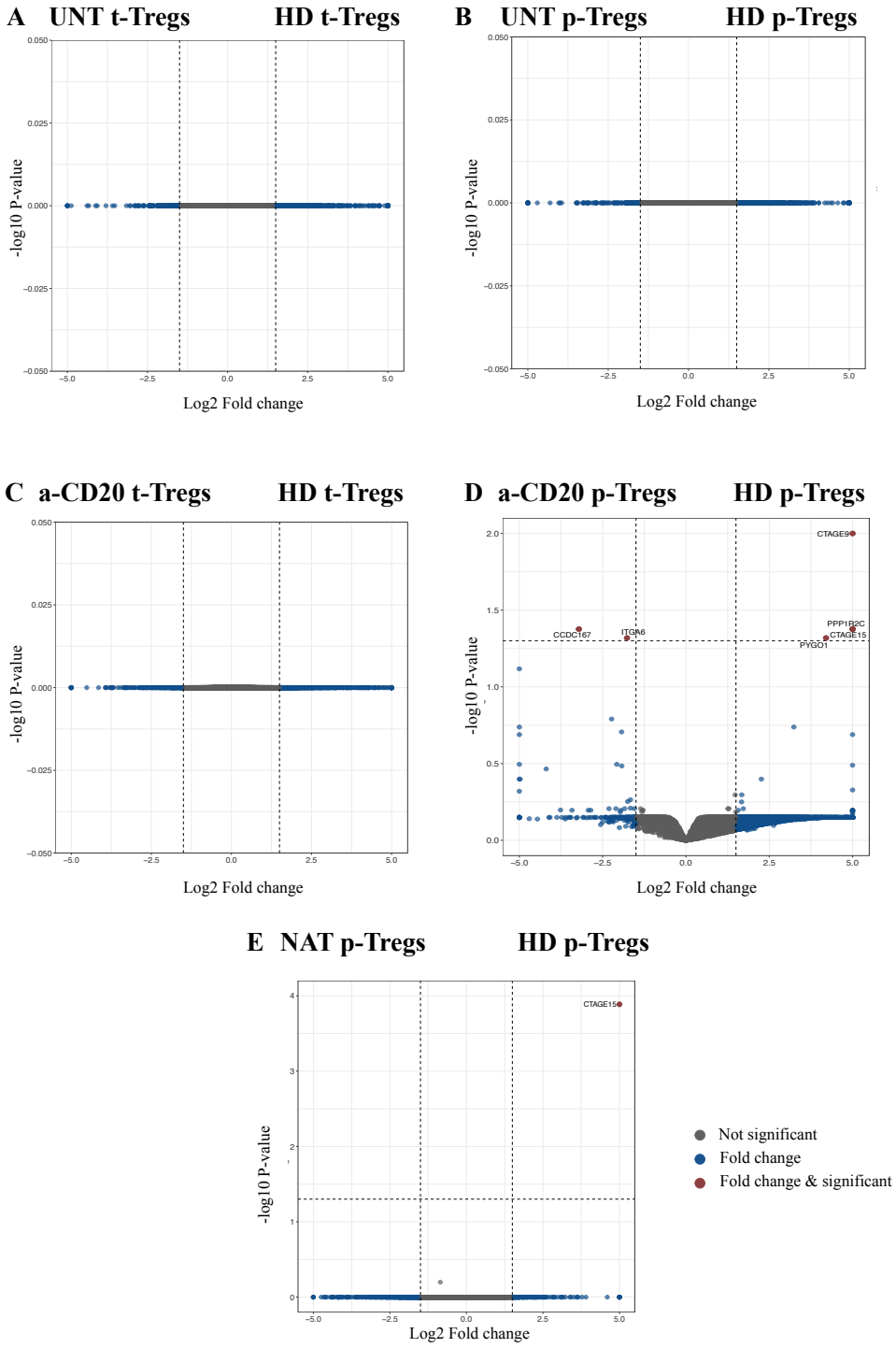

Figure 21. Transcriptomic analysis of t-Tregs and p-Tregs derived from patients with MS and HDs. (A-B) Volcano plot showing DEGs between t-Tregs and p-Tregs derived from untreated patients and HDs. **(C-D)** Volcano plot showing DEGs between t-Tregs and p-Tregs derived from anti-CD20-treated patients and HDs. **(E)** Volcano plot showing genes differentially expressed between p-Tregs derived from natalizumab-treated patients and HDs. **(A-E)** UNT: Untreated. NAT: natalizumab-treated. a-CD20: anti-CD20-treated. Log2 fold change threshold > 1.5; False Discovery Rate <0.05.

Table 14. DEGs between t-Tregs from natalizumab-treated patients and HDs show a linear correlation with Treg function.

Gene	GO BP	Slope	r^2	P value
AC008397.2	Signal transduction	2.059 ± 0.6493	0.5013	0.01
TXNIP	Response to glucose, negative regulation of cell proliferation, negative regulation of transcription, apoptosis	-145.2 ± 44.32	0.5177	0.0083
GOLM1	Metabolic process, post-translational protein modification	2.103 ± 0.7867	0.4169	0.0233
MRPL16	Translation, mitochondrial translation	-3.914 ± 1.747	0.3342	0.049
IL7R	Positive regulation of T cell differentiation in thymus, IL7-mediated signaling pathway, lymph node development	-78.71 ± 35.01	0.3357	0.0484
MAP3K19	Protein phosphorylation	2.248 ± 0.7581	0.4678	0.0142
IFI27	Type I interferon signaling pathway, apoptosis, negative regulation of transcription, innate immune response	2.978 ± 1.127	0.4113	0.0246
NLRP7	Negative regulation of IL-1β production, negative regulation of protein processing, negative regulation of inflammatory cytokine production	2.181 ± 0.6539	0.5266	0.0076
C13orf46	Unknown	-17.64 ± 5.564	0.5013	0.01
LUC7L3	mRNA processing, RNA splicing	-84.94 ± 28.20	0.4758	0.0131
PPP1R3A	Metabolic process	1.934 ± 0.8382	0.3474	0.0437
CNGA3	Signal transduction	1.514 ± 0.6026	0.3869	0.0308
CLIC2	Signal transduction	1.382 ± 0.5411	0.395	0.0286
DDX17	rRNA processing, mRNA splicing	-108.5 ± 42.28	0.397	0.0281
KLF3	Negative regulation of transcription	-54.02 ± 18.95	0.4484	0.0172
MTARC2	Oxidation-reduction process	0.9015 ± 0.3806	0.3594	0.0394
MS4A5	Signal transduction	1.811 ± 0.5739	0.4988	0.0102
SPCS1	Signal peptide processing, protein targeting to ER, proteolysis	9.296 ± 4.150	0.3341	0.049
SLC38A4	Amino acid and ion transport	0.8221 ± 0.3359	0.3745	0.0344
TENT4A	mRNA processing	-16.69 ± 6.199	0.4201	0.0226
E2F1	Positive regulation of cell proliferation	2.263 ± 0.8079	0.4397	0.0188

RNF126	Protein catabolic process, negative regulation of EGF-R signaling pathway, regulation of cell population proliferation	-7.795 ± 2.271	0.5408	0.0064
GALNTL6	Protein glycosylation, protein phosphopantetheinylation	1.899 ± 0.6304	0.4758	0.0131
IL13RA1	Positive regulation of cell population proliferation, cytokine mediated signaling pathway	0.9352 ± 0.3103	0.4759	0.013
TP63	Positive regulation of cell proliferation, negative regulation of transcription	1.543 ± 0.4636	0.5255	0.0076
TXK	Positive regulation of IFN-γ-mediated signaling pathway, integrin-mediated signaling pathway, positive regulation of gene expression	-22.37 ± 8.826	0.3911	0.0296

4.10 Myelin-specific TCR discovery based on a bioinformatic approach

Recently, the investigation of the TCR repertoire, by means of high throughput TCR sequencing (HTS), has boosted the research of antigen-specific T cells in several disease contexts. It has been shown that patients with MS share some T cell clones (TCCs) that are not present in the repertoire of patients with other neurological diseases *(121)*. These clones are defined "public" based on the identical amino acid sequence, and they might be expanded in response to a dominant pathogenic epitope *(126)*. Using HTS, we analyzed the Teff and Treg TCR repertoire of 9 patients with RRMS (3 untreated, 3 natalizumab-treated, 3 anti-CD20-treated) as compared to HDs (Table 9). We defined as public TCR an amino acid CDR3 sequence shared across at least 5/9 patients and not present in HDs. We found 157 public TCRs across patients with MS, most of them (147) were shared across Teff and Treg compartments while 10 were exclusively present in Teff compartment (Figure 22A). The mean productive frequency of public TCRs was similar between Tregs and Teffs (Figure 22B). We took advantage of available datasets where TCRs with known antigen specificities are listed. We used the McPAS-TCR and the VDJdb databases which couple TCR sequences and antigen specificities *(127, 128)*. In addition, as it has been shown that some TCCs are shared between peripheral blood and brain lesions in patients with MS, we employed the TCR Vβ sequencing data of MS brain lesions *(21)*. When we searched the top 18 public TCRs detected in patients with MS, we observed that they were mostly predicted to recognize viruses, especially cytomegalovirus (CMV), and autoantigens, but only one clone was found to be associated with MS (Figure 22C). As alternative approach, we explored the entire repertoire in order to find known antigen-specific TCRs. Using the VDJdb database, we initially investigated TCRs specific for foreign antigens, such as Influenza, CMV, and SARS-CoV2, and we found that their mean productive frequency was similar in Teffs and Tregs (Figure 22D). Employing the three databases above mentioned, we then identified 29 putative MS-specific TCRs in the repertoires analyzed. Their productive frequency did not significantly differ between Teffs and Tregs (Figure 22E), but it was significantly higher in natalizumab-treated patients as compared to a-CD20-treated patients ($p=0.0096$. Figure 22F). This might be related to the mechanism of action of natalizumab which, by preventing their migration to the CNS, sequesters lymphocytes, including autoreactive T cells, in the peripheral blood. Hence, we attempted to isolate myelin-specific Treg clones from peripheral blood of a natalizumab-treated patient with MS. The patient carried the HLA-DR15 haplotype

(DRB1*15:01 which is in linkage disequilibrium with HLA-DRB5*01:01) that has been identified as the main genetic risk factor for MS *(8)*.

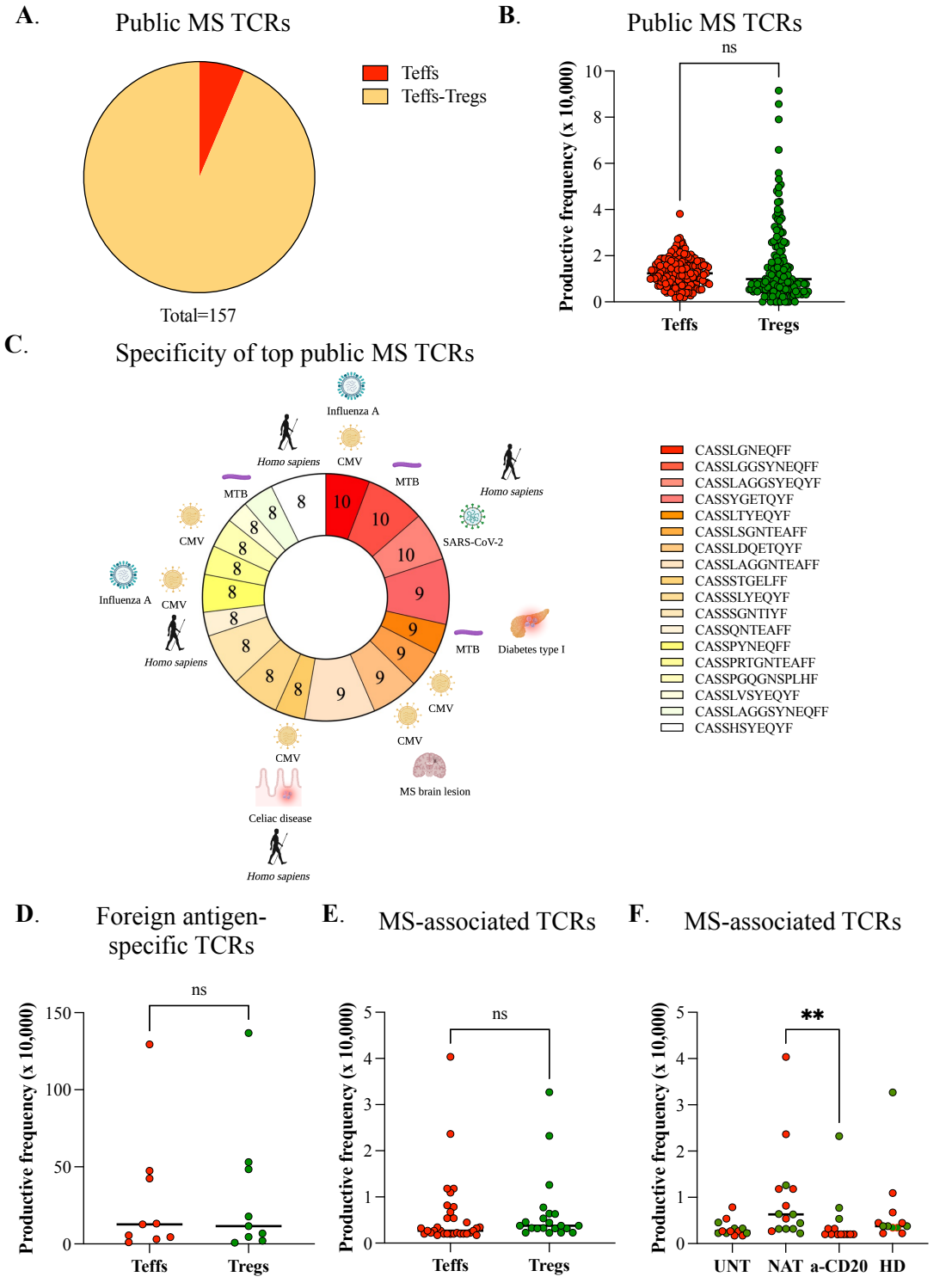

Figure 22. Bioinformatic approach to identify Ag-specific TCRs. (A) Pie chart of public TCRs present in Teff compartment (red) or shared between Teff and Treg compartments

(yellow). **(B)** Productive frequency of public TCRs in Teffs and Tregs. **(C)** Specificity prediction of top 18 public TCRs based on available databases. MTB: Mycobacterium tuberculosis, CMV: cytomegalovirus. **(D)** Productive frequency of TCRs specific for foreign antigens in Teffs and Tregs. **(E-F)** Productive frequency of 29 putative MS-specific TCRs in Teffs (red dots) and Tregs (green dots) and in patients and HDs (HD). UNT: Untreated. NAT: natalizumab-treated. a-CD20: anti-CD20-treated. **(B-D-E-F)** Scatter plot graph. Mann-Whitney test or one-way ANOVA followed by Kruskal-Wallis test. ** $p< 0.01$.

4.11 Identification of MBP-reactive Tregs

We conducted preliminary experiments to analyse the reactivity of peripheral CD45RA- T cells isolated from 20 natalizumab-treated patients with MS to known autoantigens, such as MOG, MBP, RASGRP2, TSTA3, HLA and PLP. In addition, we investigated the proliferative response to EBNA 1, BLLF1, and CEF II. We observed that 40% of patients showed reactivity to MBP pool 3 (data not shown), a pool of peptides that span the MBP sequence 78-170 (Figure 23A). Thus, we selected one of these patients (Figure 23B) to trace this reactivity in Treg compartment. For this purpose, we isolated CD25+CD127lo T cells by magnetic sorting and stimulated them in vitro using autologous irradiated monocytes either untreated or pulsed with MBP pool 3. At day 5, Tregs showed a positive response to MBP, as demonstrated by upregulation of the activation markers OX40 and CD137 (Figure 23C). Next, we compared responding (OX40+CD137+) and non-responding (OX40-CD137-) Tregs by HTS. We found that responding Tregs had a higher clonality than non-responding Tregs (Simpson clonality 0.052 as compared to 0.023), and the productive frequency of the top 50 clones was increased in responding Tregs in comparison to the non-responding ones ($p<0.0001$. Figure 23D). By contrast, CD25- T cells showed low response to MBP, as demonstrated by upregulation of OX40 and CD137, probably because these markers are not specific for Teffs (Figure 23E). Nevertheless, responding Teffs (OX40+CD137+) had a higher clonality than non-responding Teffs (Simpson clonality 0.105 as compared to 0.020) and productive frequency of the top 50 clones ($p<0.0001$. Figure 23F). Interestingly, shared clonotypes between responding Tregs and Teffs (0.8%) were enriched in comparison to the shared clonotypes between non-responding Tregs and Teffs (0.2%) (Figure 23G). Hence, our approach led us to identify MBP-responding Tregs, whose repertoire was made up of expanded clones under antigen-specific stimulation, in peripheral blood from a patient with

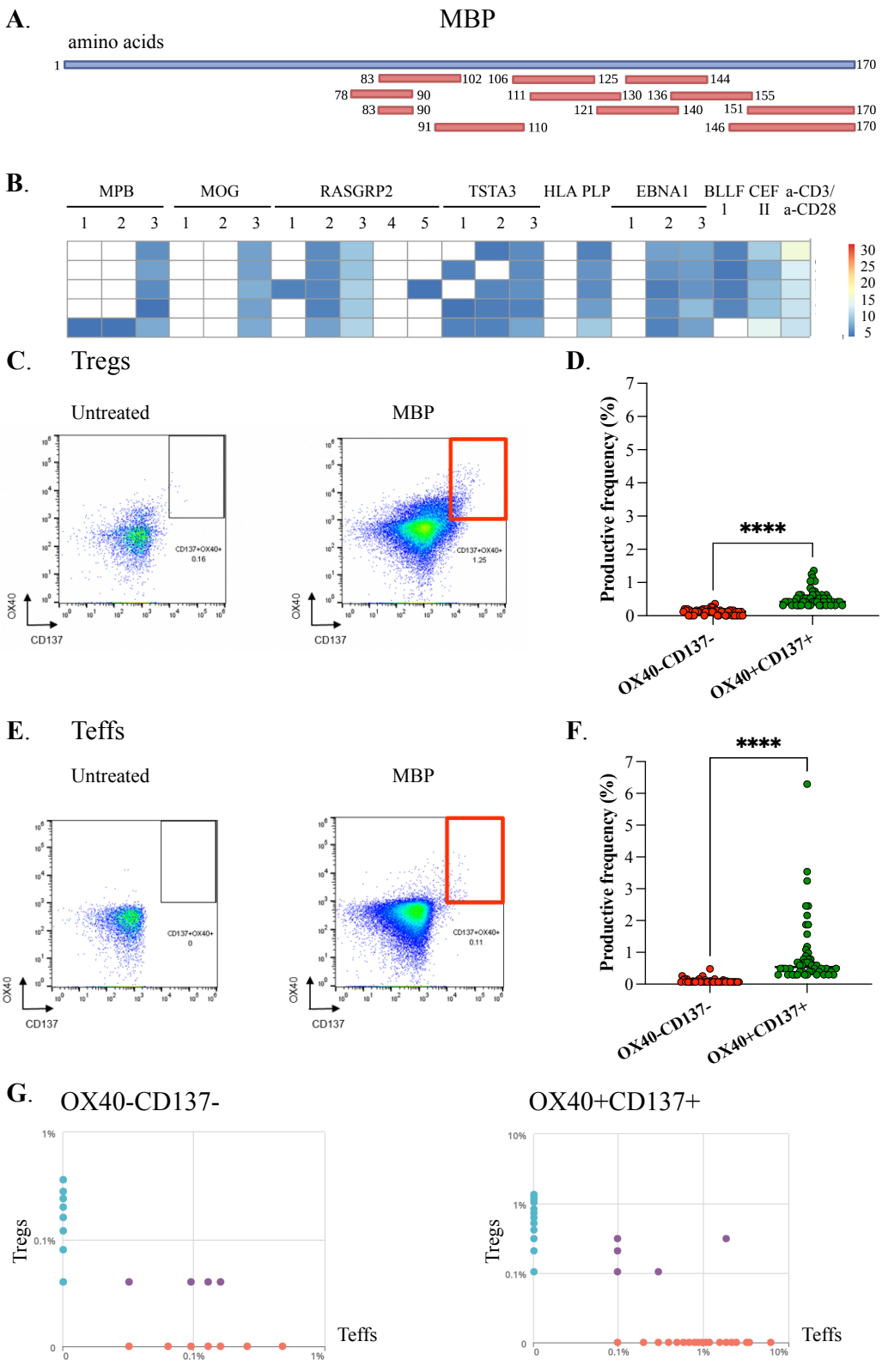

MS.

Figure 23. Identification of MBP reactive Tregs. (A) List of peptides of MBP pool 3. **(B)** Reactivity of CD45RA-PBMCs isolated from a patient with MS to known MS-associated autoantigens (MBP, MOG, RASGRP2, TSTA3, HLA, PLP) and foreign antigens (EBNA1,

BLLF, CEF II). As positive control, we used anti-CD3 and anti-CD28 beads. Response was measured as proliferation by thymidine assay. The stimulatory index is shown and indicates the ratio of cpm in the presence of the peptide versus cpm in the unstimulated control. **(C-E)** Treg and Teff activation in response to MBP stimulation in comparison to the unstimulated control. **(D-F)** Productive frequency of TCRs in OX40-CD137- and OX40+CD137+ Tregs and Teffs. Scatter plot graph. Mann-Whitney test. **** $p < 0.0001$. **(G)** Schematic representation of the frequency of shared clonotypes (violet dots) between non-responding Tregs (light blue dots) and Teffs (orange dots) and responding Tregs and Teffs, respectively.

4.12 Generation of MBP-specific TCCs

To generate autoreactive Treg clones, we performed a single-cell FACS sorting and cloning of OX40+CD137+ Tregs after stimulation with MBP pool 3. As the MBP responding fraction might contain bystander cells, we tested the 35 clones obtained with autologous irradiated monocytes either untreated or pulsed with MBP pool 3 to confirm their specificity. After 24 hours, 9 clones (25.7%) upregulated the activation marker CD69, and downregulated CD3, under stimulation with MBP pool 3, and therefore were confirmed to be specific for MBP; 7 out of 9 clones also upregulated CD137 (Figure 24A). In contrast to non-specific TCCs, specific TCCs rapidly formed clusters under antigen-specific stimulation (Figure 24B). The specificity of 7 clones was mapped to distinct peptides that spanned the MBP sequence 78-170. In particular, 3 clones recognized immunodominant sequences (amino acids 78-90 and 83-102, respectively), and 4 clones recognized sequences located at the the C-terminal region (amino acids 106-130, 121-140, and 146-170, respectively) (Figure 24C). We performed HTS of the clonotypes identified and we found a predominance of the TCR β-chain variable region (TRBV) 2 (Figure 24D). By contrast, after stimulation with MBP pool 3, OX40+CD137+ Tregs were composed of multiple clonotypes with no predominance of a Vβ family (Figure 24E). We next analyzed TCCs for cytokines production under MBP stimulation. Most of the clones mainly secreted IL-5, IL-13, IL-4 and IL-10. The cytokine profile was compatible with a Th2-like phenotype (Figure 24F). Thus, autoreactive TCCs target several MBP sequences, spreading from dominant to subdominant epitopes.

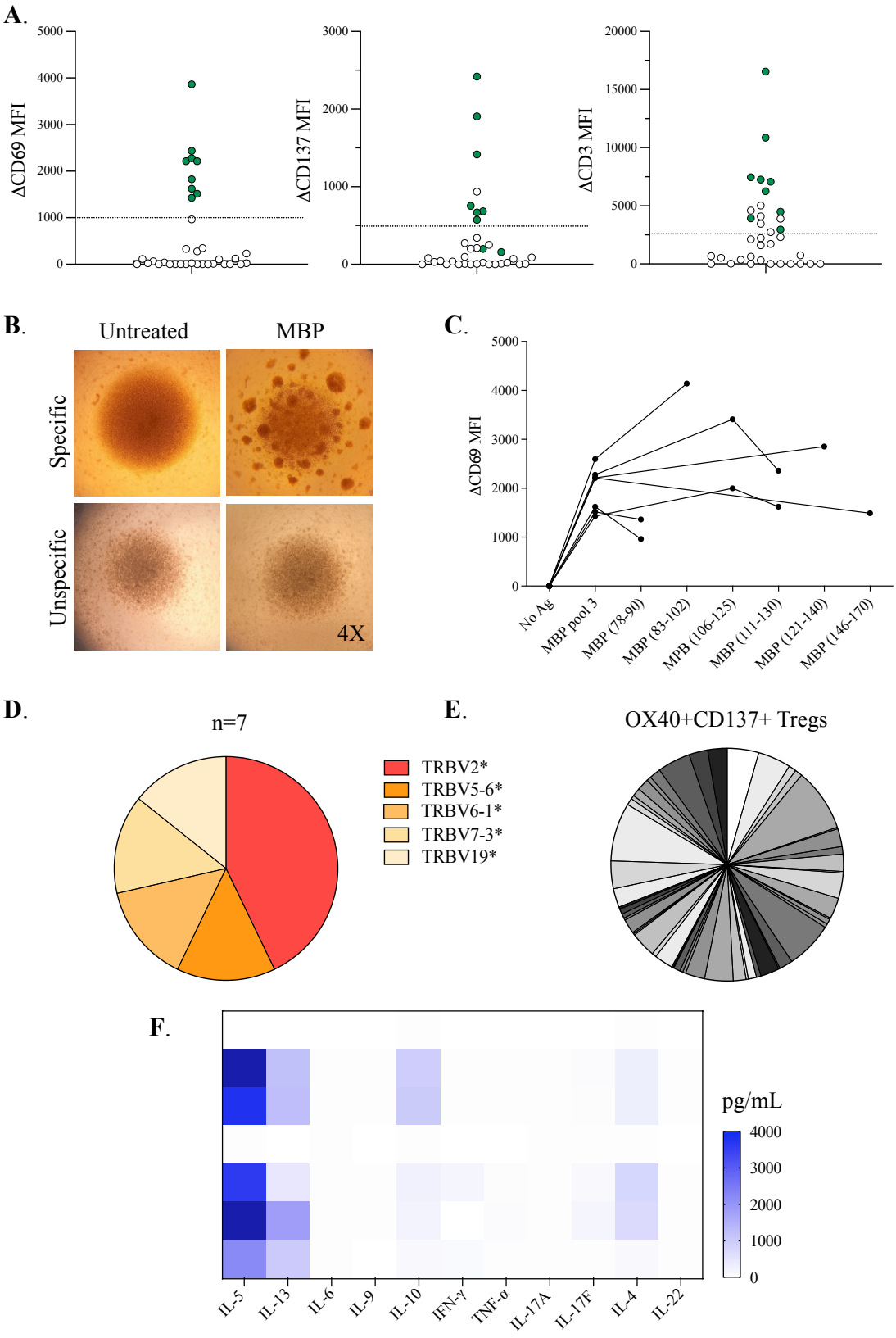

Figure 24. Generation of MBP specific TCCs. (A) Screening of 35 TCCs for activation in response to stimulation with MBP pool 3. On the Y axis the absolute value of the difference between MFI of CD69, CD137 and CD3 in stimulated and unstimulated conditions is shown. The ΔMFI was considered positive when above 1000, 500 and 2500 for CD69, CD137 and CD3, respectively. **(B)** Visual pattern of specific (above) and non-specific (below) TCCs

under stimulation with MBP. Images were captured by light microscopy. **(C)** Specificity of 7 TCCs. On the Y axis the absolute value of the difference between MFI of CD69 in stimulated and unstimulated conditions is shown. **(D)** TCRBV predominance in specific TCCs in comparison to responding Tregs. Frequency of each TCRBV is shown as part of whole in a pie chart. **(E)** Cytokines in supernatants of TCCs after co-culture with irradiated monocytes pulsed with MBP pool 3. Cytokine concentration, detected by by a bead-based immunoassay ranged from 0 (white) to 4000 (blue) pg/mL with the exception of two outliers that were above 400 pg/mL and appear as dark blue.

4.13 Some MBP-specific TCCs express Foxp3 and are fully suppressive

High expression of CD25 and lack of CD127 are the most used surface markers to identify Tregs, but they are not specific, as they can also be expressed by Teffs, especially under activation *(27)*. Thus, TCCs might have been originated either from the purified Treg fraction or from contaminating Teffs that were not targeted for depletion. To determine the origin of generated TCCs, we analyzed them by flow cytometry and we observed a variable Foxp3 expression. MFI of Foxp3 ranged from 184 to 2102 (Figure 25A). Towards the functional characterization of TCCs we co-cultured them with autologous policlonally stimulated Teffs (CD4+CD25-) at different ratios. We found that TCCs had a variable mean inhibitory capacity, ranging from 0% to 81.4% (Figure 25B and 25C). Interestingly, when polyclonal Tregs isolated from the same patient were tested for their capacity to suppress Teffs, their mean inhibitory function was 2.8% (the patient belongs to the natalizumb-treated cohort collectively analysed in Figure 18A). Moreover, TCCs that displayed the brightest Foxp3 expression held the best functionality.

We were then interested to know whether the autoreactive TCCs recognised MBP in association with HLA-DRB1*15:01 molecule. We used a fluorescent tetramer composed of a HLA-DRB1*15:01 molecule bound to the MBP(83-99) peptide. By means of this complex we could stain the TCC that was specific for MBP(83-99), thus confirming its HLA class II restriction (Figure 18D). By contrast, when we used a fluorescent tetramer composed of a HLA-DRB1*15:01 molecule bound to the CLIP peptide, the MFI was weaker, confirming the specificity of the interaction TCR-MBP(83-99). A second clonotype showed a positive response to MBP pool presented either by HLA-DRB5*01:01 (DR2a) and HLA-DRB1*15:01

(DR2b) B cell lines, thus confirming its HLA-DR15 restriction (Figure 26). Hence, we demonstrated that some of the MBP-specific TCCs have Treg properties, such as Foxp3 expression, and the ability to inhibit T effector cell proliferation.

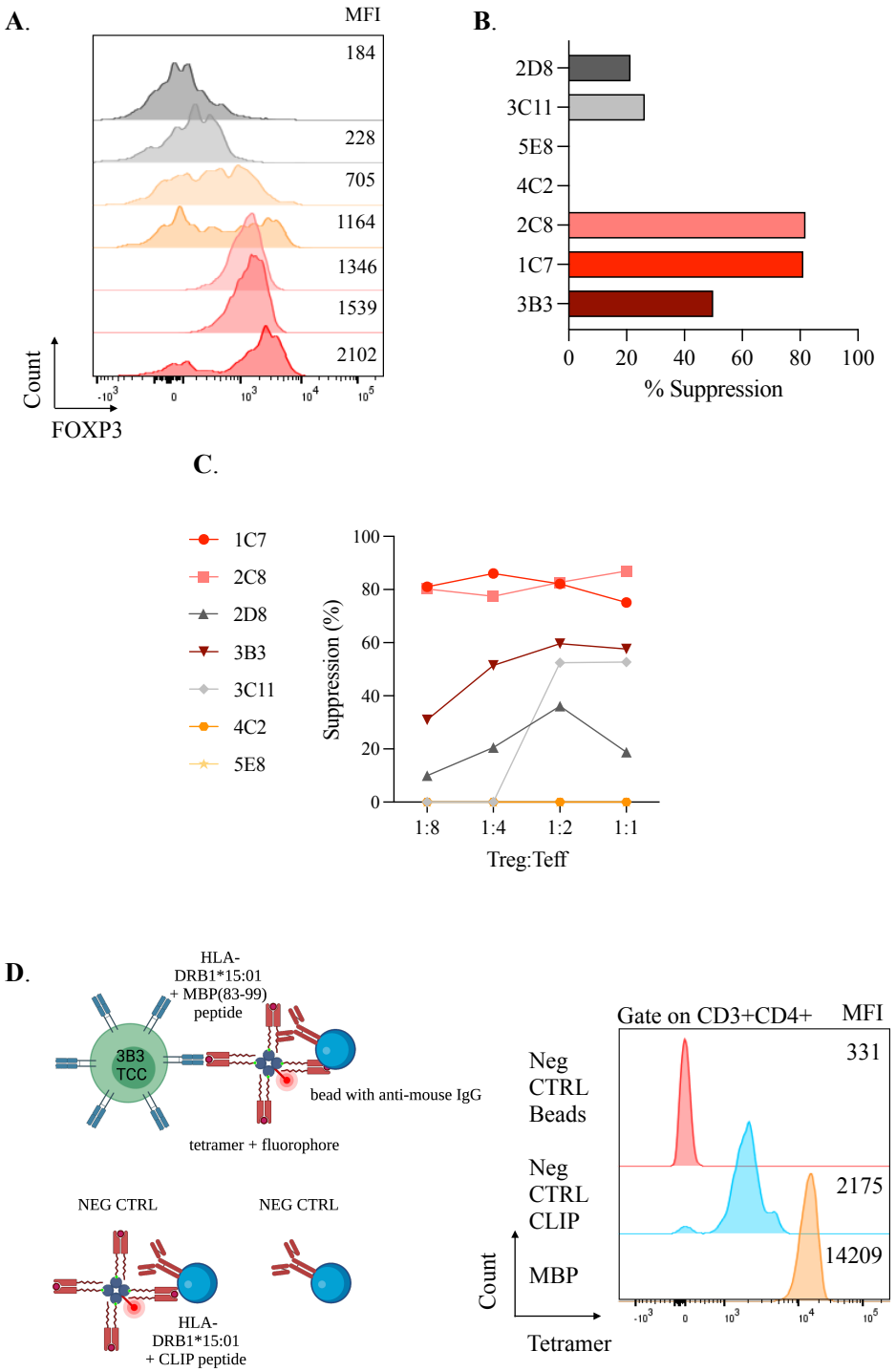

Figure 25. Identification of functional Foxp3+ Ag-specific TCCs. (A) Foxp3 expression is shown as MFI in different Ag-specific TCCs. **(B)** Suppressive capacity of Ag-specific TCCs calculated as mean of four values at different putative Treg:Teff ratios. **(C)** Individual values

of Treg inhibitory capacity are shown. **(D)** Schematic representation of tetramer staining procedure. We used a fluorescent tetramer composed of a HLA-DRB1*15:01 molecule bound to the MBP(83-99) peptide. As negative controls we used a fluorescent tetramer composed of a HLA-DRB1*15:01 molecule bound to the CLIP peptide and beads with anti-mouse IgG respectively. The MFI of the MBP (83-102)-specific TCC incubated with different constructs is shown.

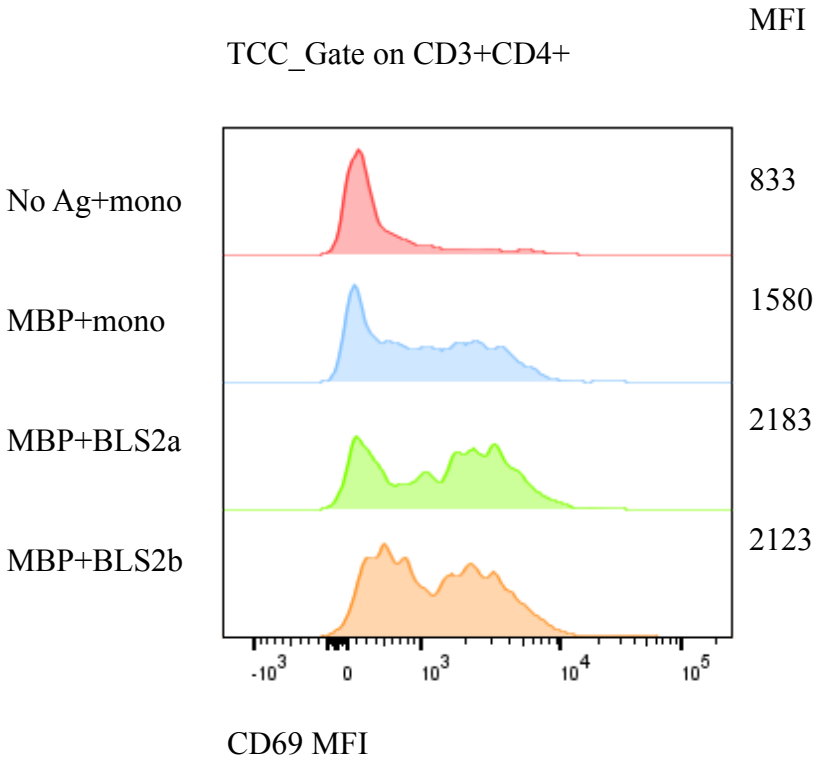

Figure 26. HLA-DR15 restriction of an antigen-specific TCC. CD69 expression, shown as MFI, of a TCC stimulated with autologous monocytes that were either untreated (No Ag+mono) or pulsed with MBP (MBP+mono). When MBP was presented either by HLA-DRB5*01:01 (DR2a) and HLA-DRB1*15:01 (DR2b) B cell lines, the clone upregulated CD69 similarly to what observed when monocytes were used as APC.

4.14 Detection of autoreactive clonotypes in TCR repertoires

By TCR sequencing, we obtained the alpha and beta chain CDR3 nucleotide sequences of MBP-specific TCCs (Figure 27A). We next examined whether the same clonotypes could be traced in the TCR repertoire of the same donor, or in different patients and healthy controls. One clonotype (CASRATVATNEKLFF) was among the top 10 expanded clones Teff fraction isolated from the same donor after stimulation with MBP pool 3 in an independent replicate (productive frequency 1.87%). The same clonotype was detected with a lower frequency (0.3%) in stimulated Treg compartment (Figure 27B). Accordingly, it has been suggested that any overlap that is present between Treg and Teff compartment occurs between Tregs and self-reactive Teffs *(123)*. A second clonotype (CASSLTGYSNQPQHF) was detected at low frequency (8 in 100,000) in the unstimulated Teff repertoire of an untreated patient with MS (Figure 5D). By contrast, none of the clonotypes was recognised either in Treg and in Teff cells isolated from three healthy donors. We next searched identified clonotypes into available datasets of TCRs with known antigen specificity and TCR Vβ sequencing data of MS brain lesions. However, no clonotypes were discovered using this method. These findings indicate that autoreactive Treg and Teff cell clones are rare and might share a public TCR Vβ clonotype.

A.

	TCRVβ				TCRVα			
TCC	**V-gene**	**J-gene**	**CDR3**	**Fraction**	**V-gene**	**J-gene**	**CDR3**	**Fraction**
TCC_1C7	TRBV2*	TRBJ1-6*	CASRPIETRSPLHF	0.68	TRAV40*	TRAJ34*	CLLSMYNTDKLIF	0.28
TCC_2C8	TRBV7-3*	TRBJ2-6*	CASSLTIGALSGANVLTF	0.76	TRAV19*	TRAJ5*	CALIREGRRALTF	0.18
TCC_2D8	TRBV19*	TRBJ1-1*	CASSMNRGGNTEAFF	0.24	TRAV26-1*	TRAJ30*	CIVRVHDDKIIF	0.64
TCC_3B3	TRBV6-1*	TRBJ2-3*	CASSTGTGGLPTQYF	0.45	TRAV17*	TRAJ8*	CATDGGNTGFQKLVF	0.30
TCC_3C11	TRBV2*	TRBJ2-3*	CASSDGGMVTDTQYF	0.78	TRAV12-1*	TRAJ44*	CVVKTGTASKLTF	0.17
TCC_4C2	TRBV2*	TRBJ1-4*	CASRATVATNEKLFF	0.67	TRAV9-2*	TRAJ11*	CALSENSGYSTLTF	0.16
TCC_5E8	TRBV5-6*	TRBJ1-5*	CASSLTGYSNQPQHF	0.61	TRAV12-3*	TRAJ54*	CAMIFQGAQKLVF	0.35

B.

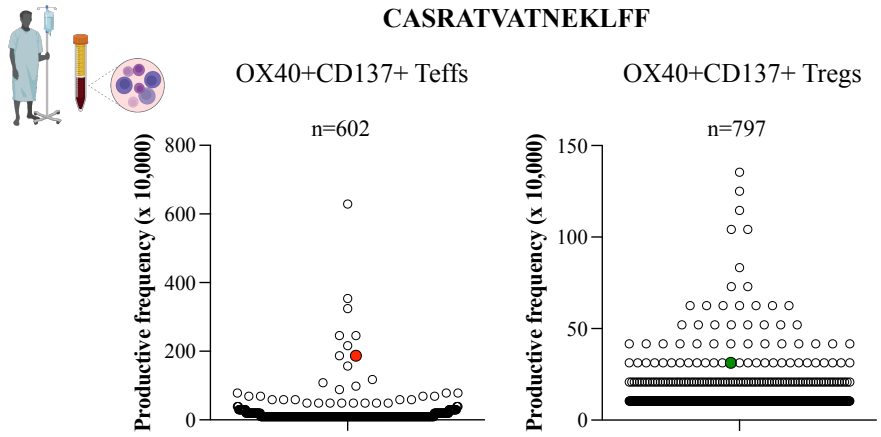

C.

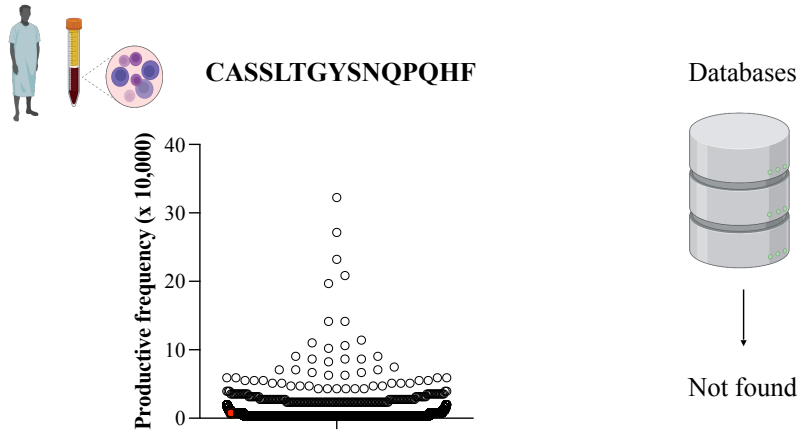

Figure 27. Detection of autoreactive clonotypes in TCR repertoires. (A) Alpha and beta chain CDR3 nucleotide sequences of MBP-specific TCCs. **(B)** One clonotype identified in TCR repertoire of the same donor either in Teff and Treg compartment after stimulation with MBP. n= number of productive TCR templates. **(C)** One clonotype found in unstimulated

Teff TCR repertoire of an untreated patient with MS. No clonotypes detected in databases of TCRs with known antigen specificity.

5.0 CONCLUSIONS

Since the discovery of Tregs, almost 30 years ago, the field of Treg research has rapidly expanded. A detailed characterisation of Tregs has been provided at the molecular, phenotypical and functional level. Novel Treg subsets have been described, including CD8+ Tregs and tissue-resident Tregs *(49, 53, 54, 58)*. Unexpected functions, such as regulation of metabolism and tissue repair and regeneration, have been discovered *(75)*. Tregs have been shown to be deleterious in some pathological settings, such as inducing immunosuppression in tumors or infections, or secreting Th-like cytokines under inflammatory conditions. By contrast, they have been found to be protective against autoimmunity, and their function has been supposed to be impaired in autoimmune diseases. The clearest example of Treg defect is represented by IPEX, a primary immunodeficiency caused by mutations in Foxp3 *(36)*. Due to the heterogeneous genotype, affected patients have low/absent or present, but unstable and impaired, Tregs *(60)*. The phenotype is characterised by autoimmune manifestations involving endocrine glands, skin and gut *(36)*. The importance of Tregs in preventing autoimmunity is evident, however their role is less intuitive in complex multifactorial autoimmune diseases, such as MS. In fact, several genetic and environmental factors have been hypothesised to predispose to MS, but their respective contribution and the way they interact are poorly understood. Previously, our group found that the HLA-DR15 haplotype, the main genetic risk factor, shapes an autoreactive T cell repertoire by presenting foreign peptides and autoantigens to autoreactive CD4+ T cells *(13)*. Additional susceptibility genes play a role in innate and adaptive immunity. Moreover, infections shape the immune system. Furthermore, several studies have reported a Treg dysfunction in some but not all the patients with MS, being Treg functionality influenced by disease stage and duration. Nevertheless, the underlying mechanisms have not been elucidated yet. We aim at providing a comprehensive analysis of the mechanisms underlying the presumed functional Treg defect in patients with MS. Towards this end, we selected a cohort of 41 individuals that recapitulated the demographical features of MS. The age of the patients ranged between 21 and 62 years (Table 9), reflecting the age distribution of the disease *(2)*. The female:male ratio was 3:2 and was

not significantly different between patients and HDs, whereas it is generally reported to range from 2:1 to 3:1 *(2)*. In contrast to HDs, the majority of patients carried the HLA-DR15 allele. Thus, we cannot exclude an effect of HLA-DR15 haplotype on T cell immunophenotype. Furthermore, our cohort included untreated individuals and patients treated with natalizumab and anti-CD20 therapy. It is important to note that all the patients are recommended to start a disease-modifying treatment (DMT) soon after diagnosis to reduce the risk of new brain lesions and relapses and slow disease progression *(141)*. The most common approach in patients with moderately active disease is to start with a base therapy, such as IFN-β, glatiramer acetate, teriflunomide, and dimethyl fumarate *(141)*. Natalizumab and anti-CD20 therapy are considered higher-efficacy agents and used for initial therapy in patients with highly active or rapidly evolving aggressive disease *(141)*. The a-CD20 agent ocrelizumab is the only DMT approved to treat PPMS. Nevertheless, each therapeutic approach needs to be personalised. Untreated patients were assessed before starting the initial treatment, or were treated with a base therapy and had discontinued the treatment for at least three months because they were clinically stable. Untreated patients have been suggested to have a lower clinical severity and thus they might have shown a milder phenotype *(142)*. Natalizumab blocks the interaction between α4 integrins and VCAM-1 that is important not only for leukocyte adhesion to the endothelium and transmigration across the brain barrier, but also for lymphocyte activation and proliferation *(92)* and for retention of B cells in the bone marrow and secondary lymphoid organs *(94)*. The main mechanism of anti-CD20 therapy is binding to CD20, expressed on the surface of all B cells, except early pro-B cells, plasma blasts and plasma cells, and inducing lysis by antibody-dependent complement- or cell-mediated cytotoxicity *(95)*. Whereas a small fraction of CD20-expressing T cells is depleted *(96)*, T cells are mostly diminished because in absence of B cells, they are not supported by antigen presentation, and are thus deprived of a stimulus necessary for their activation and proliferation *(96)*.

To characterise Treg compartment we applied multiple experimental approaches, including immunophenotyping, functional tests, Treg TCR repertoire analysis and next generation RNA sequencing (Figure 28). We used a novel gating strategy, based on the expression of CD45RA and GPA33, to identify two subsets of Tregs with a differential gene expression that was compatible with their thymic or peripheral origin. In addition, we observed a small subset of CD45RA-GPA33+ Tregs that would require additional studies to address whether it is a

distinct entity, for instance by transcriptome analysis. We found no evidence for reduced numbers of CD25+CD127lo T cells, but we observed a reduced Foxp3 expression in Tregs derived from patients, in agreement with previous reports *(79, 143)*. One limitation of our study was the unavailability of the absolute blood lymphocyte numbers. As the frequency of CD3+CD4+ cells was reduced in patients, it would have been meaningful to check whether the absolute number of Tregs was secondarily decreased. Furthermore, we detected an increased expression of CD127 and CD39 on Tregs. These molecules identify activated and functional Tregs *(144)*. Accordingly, the frequency of CD39+ Tregs inversely correlated with the percentage of t-Tregs. Whereas CD39 has been described to be abnormally upregulated in patients with active disease *(88)*, CD127 high Tregs have been associated with decreased inhibitory function *(145)*. Of note, the reduced frequency of Foxp3+ Tregs and the increased CD127 expression on Tregs were predominant in a-CD20-treated in comparison to untreated patients. Moreover, we found a reduced expression of CD49d mainly in Tregs derived from natalizumab-treated patients. As Tregs constitutively express lower surface levels of CD49d, they have been expected to be influenced less by natalizumab. By contrast, we confirmed their susceptibility to the treatment *(146)*. Next, we observed a reduced frequency of t-Tregs in younger, but not in older, patients with MS. This may reflect a reduced thymic output during early disease stages that has already been reported *(83)*. Accordingly, the proportion of t-Tregs was correlated with the diversity of Treg TCR repertoire. The etiology of premature thymic involution is unknown, but viruses causing intrathymic inflammation, such as EBV, a well-known environmental risk factor for MS, might play a role. This hypothesis has already been suggested as possible pathogenic mechanism for myasthenia gravis, but additional studies are required to fully address this *(147)*. Moreover, the finding of a reduced Foxp3 expression not only in t-Tregs, but also in p-Tregs, supports the existence of additional peripheral pathogenic mechanisms. The total number of Tregs is maintained constant during ageing by compensatory mechanisms, such as homeostatic proliferation and conversion of Teffs into Tregs *(148)*. The frequency of p-Tregs, which are supposed to derive from Teffs, was increased, but not significantly, in our cohort. In older patients we found an increased frequency of CD45RA-GPA33+ t-Tregs. This subset might have some similarities with memory-like CD45RAlow Tregs that have been detected in older patients with MS with longer clinical remission *(87, 149)*. Furthermore, Tregs can recirculate between blood, lymph nodes and tissues, where they have been shown to accumulate with age *(148)*. Peripheral

Tregs can even migrate to the thymus to regulate T cell development by feedback mechanisms. Due to age-dependent Treg compartmentalization, it is still not clear how Treg number and function evolve with ageing. Current available evidences are conflicting. Treg function has been described to be alternatively reduced predisposing to autoimmunity, or increased predisposing to cancer and infections in the elderly *(119)*. Additional studies are required to address the age-dependent changes of Treg homeostasis, both in healthy individuals and in patients with MS.

The frequency of t-Tregs was correlated with Treg inhibitory capacity, but we found that this was reduced only in natalizumab-treated patients. Numerous studies have reported a functional Treg defect in patients with MS *(76, 78, 81)*, but this report was inconstant, being Treg function variable during the disease process and more affected in the early phase *(82)*. Nevertheless, previous studies were mostly performed on cohorts of untreated patients or mixed cohorts of treated and untreated subjects, but did not compare groups treated with different immunomodulatory therapies. Some longitudinal studies assessed Treg function pre- and after-treatment, for instance Stenner et al. excluded direct changes in Treg function after natalizumab infusion *(81)*. The design of our study, that was not longitudinal, limits our conclusions regarding a direct relationship between treatment and phenotype. Nevertheless, several limitations are related to the *in vitro* analysis of Treg function: we used a standardised number of cells, potentially correcting any numerical Treg defect, and we did not examine in depth the intrinsic Teff proliferative capacity. In fact, an enhanced T cell autoproliferation with production of proinflammatory cytokines after natalizumab treatment has been reported *(13)*. This autoproliferation might be sustained by circulating B cells that are increased *(13)*. In contrast, a-CD20 therapy inhibits T cell autoproliferation and proinflammatory cytokines secretion *(13)*. When we analysed the TCR repertoire for clonotypes reported in publicly available databases to be associated with MS, we observed that we they were augmented in natalizumab-treated patients as compared to a-CD20-treated individuals, suggesting a retention of autoreactive T cells in the periphery. Consistently, we found increased inflammatory cytokines in the supernatants from suppression assays performed in natalizumab-treated as compared to a-CD20 treated patients. However, we could not determine whether the decreased Treg function in natalizumab-treated patients was due to an intrinsic Treg defect or whether Teffs were refractory to suppression due to an increased autoproliferation.

Regarding the TCR repertoire of Tregs, Föhse *et al*. suggested that the breath of the repertoire influences Treg function *(124)*. Overall, we observed a reduced repertoire diversity of Tregs in comparison to Teffs and the overlap between the two repertoires was limited. Treg TCR repertoire diversity was not significantly decreased in patients as compared to HDs and we did not find a correlation between Treg repertoire diversity and Treg inhibitory capacity. However, the number of individuals that we studied by TCR sequencing was limited, and additional data are needed to understand the role of Treg TCR repertoire in MS pathogenesis.

Furthermore, we detected severe gene expression alterations in t-Tregs, but not in p-Tregs derived from natalizumab-treated patients. Most of the genes, especially those involved in T cell activation, proliferation, and metabolism, were downregulated in comparison to HDs. Some of the genes with an altered expression are listed among the risk susceptibility genes for MS *(7)*. Among these genes, we observed an upregulation of IL7R (CD127) that was negatively correlated with Treg function. IL7R is involved in thymic T cell differentiation and influences T cell response to immunological stimuli *(150, 151)*. In a mouse model for MS, it has been shown that t-Tregs express IL7R during active disease *(152)*. Thus, the increased CD127 expression in patients with MS could be a consequence to counterbalance the reduced thymic Treg neogenesis and contribute to the functional Treg impairment. Moreover, we detected an altered expression of TXK and STAB1. TXK is implicated in Th1 differentiation. An altered differentiation program has been shown to render Tregs dysfunctional *(85)*. An additional candidate that could account for t-Treg dysfunction is TXNIP. Similarly to IL7R, it might be induced in t-Tregs and contribute to their reduced proliferative capacity. Interestingly, TXNIP transcript showed the most significant induction in twins with MS compared with unaffected twins *(153)*. The evidence of a "pathogenic" transcriptome in natalizumab-treated patients suggests an intrinsic defect in t-Tregs that might be related to a thymic dysfunction. DiGeorge syndrome, caused by the 22q11.2 deletion and characterized by defective heart and thymus embryogenesis, shows the effects of thymic abnormalities on T cell homeostasis. Indeed, patients with this syndrome display variable degrees of T cell deficiency and loss of Treg suppressive capacity leading to autoimmune manifestations *(154)*. Following a reduced thymic output of CD4+ T cells, a compensatory homeostatic proliferative response might be induced, leading to the generation of autoreactive T cells *(155)*. In conclusion, we found several possible pathogenic mechanisms that could account for Treg dysfunction in patients with MS, such as a reduced frequency of t-Tregs, an altered gene

expression in t-Tregs, compromising their proliferative capacity, and an increased Teff autoproliferation (Figure 28). In addition, we detected compensatory mechanisms that might improve or worsen Treg function, such as CD39, CD127 and CD45RA expression (Figure 28). These findings have implications for the adoptive Treg therapy as strategy to replace Treg function. The use of t-Tregs might be preferable to compensate the impaired thymic T cell development. The group of patients that would benefit of adoptive Treg therapy has to be defined. Natalizumab-treated patients, having a more compromised function, would benefit more, but infusing back into such patients defective Tregs might be useless. As there are already highly effective treatments for MS, it is not clear whether Treg-based therapy should be reserved to the non-responsive forms, such as primary progressive or generally progressive patients, or should be the first-line option. Further research is necessary to design the best strategy for adoptive transfer of Tregs. Treg-based therapy should be safe, antigen-specific, with a low risk of general immunosuppression and conversion of Tregs into Teffs, and more durable than conventional therapies. In peripheral blood from a patient with MS, we identified Tregs responsive to MBP which expanded under antigen-specific stimulation. Here, we provide the first description of functional myelin-specific Treg-derived clones. We found that they recognised not only immunodominant MBP sequences, but also sequences located at the C-terminal region of MBP, suggesting an epitope spreading in the same patient. Furthermore, they did not produce IFN-γ. We also observed that they differ for stability of Foxp3 expression and suppressive capacity. Three clones showed high Foxp3 expression and were fully suppressive. One clone was among the most-frequent expanded clonotypes after antigen-specific stimulation. Additional investigations are ongoing to understand the origin of these clones, whether they are actually Tregs or Teffs, and their potential use as source of TCRs for adoptive Treg therapy.

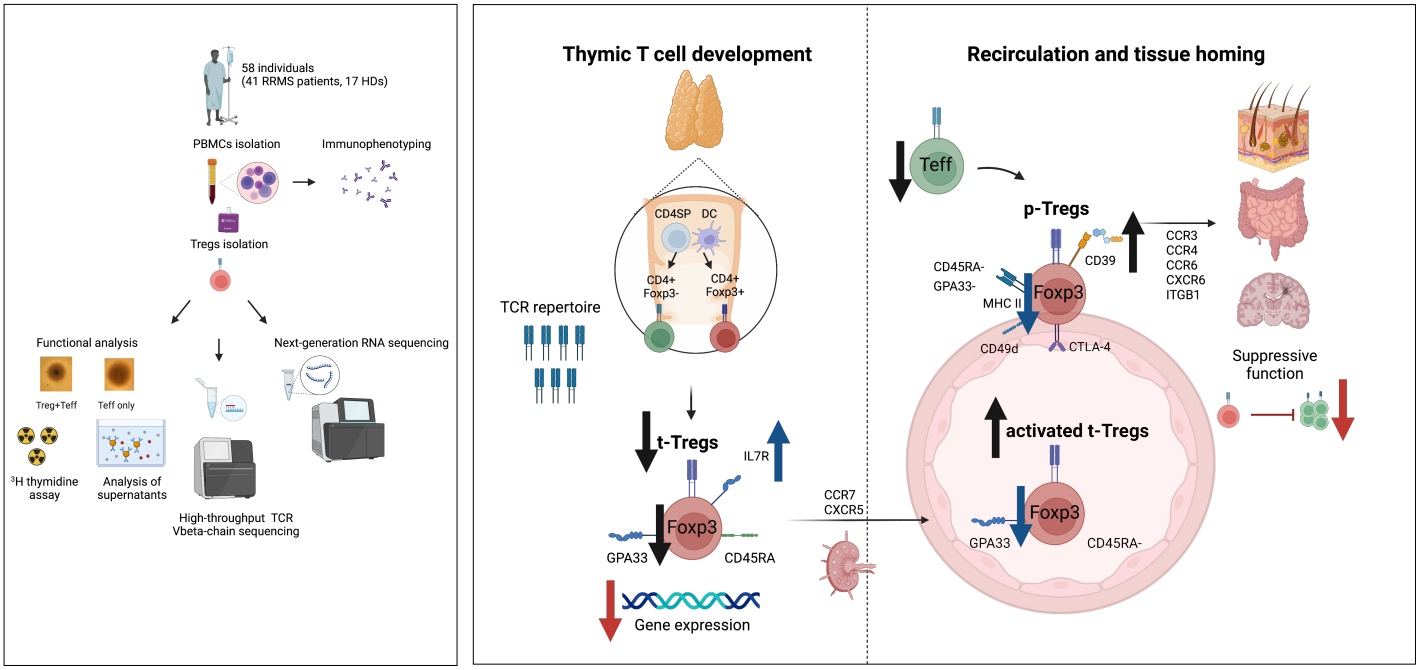

Figure 28. **Summary of the spectrum of Treg alterations in patients with RRMS.** The panel on the left shows the experimental strategy used to analyze Treg compartment in 41 patients with RRMS as compared to 17 HDs. The panel on the right summarizes Treg alterations, variably affecting thymus- and peripherally-derived compartments, in patients with MS. Black arrow: alteration found in patients with MS; red arrow: alteration mostly detected in natalizumab-treated patients; blue arrow: alteration mainly affecting a-CD20-treated patients. Created with Biorender.com.

5.1 Contributions

This research was funded by the University of Zurich via the Clinical Research Priority Project Precision-MS awarded to R. Martin. Blood samples were collected by the clinical team and processed by the members of the laboratory team at NIMS. Leukaphereses were performed by the staff of the Hematology Clinic, University Hospital Zurich. The staff of the MS Outpatient Clinic and Day Hospital-Neurology Clinic followed patient care-related aspects of the study. RNA sequencing was performed at the Functional Genomics Center Zurich with the technical support of C.F. Aquino. L. Opitz performed the bioinformatic analysis of the RNA sequencing data. M. J. Docampo designed a panel for Treg analysis by flow cytometry. J. Ruder supported the TCR sequencing data analysis. R. Naghavian designed the peptide pool shown in Fig. 22A. S. Stutz performed the experiment shown in Fig. 22B and found that 40% of natalizumab-treated patients showed reactivity to MBP pool 3. W. Faigle designed the tetramers used in Fig. 25D, wrote the paragraph 3.8, and supervised the whole project. R. Martin conceptualised, administered, supervised the project and acquired fundings. D. J. Mathis, W. Faigle, L. Opitz, M. J. Docampo and J. Ruder reviewed part of the thesis. R. Martin reviewed and edited the thesis.

6.0 BIBLIOGRAPHY

1. M. Sospedra, R. Martin. Immunology of Multiple Sclerosis. *Semin. Neurol.* 36(2):115-127 (2016).

2. C. Walton, R. King, L. Rechtman, W. Kaye, E. Leray, R.A. Marrie, N. Robertson, N. La Rocca, B. Uitdehaag, I. van der Mei, M. Wallin, A. Helme, C. Angood Napier, N. Rijke, P. Baneke. Rising prevalence of multiple sclerosis worldwide: Insights from the Atlas of MS, third edition. *Mult. Scler.* 26(14):1816-1821 (2020).

3. M. Charcot. Histologie de la sclerose en plaques. *Gaz Hosp*. 141:554–5. 557–8 (1868).

4. A. J. Thompson, B. L. Banwell, F. Barkhof, W. M. Carroll, T. Coetzee, G. Comi, J. Correale, F. Fazekas, M. Filippi, M. S. Freedman. Diagnosis of multiple sclerosis: 2017 revisions of the McDonald criteria. *Lancet. Neurol.* 17:162–173 (2018).

5. C. Loeb, E. Favale. Neurologia. *Società Editrice Universo* (2003).

6. R. Dutta, B. D. Trapp. Relapsing and progressive forms of multiple sclerosis: insights from pathology. *Curr. Opin. Neurol*. 27(3):271-8 (2014).

7. International Multiple Sclerosis Genetics Consortium. Multiple sclerosis genomic map implicates peripheral immune cells and microglia in susceptibility. *Science*. 365(6460):eaav7188 (2019).

8. R. Martin, M. Sospedra, T. Eiermann, T. Olsson. Multiple sclerosis: doubling down on MHC. *Trends Genet*. 37(9):784-797 (2021).

9. A. Ascherio. Environmental factors in multiple sclerosis. *Expert Rev. Neurother*. 13(12 Suppl):3-9 (2013).

10. J. Menegatti, D. Schub, M. Schäfer, F. A. Grässer, K. Ruprecht. HLA-DRB1*15:01 is a co-receptor for Epstein-Barr virus, linking genetic and environmental risk factors for multiple sclerosis. *Eur. J. Immunol.* 51(9):2348-2350 (2021).

11. A. G. Baxter. The origin and application of experimental autoimmune encephalomyelitis. *Nat. Rev. Immunol*. 7(11):904–912 (2007).

12. R. Martin, H. F. McFarland, D. E. McFarlin. Immunological aspects of demyelinating diseases. *Annu. Rev. Immunol*. 10:153-87 (1992).

13. J. Wang, I. Jelcic, L. Mühlenbruch, V. Haunerdinger, N. C. Toussaint, Y. Zhao, C. Cruciani, W. Faigle, R. Naghavian, M. Foege, T. M. C. Binder, T. Eiermann, L. Opitz, L. Fuentes-Font, R. Reynolds, W. W. Kwok, J. T. Nguyen, J. H. Lee, A. Lutterotti, C. Münz, H. G. Rammensee, M. Hauri-Hohl, M. Sospedra, S. Stevanovic, R. Martin. HLA-DR15 Molecules Jointly Shape an Autoreactive T Cell Repertoire in Multiple Sclerosis. *Cell*. 183(5):1264-1281.e20 (2020).

14. I. Jelcic, F. Al Nimer, J. Wang, V. Lentsch, R. Planas, I. Jelcic, A. Madjovski , S. Ruhrmann, W. Faigle, K. Frauenknecht, C. Pinilla, R. Santos, C. Hammer, Y. Ortiz, L. Opitz, H. Grönlund, G. Rogler, O. Boyman, R. Reynolds, A. Lutterotti, M. Khademi, T. Olsson, F. Piehl, M. Sospedra, R. Martin. Memory B Cells Activate Brain-Homing, Autoreactive CD4+ T Cells in Multiple Sclerosis. *Cell*. 175(1):85-100.e23 (2018).

15. R. Martin, M. Sospedra, M. Rosito, B. Engelhardt. Current multiple sclerosis treatments have improved our understanding of MS autoimmune pathogenesis. *Eur. J. Immunol*. 46(9):2078-90 (2016).

16. R. Planas, R. Santos, P. Tomas-Ojer, C, Cruciani, A. Lutterotti, W. Faigle, N. Schaeren-Wiemers, C. Espejo, H. Eixarch, C. Pinilla, R. Martin, M. Sospedra. GDP-l-fucose synthase is a CD4+ T cell-specific autoantigen in DRB3*02:02 patients with multiple sclerosis. *Sci. Transl. Med*. 10(462):eaat4301 (2018).

17. I. Bechmann, I. Galea, V. H. Perry. What is the blood-brain barrier (not)? *Trends Immunol.* 28(1):5-11 (2007).

18. J. M. Fletcher, S. J. Lalor, C. M. Sweeney, N. Tubridy, K. H. Mills. T cells in multiple sclerosis and experimental autoimmune encephalomyelitis. *Clin. Exp. Immunol*. 162(1):1-11 (2010).

19. H. Kebir, K. Kreymborg, I. Ifergan, A. Dodelet-Devillers, R. Cayrol, M. Bernard, F. Giuliani, N. Arbour, B. Becher, A. Prat. Human TH17 lymphocytes promote blood-brain barrier disruption and central nervous system inflammation. *Nat. Med*. 13(10):1173-5 (2007).

20. I. Cosorich, G. Dalla-Costa, C. Sorini, R. Ferrarese, M. J. Messina, J. Dolpady, E. Radice, A. Mariani, P. A. Testoni, F. Canducci, G. Comi, V. Martinelli, M. Falcone. High frequency

of intestinal TH17 cells correlates with microbiota alterations and disease activity in multiple sclerosis. *Sci Adv*. 12;3(7):e1700492 (2017).

21. R. Planas, I. Metz, R. Martin, M. Sospedra. Detailed Characterization of T Cell Receptor Repertoires in Multiple Sclerosis Brain Lesions. *Front. Immunol*. 9:509 (2018).

22. C. M. Costantino, C. Baecher-Allan, D. A. Hafler. Multiple sclerosis and regulatory T cells. J. Clin. Immunol. 28(6):697-706 (2008).

23. M. Mimpen, J. Smolders, R. Hupperts, J. Damoiseaux. Natural killer cells in multiple sclerosis: A review. *Immunol. Lett*. 222:1-11 (2020).

24. J. Ruder, J. Rex, S. Obahor, M. J. Docampo, A. M. S. Müller, U. Schanz, I. Jelcic, R. Martin. NK Cells and Innate-Like T Cells After Autologous Hematopoietic Stem Cell Transplantation in Multiple Sclerosis. *Front. Immunol.* 12:794077 (2021).

25. M. T. Cencioni, M. Mattoscio, R. Magliozzi, A. Bar-Or, P. A. Muraro. B cells in multiple sclerosis - from targeted depletion to immune reconstitution therapies. *Nat. Rev. Neurol*. 17(7):399-414 (2021).

26. B. Thi Cuc, J. Pohar, S. Fillatreau. Understanding regulatory B cells in autoimmune diseases: the case of multiple sclerosis. *Curr. Opin. Immunol*. 61:26-32 (2019).

27. B. L. Guerrero, N. L. Sicotte. Microglia in Multiple Sclerosis: Friend or Foe? *Front. Immunol*. 20;11:374 (2020).

28. M. De Bondt, N. Hellings, G. Opdenakker, S. Struyf. Neutrophils: Underestimated Players in the Pathogenesis of Multiple Sclerosis (MS). *Int. J. Mol. Sci*. 26;21(12):4558 (2020).

29. R. K. Gershon, K. Kondo. Cell interactions in the induction of tolerance: the role of thymic lymphocytes. *Immunology.* 18(5):723-37 (1970).

30. S. Sakaguchi. Regulatory T cells: history and perspective. *Methods Mol. Biol*. 707:3-17. (2011).

31. S. Sakaguchi, N. Sakaguchi, M. Asano, M. Itoh, M. Toda. Immunologic self-tolerance maintained by activated T cells expressing IL-2 receptor alpha-chains (CD25). Breakdown of a single mechanism of self-tolerance causes various autoimmune diseases. *J. Immunol*. 155(3):1151-64 (1995).

32. H. Groux, A. O'Garra, M. Bigler, M. Rouleau, S. Antonenko, J. E. de Vries, M. G. Roncarolo. A CD4+ T-cell subset inhibits antigen-specific T-cell responses and prevents colitis. *Nature*. 16;389(6652):737-42 (1997).

33. M. E. Brunkow, E. W. Jeffery, K. A. Hjerrild, B. Paeper, L. B. Clark, S. A. Yasayko, J. E. Wilkinson, D. Galas, S. F. Ziegler, F. Ramsdell. Disruption of a new forkhead/winged-helix protein, scurfin, results in the fatal lymphoproliferative disorder of the scurfy mouse. *Nat. Genet.* 27(1):68-73 (2001).

34. E. Bettelli, M. Dastrange, M. Oukka. Foxp3 interacts with nuclear factor of activated T cells and NF-kappa B to repress cytokine gene expression and effector functions of T helper cells. *Proc. Natl. Acad. Sci. USA*. 102(14):5138-43 (2005).

35. U. Baron, S. Floess, G. Wieczorek, K. Baumann, A. Grützkau, J. Dong, A. Thiel, T. J. Boeld, P. Hoffmann, M. Edinger, I. Türbachova, A. Hamann, S. Olek, J. Huehn. DNA demethylation in the human FOXP3 locus discriminates regulatory T cells from activated FOXP3(+) conventional T cells. *Eur. J. Immunol*. 37(9):2378-89 (2007).

36. R. S. Wildin, F. Ramsdell, J. Peake, F. Faravelli, J. L. Casanova, N. Buist, E. Levy-Lahad, M. Mazzella, O. Goulet, L. Perroni, F. D. Bricarelli, G. Byrne, M. McEuen, S. Proll, M. Appleby, M. E. Brunkow. X-linked neonatal diabetes mellitus, enteropathy and endocrinopathy syndrome is the human equivalent of mouse scurfy. *Nat. Genet.* 27(1):18–20 (2001).

37. W. Liu, A. L. Putnam, Z. Xu-Yu, G. L. Szot, M. R. Lee, S. Zhu, P. A. Gottlieb, P. Kapranov, T. R. Gingeras, B. Fazekas de St Groth, C. Clayberger, D. M. Soper, S. F. Ziegler, J. A. Bluestone. CD127 expression inversely correlates with FoxP3 and suppressive function of human CD4+ T reg cells. *J. Exp. Med*. 10;203(7):1701-11 (2006).

38. J. H. Buckner. Mechanisms of impaired regulation by CD4(+)CD25(+)FOXP3(+) regulatory T cells in human autoimmune diseases. *Nat. Rev. Immunol*. 10(12):849-59 (2010).

39. X. Chen, J. J. Oppenheim. Resolving the identity myth: key markers of functional CD4+FoxP3+ regulatory T cells. *Int. Immunopharmacol*. 11(10):1489-96 (2011).

40. E. Cuadrado, M. van den Biggelaar, S. de Kivit, Y. Y. Chen, M. Slot, I. Doubal, A. Meijer, R. A. W. van Lier, J. Borst, D. Amsen. Proteomic Analyses of Human Regulatory T Cells Reveal Adaptations in Signaling Pathways that Protect Cellular Identity. *Immunity*. 48(5):1046-1059.e6 (2018).

41. M. Sambucci, F. Gargano, G. Guerrera, L. Battistini, G. Borsellino. One, No One, and One Hundred Thousand: T Regulatory Cells' Multiple Identities in Neuroimmunity. *Front. Immunol*. 20;10:2947 (2019).

42. A. M. Thornton, P. E. Korty, D. Q. Tran, E. A. Wohlfert, P. E. Murray, Y. Belkaid, E. M. Shevach. Expression of Helios, an Ikaros transcription factor family member, differentiates thymic-derived from peripherally induced Foxp3+ T regulatory cells. *J. Immunol*. 184(7):3433-41 (2010).

43. J. B. Wing, A. Tanaka, S. Sakaguchi. Human FOXP3+ Regulatory T Cell Heterogeneity and Function in Autoimmunity and Cancer. *Immunity*. 50(2):302-316 (2019).

44. K. Bin Dhuban, E. d'Hennezel, E. Nashi, A. Bar-Or, S. Rieder, E. M. Shevach, S. Nagata, C. A. Piccirillo. Coexpression of TIGIT and FCRL3 identifies Helios+ human memory regulatory T cells. *J. Immunol*. 194(8):3687-96 (2015).

45. A. Nowak, D. Lock, P. Bacher, T. Hohnstein, K. Vogt, J. Gottfreund, P. Giehr, J. K. Polansky, B. Sawitzki, A. Kaiser, J. Walter, A. Scheffold. CD137+CD154- Expression As a Regulatory T Cell (Treg)-Specific Activation Signature for Identification and Sorting of Stable Human Tregs from In Vitro Expansion Cultures. *Front. Immunol*. 9:199 (2018).

46. A. S. Gautron, M. Dominguez-Villar, M. de Marcken, D. A. Hafler. Enhanced suppressor function of TIM-3+ FoxP3+ regulatory T cells. *Eur. J. Immunol*. 44(9):2703-2711 (2014).

47. C. T. Huang, C. J. Workman, D. Flies, X. Pan, A. L. Marson, G. Zhou, E. L. Hipkiss, S. Ravi, J. Kowalski, H. I. Levitsky, J. D. Powell, D. M. Pardoll, C. G. Drake, D. A. Vignali. Role of LAG-3 in regulatory T cells. *Immunity*. 21(4):503-13 (2004).

48. E. Kieback, E. Hilgenberg, U. Stervbo, V. Lampropoulou, P. Shen, M. Bunse, Y. Jaimes, P. Boudinot, A. Radbruch, U. Klemm, A. A. Kühl, R. Liblau, N. Hoevelmeyer, S. M. Anderton, W. Uckert, S. Fillatreau. Thymus-Derived Regulatory T Cells Are Positively

Selected on Natural Self-Antigen through Cognate Interactions of High Functional Avidity. *Immunity*. 17;44(5):1114-26 (2016).

49. R. Opstelten, D. Amsen. Separating the wheat from the chaff: Making sense of Treg heterogeneity for better adoptive cellular therapy. *Immunol. Lett*. 239:96-112 (2021).

50. R. Opstelten, S. de Kivit, M. C. Slot, M. van den Biggelaar, D. Iwaszkiewicz-Grześ, M. Gliwiński, A. M. Scott, B. Blom, P. Trzonkowski, J. Borst, E. Cuadrado, D. Amsen. GPA33: A Marker to Identify Stable Human Regulatory T Cells. *J. Immunol*. 204(12):3139-3148 (2020).

51. W. Lee, G. R. Lee. Transcriptional regulation and development of regulatory T cells. *Exp. Mol. Med*. 50(3):e456 (2018).

52. M. G. Roncarolo, S. Gregori, R. Bacchetta, M. Battaglia, N. Gagliani. The Biology of T Regulatory Type 1 Cells and Their Therapeutic Application in Immune-Mediated Diseases. Immunity. 49(6):1004-1019 (2018).

53. S. Mishra, S. Srinivasan, C. Ma, N. Zhang. CD8+ Regulatory T Cell - A Mystery to Be Revealed. *Front. Immunol*. 12:708874 (2021).

54. A. Levescot, N. Cerf-Bensussan. Regulatory CD8+ T cells suppress disease. *Science*. 376(6590):243-244 (2022).

55. H. Zhao, R. Feng, A. Peng, G. Li, L. Zhou. The expanding family of noncanonical regulatory cell subsets. *J. Leukoc. Biol.* 106(2):369-383 (2019).

56. T. Duhen. R. Duhen, A. Lanzavecchia, F. Sallusto, D. J. Campbell. Functionally distinct subsets of human FOXP3+ Treg cells that phenotypically mirror effector Th cells. *Blood*. 119(19):4430-40 (2012).

57. G. R. Lee. The Balance of Th17 versus Treg Cells in Autoimmunity. *Int. J. Mol. Sci*. 19(3):730 (2018).

58. R. Zhang, J. Miao, P. Zhu. Regulatory T cell heterogeneity and therapy in autoimmune diseases. *Autoimmun. Rev*. 20(5):102715 (2021).

59. A. K. Abbas, C. Benoist, J. A. Bluestone, D. J. Campbell, S. Ghosh, S. Hori, S. Jiang, V. K. Kuchroo, D. Mathis, M. G. Roncarolo, A. Rudensky, S. Sakaguchi, E. M. Shevach, D.

A. Vignali, S. F. Ziegler. Regulatory T cells: recommendations to simplify the nomenclature. *Nat. Immunol*. 14(4):307-8 (2013).

60. F. Barzaghi, L. Passerini. IPEX Syndrome: Improved Knowledge of Immune Pathogenesis Empowers Diagnosis. *Front. Pediatr*. 9:612760 (2021).

61. H. D. Ochs, M. Oukka, T. R. Torgerson. TH17 cells and regulatory T cells in primary immunodeficiency diseases. *J. Allergy Clin. Immunol*. 123(5):977-83 (2009).

62. P. Pandiyan, L. Zheng, S. Ishihara, J. Reed, M. J. Lenardo. CD4+CD25+Foxp3+ regulatory T cells induce cytokine deprivation-mediated apoptosis of effector CD4+ T cells. *Nat. Immunol*. 8(12):1353-62 (2007).

63. D. A. Vignali, L. W. Collison, C. J. Workman. How regulatory T cells work. *Nat. Rev. Immunol*. 8(7):523-32 (2008).

64. L. Strauss, C. Bergmann, T. L. Whiteside. Human circulating CD4+CD25highFoxp3+ regulatory T cells kill autologous CD8+ but not CD4+ responder cells by Fas-mediated apoptosis. *J. Immunol*. 182(3):1469-80 (2009).

65. N. Mitsuiki, C. Schwab, B. Grimbacher. What did we learn from CTLA-4 insufficiency on the human immune system? *Immunol. Rev.* 287(1):33-49 (2019).

66. P. Gu, J. F. Gao, C. A. D'Souza, A. Kowalczyk, K. Y. Chou, L. Zhang. Trogocytosis of CD80 and CD86 by induced regulatory T cells. *Cell. Mol. Immunol*. 9(2):136-46 (2012).

67. A. Corthay. How do regulatory T cells work? *Scand. J. Immunol*. 70(4):326-36 (2009).

68. A. Kitz, M. Dominguez-Villar. Molecular mechanisms underlying Th1-like Treg generation and function. *Cell. Mol. Life Sci*. 74(22):4059-4075 (2017).

69. J. Pohar, Q. Simon, S. Fillatreau. Antigen-Specificity in the Thymic Development and Peripheral Activity of CD4+FOXP3+ T Regulatory Cells. *Front. Immunol*. 9:1701 (2018).

70. M. Izraelson, T. O. Nakonechnaya, B. Moltedo, E. S. Egorov, S. A. Kasatskaya, E. V. Putintseva, I. Z. Mamedov, D. B. Staroverov, I. I. Shemiakina, M. Y. Zakharova, A. N. Davydov, D. A. Bolotin, M. Shugay, D. M. Chudakov, A. Y. Rudensky, O. V. Britanova. Comparative analysis of murine T-cell receptor repertoires. *Immunology*. 153(2):133-144 (2018).

71. R. Pacholczyk, J. Kern, N. Singh, M. Iwashima, P. Kraj, L. Ignatowicz. Non self-antigens are the cognate specificities of Foxp3+ regulatory T cells. *Immunity*. 27(3):493-504 (2007).

72. H. M. van Santen, C. Benoist, D. Mathis. Number of T reg cells that differentiate does not increase upon encounter of agonist ligand on thymic epithelial cells. *J. Exp. Med*. 200(10):1221-30 (2004).

73. N. Fazilleau, H. Bachelez, M. L. Gougeon, M. Viguier. Cutting edge: size and diversity of CD4+CD25high Foxp3+ regulatory T cell repertoire in humans: evidence for similarities and partial overlapping with CD4+CD25- T cells. *J. Immunol*. 179(6):3412-6 (2007).

74. X. Zhang, D. N. Koldzic, L. Izikson, J. Reddy, R. F. Nazareno, S. Sakaguchi, V. K. Kuchroo, H. L. Weiner. IL-10 is involved in the suppression of experimental autoimmune encephalomyelitis by CD25+CD4+ regulatory T cells. *Int. Immunol*. 16(2):249-56 (2004).

75. Y. Dombrowski, T. O'Hagan, M. Dittmer, R. Penalva, S. R. Mayoral, P. Bankhead, S. Fleville, G. Eleftheriadis, C. Zhao, M. Naughton, R. Hassan, J. Moffat, J. Falconer, A. Boyd, P. Hamilton, I. V. Allen, A. Kissenpfennig, P. N. Moynagh, E. Evergren, B. Perbal, A. C. Williams, R. J. Ingram, J. R. Chan, R. J. M. Franklin, D. C. Fitzgerald. Regulatory T cells promote myelin regeneration in the central nervous system. *Nat. Neurosci*. 20(5):674-680 (2017).

76. V. Viglietta, C. Baecher-Allan, H. L. Weiner, D. A. Hafler. Loss of functional suppression by CD4+CD25+ regulatory T cells in patients with multiple sclerosis. *J. Exp. Med*. 199(7):971-9 (2004).

77. U. Feger, C. Luther, S. Poeschel, A. Melms, E. Tolosa, H. Wiendl. Increased frequency of CD4+ CD25+ regulatory T cells in the cerebrospinal fluid but not in the blood of multiple sclerosis patients. *Clin. Exp. Immunol*. 147(3):412-8 (2007).

78. K. Venken, N. Hellings, M. Thewissen, V. Somers, K. Hensen, J. L. Rummens, R. Medaer, R. Hupperts, P. Stinissen. Compromised CD4+ CD25(high) regulatory T-cell function in patients with relapsing-remitting multiple sclerosis is correlated with a reduced frequency of FOXP3-positive cells and reduced FOXP3 expression at the single-cell level. *Immunology.* 123(1):79-89 (2008).

79. Y. F. Li, S.X. Zhang, X. W. Ma, Y. L. Xue, C. Gao, X.Y. Li, A. D. Xu. The proportion of peripheral regulatory T cells in patients with Multiple Sclerosis: A meta-analysis. *Mult. Scler. Relat. Disord*. 28:75-80 (2019).

80. B. Fritzsching, J. Haas, F. König, P. Kunz, E. Fritzsching, J. Pöschl, P. H. Krammer, W. Brück, E. Suri-Payer, B. Wildemann. Intracerebral human regulatory T cells: analysis of CD4+ CD25+ FOXP3+ T cells in brain lesions and cerebrospinal fluid of multiple sclerosis patients. *PLoS One*. 6(3):e17988 (2011).

81. J. Haas, A. Hug, A. Viehöver, B. Fritzsching, C. S. Falk, A. Filser, T. Vetter, L. Milkova, M. Korporal, B. Fritz, B. Storch-Hagenlocher, P. H. Krammer, E. Suri-Payer, B. Wildemann. Reduced suppressive effect of CD4+CD25high regulatory T cells on the T cell immune response against myelin oligodendrocyte glycoprotein in patients with multiple sclerosis. *Eur. J. Immunol*. 35(11):3343-52 (2005).

82. K. Venken, N. Hellings, K. Hensen, J. L. Rummens, R. Medaer, M. B. D'hooghe, B. Dubois, J. Raus, P. Stinissen. Secondary progressive in contrast to relapsing-remitting multiple sclerosis patients show a normal CD4+CD25+ regulatory T-cell function and FOXP3 expression. *J. Neurosci. Res*. 83(8):1432-46 (2006).

83. J. Haas, B. Fritzsching, P. Trübswetter, M. Korporal, L. Milkova, B. Fritz, D. Vobis, P. H. Krammer, E. Suri-Payer, B. Wildemann. Prevalence of newly generated naive regulatory T cells (Treg) is critical for Treg suppressive function and determines Treg dysfunction in multiple sclerosis. *J. Immunol*. 179(2):1322-30 (2007).

84. B. Balint, J. Haas, A. Schwarz, S. Jarius, A. Fürwentsches, K. Engelhardt, C. Bussmann, F. Ebinger, B. Fritzsching, F. Paul, U. Seidel, S. Vlaho, P. Huppke, J. Gärtner, B. Wildemann. T-cell homeostasis in pediatric multiple sclerosis: old cells in young patients. *Neurology*. 81(9):784-92 (2013).

85. M. Dominguez-Villar, C. M. Baecher-Allan, D. A. Hafler. Identification of T helper type 1-like, Foxp3+ regulatory T cells in human autoimmune disease. *Nat. Med*. 17(6):673-5 (2011).

86. A. Colamatteo, F. Carbone, S. Bruzzaniti, M. Galgani, C. Fusco, G. T. Maniscalco, F. Di Rella, P. de Candia, V. De Rosa. Molecular Mechanisms Controlling Foxp3 Expression in

Health and Autoimmunity: From Epigenetic to Post-translational Regulation. *Front. Immunol*. 10:3136 (2020).

87. N. D. Verma, A. D. Lam, C. Chiu, G. T. Tran, B. M. Hall, S. J. Hodgkinson. Multiple sclerosis patients have reduced resting and increased activated CD4+CD25+FOXP3+T regulatory cells. *Sci. Rep*. 11(1):10476 (2021).

88. N. Álvarez-Sánchez, I. Cruz-Chamorro, M. Díaz-Sánchez, P. J. Lardone, J. M. Guerrero, A. Carrillo-Vico. Peripheral CD39-expressing T regulatory cells are increased and associated with relapsing-remitting multiple sclerosis in relapsing patients. *Sci. Rep*. 9(1):2302 (2019).

89. G. Borsellino, M. Kleinewietfeld, D. Di Mitri, A. Sternjak, A. Diamantini, R. Giometto, S. Höpner, D. Centonze, G. Bernardi, M. L. Dell'Acqua, P. M. Rossini, L. Battistini, O. Rötzschke, K. Falk. Expression of ectonucleotidase CD39 by Foxp3+ Treg cells: hydrolysis of extracellular ATP and immune suppression. *Blood*. 110(4):1225-32 (2007).

90. A. L. Astier, G. Meiffren, S. Freeman, D. A. Hafler. Alterations in CD46-mediated Tr1 regulatory T cells in patients with multiple sclerosis. *J. Clin. Invest*. 116(12):3252-7 (2006).

91. T. F. Benkert, L. Dietz, E. M. Hartmann, E. Leich, A. Rosenwald, E. Serfling, M. Buttmann, F. Berberich-Siebelt. Natalizumab exerts direct signaling capacity and supports a pro-inflammatory phenotype in some patients with multiple sclerosis. *PLoS One*. 7(12):e52208 (2012).

92. N. K. Damle, A. Aruffo. Vascular cell adhesion molecule 1 induces T-cell antigen receptor-dependent activation of CD4+T lymphocytes. *Proc. Natl. Acad. Sci. USA*. 88(15):6403-7 (1991).

93. J. R. Berger. Natalizumab and progressive multifocal leucoencephalopathy. *Ann. Rheum. Dis*. 65 Suppl 3(Suppl 3):iii48-53 (2006).

94. C. E. Leuker, M. Labow, W. Müller, N. Wagner. Neonatally induced inactivation of the vascular cell adhesion molecule 1 gene impairs B cell localization and T cell-dependent humoral immune response. *J. Exp. Med*. 193(6):755-68 (2001).

95. Q. Howlett-Prieto, X. Feng, J. F. Kramer, K. J. Kramer, T. W. Houston, A. T. Reder. Anti-CD20 therapy corrects a CD8 regulatory T cell deficit in multiple sclerosis. Mult. Scler. 27(14):2170-2179 (2021).

96. C. A. Roach, A. H. Cross. Anti-CD20 B Cell Treatment for Relapsing Multiple Sclerosis. *Front. Neurol*. 22;11:595547 (2021).

97. P. A. Muraro, R. Martin, G. L. Mancardi, R. Nicholas, M. P. Sormani, R. Saccardi. Autologous haematopoietic stem cell transplantation for treatment of multiple sclerosis. *Nat. Rev. Neurol*. 13(7):391-405 (2017).

98. A. Lutterotti, S. Yousef, A. Sputtek, K. H. Stürner, J. P. Stellmann, P. Breiden, S. Reinhardt, C. Schulze, M. Bester, C. Heesen, S. Schippling, S. D. Miller, M. Sospedra, R. Martin. Antigen-specific tolerance by autologous myelin peptide-coupled cells: a phase 1 trial in multiple sclerosis. *Sci. Transl. Med.* 5(188):188ra75 (2013).

99. M. Korporal, J. Haas, B. Balint, B. Fritzsching, A. Schwarz, S. Moeller, B. Fritz, E. Suri-Payer, B. Wildemann. Interferon beta-induced restoration of regulatory T-cell function in multiple sclerosis is prompted by an increase in newly generated naive regulatory T cells. *Arch. Neurol*. 65(11):1434-9 (2008).

100. M. Chiarini, R. Capra, F. Serana, D. Bertoli, A. Sottini, V. Giustini, C. Scarpazza, M. Rovaris, V. Torri Clerici, D. Ferraro, S. Galgani, C. Solaro, M. Z. Conti, A. Visconti, L. Imberti; SURROGATE Study Group. Simultaneous quantification of natural and inducible regulatory T-cell subsets during interferon-β therapy of multiple sclerosis patients. *J. Transl. Med*. 18(1):169 (2020).

101. J. Haas, M. Korporal, B. Balint, B. Fritzsching, A. Schwarz, B. Wildemann. Glatiramer acetate improves regulatory T-cell function by expansion of naive CD4(+)CD25(+)FOXP3(+)CD31(+) T-cells in patients with multiple sclerosis. *J. Neuroimmunol*. 216(1-2):113-7 (2009).

102. P. Putheti, M. Soderstrom, H. Link, Y. M. Huang. Effect of glatiramer acetate (Copaxone) on CD4+CD25high T regulatory cells and their IL-10 production in multiple sclerosis. *J. Neuroimmunol*. 144(1-2):125-31 (2003).

103. M. P. Stenner, A. Waschbisch, D. Buck, S. Doerck, H. Einsele, K. V. Toyka, H. Wiendl. Effects of natalizumab treatment on Foxp3+ T regulatory cells. *PLoS One*. 6;3(10):e3319 (2008).

104. N. Muls, H. A. Dang, C. J. Sindic, V. van Pesch. Fingolimod increases CD39-expressing regulatory T cells in multiple sclerosis patients. *PLoS One*. 20;9(11):e113025 (2014).

105. J. Schlöder, C. Berges, F. Luessi, H. Jonuleit. Dimethyl Fumarate Therapy Significantly Improves the Responsiveness of T Cells in Multiple Sclerosis Patients for Immunoregulation by Regulatory T Cells. *Int. J. Mol. Sci*. 18(2):271 (2017).

106. J. Haas, C. Würthwein, M. Korporal-Kuhnke, A. Viehoever, S. Jarius, T. Ruck, S. Pfeuffer, S. G. Meuth, B. Wildemann. Alemtuzumab in Multiple Sclerosis: Short- and Long-Term Effects of Immunodepletion on the Peripheral Treg Compartment. *Front Immunol*. 10:1204 (2019).

107. U. Oh, G. Blevins, C. Griffith, N. Richert, D. Maric, C. R. Lee, H. McFarland, S. Jacobson. Regulatory T cells are reduced during anti-CD25 antibody treatment of multiple sclerosis. *Arch. Neurol*. 66(4):471-9 (2009).

108. B. Bielekova, M. Catalfamo, S. Reichert-Scrivner, A. Packer, M. Cerna, T. A. Waldmann, H. McFarland, P. A. Henkart, R. Martin. Regulatory CD56(bright) natural killer cells mediate immunomodulatory effects of IL-2Ralpha-targeted therapy (daclizumab) in multiple sclerosis. *Proc. Natl. Acad. Sci. U. S. A*. 103(15):5941-6 (2006).

109. C. A. Dendrou, L. Fugger. Immunomodulation in multiple sclerosis: promises and pitfalls. *Curr. Opin. Immunol*. 49:37-43 (2017).

110. S. S. Duffy, B. A. Keating, G. Moalem-Taylor. Adoptive Transfer of Regulatory T Cells as a Promising Immunotherapy for the Treatment of Multiple Sclerosis. Front. Neurosci. 13:1107 (2019).

111. C. Raffin, L. T. Vo, J. A. Bluestone. Treg cell-based therapies: challenges and perspectives. Nat. Rev. Immunol. 20(3):158-172 (2020).

112. K. Chwojnicki, D. Iwaszkiewicz-Grześ, A. Jankowska, M. Zieliński, P. Łowiec, M. Gliwiński, M. Grzywińska, K. Kowalczyk, A. Konarzewska, P. Glasner, J. Sakowska, J. Kulczycka, A. Jaźwińska-Curyłło, M. Kubach, B. Karaszewski, W. Nyka, E. Szurowska, P.

Trzonkowski. Administration of CD4+CD25highCD127-FoxP3+ Regulatory T Cells for Relapsing-Remitting Multiple Sclerosis: A Phase 1 Study. *BioDrugs*. 35(1):47-60 (2021).

113. M. Vergelli, B. Mazzanti, E. Traggiai, T. Biagioli, C. Ballerini, A. Parigi, A. Konse, G. Pellicanò, L. Massacesi. Short-term evolution of autoreactive T cell repertoire in multiple sclerosis. *J. Neurosci. Res*. 66(3):517-24 (2001).

114. Y. C. Kim, A. H. Zhang, J. Yoon, W. E. Culp, J. R. Lees, K. W. Wucherpfennig, D. W. Scott. Engineered MBP-specific human Tregs ameliorate MOG-induced EAE through IL-2-triggered inhibition of effector T cells. *J. Autoimmun*. 92:77-86 (2018).

115. M. Fransson, E. Piras, J. Burman, B. Nilsson, M. Essand, B. Lu, R. A. Harris, P. U. Magnusson, E. Brittebo, A. S. Loskog. CAR/FoxP3-engineered T regulatory cells target the CNS and suppress EAE upon intranasal delivery. *J. Neuroinflammation*. 9:112 (2012).

116. M. Malviya, A. Saoudi, J. Bauer, S. Fillatreau, R. Liblau. Treatment of experimental autoimmune encephalomyelitis with engineered bi-specific Foxp3+ regulatory CD4+ T cells. *J. Autoimmun*. 108:102401 (2020).

117. S. Gregori, M. G. Roncarolo. Engineered T Regulatory Type 1 Cells for Clinical Application. *Front. Immunol*. 9:233 (2018).

118. C. S. Carlson, R. O. Emerson, A. M. Sherwood, C. Desmarais, M. W. Chung, J. M. Parsons, M. S. Steen, M. A. LaMadrid-Herrmannsfeldt, D. W. Williamson, R. J. Livingston, D. Wu, B. L. Wood, M. J. Rieder, H. Robins. Using synthetic templates to design an unbiased multiplex PCR assay. *Nat. Commun*. 4:2680 (2013).

119. C. Krishna, D. Chowell, M. Gönen, Y. Elhanati, T. A. Chan. Genetic and environmental determinants of human TCR repertoire diversity. *Immun. Ageing*. 17:26 (2020).

120. A. Lossius, J. N. Johansen, F. Vartdal, T. Holmøy. High-throughput sequencing of immune repertoires in multiple sclerosis. *Ann. Clin. Transl. Neurol*. 25;3(4):295-306 (2016).

121. A. de Paula Alves Sousa, K. R. Johnson, R. Nicholas, S.Darko, D. A. Price, D. C. Douek, S. Jacobson, P. A. Muraro. Intrathecal T-cell clonal expansions in patients with multiple sclerosis. *Ann. Clin. Transl. Neurol.* 3(6):422-33 (2016).

122. F. Hayashi, N. Isobe, J. Glanville, T. Matsushita, G. Maimaitijiang, S. Fukumoto, M. Watanabe, K. Masaki, J. I. Kira. A new clustering method identifies multiple sclerosis-specific T-cell receptors. *Ann. Clin. Transl. Neurol.* 8(1):163-176 (2021).

123. J. B. Wing, S. Sakaguchi. TCR diversity and Treg cells, sometimes more is more. *Eur. J. Immunol*. 41:3097-3100 (2011).

124. L. Föhse, J. Suffner, K. Suhre, B. Wahl, C. Lindner, C. W. Lee, S. Schmitz, J.D. Haas, S. Lamprecht, C. Koenecke, A. Bleich, G. J. Hämmerling, B. Malissen, S. Suerbaum, R. Förster, I. Prinz. High TCR diversity ensures optimal function and homeostasis of Foxp3+ regulatory T cells. *Eur. J. Immunol.* 41(11):3101-13 (2011).

125. R. Amoriello, M. Chernigovskaya, V. Greiff, A. Carnasciali, L. Massacesi, A. Barilaro, A. M. Repice, T. Biagioli, A. Aldinucci, P. A. Muraro, D. A. Laplaud, A. Lossius, C. Ballerini. TCR repertoire diversity in Multiple Sclerosis: High-dimensional bioinformatics analysis of sequences from brain, cerebrospinal fluid and peripheral blood. *EBioMedicine*. 68:103429 (2021).

126. N. P. Smith, B. Ruiter, Y. V. Virkud, A. A. Tu, B. Monian, J. J. Moon, J. C. Love, W. G. Shreffler. Identification of antigen-specific TCR sequences based on biological and statistical enrichment in unselected individuals. *JCI Insight*. 6(13):e140028 (2021).

127. N. Tickotsky, T. Sagiv, J. Prilusky, E. Shifrut, N. Friedman. McPAS-TCR: a manually curated catalogue of pathology-associated T cell receptor sequences. *Bioinformatics*. 33(18):2924-2929 (2017).

128. M. Shugay, D. V. Bagaev, I. V. Zvyagin, R. M. Vroomans, J. C. Crawford, G. Dolton, E. A. Komech, A. L. Sycheva, E. A. Koneva, E. S. Egorov, A. V. Eliseev, E. Van Dyk, P. Dash, M. Attaf, C. Rius, K. Ladell, J. E. McLaren, K. K. Matthews, E. B. Clemens, D. C. Douek, F. Luciani, D. van Baarle, K. Kedzierska, C. Kesmir, P. G. Thomas, D. A. Price, A. K. Sewell, D. M. Chudakov. VDJdb: a curated database of T-cell receptor sequences with known antigen specificity. Nucleic Acids Res. 46(D1):D419-D427 (2018).

129. S. S. Vollers, L. J. Stern. Class II major histocompatibility complex tetramer staining: progress, problems, and prospects. *Immunology*. 123, 305-313 (2008).

130. S. Gregori, R. Bacchetta, L. Passerini, M. K. Levings, M. G. Roncarolo. Isolation, expansion, and characterization of human natural and adaptive regulatory T cells. *Methods Mol. Biol*. 380:83-105 (2007).

131. BIO675 -Transcriptomics course- 29th November-3rd December 2021. Functional Genomic Center. Zürich.

132. K. P. Nishimoto, D. Newkirk, S. Hou, J. Fruehauf, E. L. Nelson. Fluorescence activated cell sorting (FACS) using RNAlater to minimize RNA degradation and perturbation of mRNA expression from cells involved in initial host microbe interactions. *J. Microbiol*. Methods. 70(1):205-8 (2007).

133. N. L. Bray, H. Pimentel, P. Melsted, L. Pachter. Near-optimal probabilistic RNA-seq quantification. *Nat. Biotechnol*. 34(5):525-7 (2016).

134. H. Varet, L. Brillet-Guéguen, J. Y. Coppée, M. A. Dillies. SARTools: A DESeq2- and EdgeR-Based R Pipeline for Comprehensive Differential Analysis of RNA-Seq Data. *PLoS One*. 11(6):e0157022 (2016).

135. M. Battaglia, A. Stabilini, M. G. Roncarolo. Rapamycin selectively expands CD4+CD25+FoxP3+ regulatory T cells. *Blood*. 105(12):4743-8 (2005).

136. M. Schmaler, M. A. Broggi, N. Lagarde, B. F. Stöcklin, C. G. King, D. Finke, S. W. Rossi. IL-7R signaling in regulatory T cells maintains peripheral and allograft tolerance in mice. *Proc. Natl. Acad. Sci. U S A*. 112(43):13330-5 (2015).

137. R. Geiger, T. Duhen, A. Lanzavecchia, F. Sallusto. Human naive and memory CD4+ T cell repertoires specific for naturally processed antigens analyzed using libraries of amplified T cells. *J. Exp. Med*. 206(7):1525-34 (2009).

138. K. Venken, M. Thewissen, N. Hellings, V. Somers, K. Hensen, J. L. Rummens, P. Stinissen. A CFSE based assay for measuring CD4+CD25+ regulatory T cell mediated suppression of auto-antigen specific and polyclonal T cell responses. *J. Immunol. Methods*. 322(1-2):1-11 (2007).

139. J. Muri, S. Heer, M. Matsushita, L. Pohlmeier, L. Tortola, T. Fuhrer, M. Conrad, N. Zamboni, J. Kisielow, M. Kopf. The thioredoxin-1 system is essential for fueling DNA

synthesis during T-cell metabolic reprogramming and proliferation. *Nat. Commun*. 9(1):1851 (2018).

140. J. Muri, H. Thut, M. Kopf. The thioredoxin-1 inhibitor Txnip restrains effector T-cell and germinal center B-cell expansion. *Eur. J. Immunol*. 51(1):115-124 (2021).

141. M. S. Freedman, V. Devonshire, P. Duquette, P. S. Giacomini, F. Giuliani, M. C. Levin, X. Montalban, S. A. Morrow, J. Oh, D. Rotstein, E. A. Yeh; Canadian MS Working Group. Treatment Optimization in Multiple Sclerosis: Canadian MS Working Group Recommendations. *Can. J. Neurol. Sci*. 47(4):437-455 (2020).

142. X. Moisset, A. A. Fouchard, B. Pereira, F. Taithe, G. Mathey, G. Edan, J. Ciron, B. Brochet, J. De Sèze, C. Papeix, P. Vermersch, P. Labauge, G. Defer, C. Lebrun-Frenay, T. Moreau, D. Laplaud, E. Berger, J. Pelletier, B. Stankoff, O. Gout, E. Thouvenot, O. Heinzlef, A. Al-Khedr, B. Bourre, O. Casez, P. Cabre, A. Montcuquet, A. Créange, J. P. Camdessanché, S. Bakchine, A. Maurousset, K. Hankiewicz, C. Pottier, N. Maubeuge, D. Dimitri Boulos, C. Nifle, S. Vukusic, P. Clavelou; OFSEP investigators. Untreated patients with multiple sclerosis: A study of French expert centers. *Eur. J. Neurol*. 28(6):2026-2036 (2021).

143. J. Huan, N. Culbertson, L. Spencer, R. Bartholomew, G. G. Burrows, Y. K. Chou, D. Bourdette, S. F. Ziegler, H. Offner, A. A. Vandenbark. Decreased FOXP3 levels in multiple sclerosis patients. *J. Neurosci. Res*. 81(1):45-52 (2005).

144. F. Simonetta, A. Chiali, C. Cordier, A. Urrutia, I. Girault, S. Bloquet, C. Tanchot, C. Bourgeois. Increased CD127 expression on activated FOXP3+CD4+ regulatory T cells. *Eur. J. Immunol*. 40(9):2528-38 (2010).

145. L. Michel, L. Berthelot, S. Pettré, S. Wiertlewski, F. Lefrère, C. Braudeau, S. Brouard, J. P. Soulillou, D. A. Laplaud. Patients with relapsing-remitting multiple sclerosis have normal Treg function when cells expressing IL-7 receptor alpha-chain are excluded from the analysis. *J. Clin. Invest.* 118(10):3411-9 (2008).

146. K. Kimura, M. Nakamura, W. Sato, T. Okamoto, M. Araki, Y. Lin, M. Murata, R. Takahashi, T. Yamamura. Disrupted balance of T cells under natalizumab treatment in multiple sclerosis. *Neurol. Neuroimmunol. Neuroinflamm*. 3(2):e210 (2016).

147. P. Cavalcante, B. Galbardi, S. Franzi, S. Marcuzzo, C. Barzago, S. Bonanno, G. Camera, L. Maggi, D. Kapetis, F. Andreetta, A. Biasiucci, T. Motta, C. Giardina, C. Antozzi, F. Baggi, R. Mantegazza, P. Bernasconi. Increased expression of Toll-like receptors 7 and 9 in myasthenia gravis thymus characterized by active Epstein-Barr virus infection. *Immunobiology.* 221(4):516-27 (2016).

148. J. Fessler, A. Ficjan, C. Duftner, C. Dejaco. The impact of aging on regulatory T-cells. *Front. Immunol.* 4:231 (2013).

149. K. Venken, N. Hellings, T. Broekmans, K. Hensen, J. L. Rummens, P. Stinissen. Natural naive CD4+CD25+CD127low regulatory T cell (Treg) development and function are disturbed in multiple sclerosis patients: recovery of memory Treg homeostasis during disease progression. *J. Immunol*. 1;180(9):6411-20 (2008).

150. S. Tavakolpour. Interleukin 7 receptor polymorphisms and the risk of multiple sclerosis: A meta-analysis. *Mult. Scler. Relat. Disord*. 8:66-73 (2016).

151. J. Jäger, C. Schulze, S. Rösner, R. Martin. IL7RA haplotype-associated alterations in cellular immune function and gene expression patterns in multiple sclerosis. *Genes Immun*. 14(7):453-61 (2013).

152. X. Chen, L. Fang, S. Song, T. B. Guo, A. Liu, J. Z. Zhang. Thymic regulation of autoimmune disease by accelerated differentiation of Foxp3+ regulatory T cells through IL-7 signaling pathway. *J. Immunol*. 183(10):6135-44 (2009).

153. F. Ingelfinger, L. A. Gerdes, V. Kavaka, S. Krishnarajah, E. Friebel, E. Galli, P. Zwicky, R. Furrer, C. Peukert, C. A. Dutertre, K. M. Eglseer, F. Ginhoux, A. Flierl-Hecht, T. Kümpfel, D. De Feo, B. Schreiner, S. Mundt, M. Kerschensteiner, R. Hohlfeld, E. Beltrán, B. Becher. Twin study reveals non-heritable immune perturbations in multiple sclerosis. *Nature*. 603(7899):152-158 (2022).

154. G. E. Marcovecchio, I. Bortolomai, F. Ferrua, E. Fontana, L. Imberti, E. Conforti, D. Amodio, S. Bergante, G. Macchiarulo, V. D'Oria, F. Conti, S. Di Cesare, G. Fousteri, A. Carotti, A. Giamberti, P. L. Poliani, L. D. Notarangelo, C. Cancrini, A. Villa, M. Bosticardo. Thymic Epithelium Abnormalities in DiGeorge and Down Syndrome Patients Contribute to Dysregulation in T Cell Development. *Front. Immunol*. 10:447 (2019).

155. D. A. Duszczyszyn, J. L. Williams, H. Mason, Y. Lapierre, J. Antel, D. G. Haegert. Thymic involution and proliferative T-cell responses in multiple sclerosis. *J. Neuroimmunol*. 221(1-2):73-80 (2010).

7.0 ACKNOWLEDGMENT

This dissertation is the result of my PhD journey started in 2019, after obtaining a specialization in Pediatrics at the University of Brescia, Italy. The aim to understand the immunological mechanisms underlying diseases motivated me to pursue a career in research. I would like to thank my advisor Prof. Dr. Roland Martin for giving me the opportunity to follow this research project in his laboratory, supporting and guiding me all the time of research and writing. I express my gratitude to Prof. Dr. Federica Sallusto, who offered me the chance to pursue a PhD in Immunology and gave me insightful comments. I would like to thank the rest of my PhD Committee: Prof. Dr. Diane Mathis and Prof. Dr. Manfred Kopf for their suggestions and questions. My thank also goes to Dr. Wolfgang Faigle, who helped me with his expertise, patience and erudition, and to all the co-authors of the manuscript for their contribution. I am grateful to all the members of the laboratory for their helpfulness, inclusivity, enthusiasm about science and availability to discuss problems arising during the daily laboratory life. I thank the team of Abata Therapeutics for the periodic meetings with fruitful discussion, the members of the Functional Genomics Center of Zurich for teaching and technical support with RNA sequencing, the staff of the MS Outpatient Clinic and Day Hospital, Neurology Clinic, for patient care-related aspects of the projects, and patients for donating blood samples. I thankfully acknowledge the inspiration I received from my mentors at the Pediatric Clinic, University of Brescia, Italy who introduced me to the field of Immunology: Prof. Dr. Alessandro Plebani, Prof. Dr. Vassilios Lougaris and Prof. Dr. Raffaele Badolato.

I wish to express gratitude to my family and friends, especially my mum, my sister and Francesco, for their constant support, encouragement, and devotion. Lastly, I would like to thank all the people I did not cite, but I have met during my journey, and have somehow contributed to my personal growth.